VOT 72229

THE DEVELOPMENT OF ADSORBENT BASED NATURAL GAS STORAGE FOR VEHICLE APPLICATION

(PEMBANGUNAN STORAN GAS ASLI BERASASKAN PENJERAP BAGI KEGUNAAN KENDERAAN)

ASSOCIATE PROFESSOR DR. HANAPI BIN MAT

ZAINAL ZAKARIA

TERRY GEORGE PAOU

DEPARTMENT OF CHEMICAL ENGINEERING

FACULTY OF CHEMICAL AND NATURAL RESOURCES ENGINEERING

UNIVERSITI TEKNOLOGI MALAYSIA

2006

ACKNOWLEDGEMENT

The financial support from the Ministry of Science, Technology and Innovation (MOSTI) on the project (Project No. 02-02-06-0092/VOT 72229) is gratefully acknowledged.

ABSTRACT

THE DEVELOPMENT OF ADSORBENT BASED NATURAL GAS STORAGE FOR VEHICLE APPLICATION

(Keywords: Adsorptive gas storage, natural gas, adsorbent, zeolites, activated carbon)

Storage of natural gas by adsorption has a potential to replace Compressed Natural Gas (CNG) in mobile storage applications, such as in vehicles. Storage by adsorption at moderate pressure of 500 psig could be expected to reduce the problem of bulky high-pressure CNG storage within a confined space used in vehicle. In adsorptive storage, the amount of gas stored at lower pressure increases when a large portion of gas adsorbs on the adsorbent. However, its capacity and performance depend on adsorbent types and properties. This study is focused on the storage capacity and delivery performance of Adsorptive Natural Gas (ANG) storage employing different types of commercial adsorbents which were carried out by performing experimental work on an ANG storage system. Methane adsorptive storage was done in a 0.5-liter adsorbent-filled gas vessel under isothermal and dynamic conditions. The ANG vessel was charged with methane up to 500 psig at different rates of filling and was discharged under dynamic condition at a varied rate of discharge. The results show that the storage capacity obtained under isothermal condition is higher than under dynamic condition due to continuous temperature rise experienced during dynamic charging. Higher storage capacities were obtained for adsorbent with larger surface area and micropore volume but smaller interparticle void. Adsorbent that has high heat capacity and low heat of methane adsorption yields lesser temperature rise during adsorption and lesser temperature fall during desorption. Consequently, these characteristics lead to a better storage and delivery capacities. At faster charging rate, lower storage capacity was obtained and faster discharging rate caused inefficient gas delivery. Under cyclic operation, adsorbents performances deteriorate when adsorbent structure is gradually damaged under high-pressure operation. Among the adsorbents tested, palm shell activated carbon shows the highest storage and delivery capacity which are 87.4 *V/V* and 75.8 *V/V* respectively.

Key Researchers:

Associate Professor Dr. Hanapi Bin Mat
Mr. Zainal Zakaria
Mr. Terry George Paou

Email: hbmat@fkkksa.utm.my
Tel. No.: +607-5535590
Fax No.: +607-5581463
Vote No.: 72229

ABSTRAK

PEMBANGUNAN STORAN GAS ASLI BERASASKAN PENJERAP BAGI KEGUNAAN KENDERAAN

(Kata kunci: Storan gas berpenjerap, gas asli, penjerap, zeolit, karbon teraktif)

Storan gas asli secara penjerapan berpotensi untuk menggantikan storan gas asli termampat (CNG) bagi kegunaan kenderaan. Storan secara penjerapan bertekanan sederhana pada 500 psig boleh dimanfaatkan untuk mengatasi masalah saiz tangki gas asli termampat yang besar dalam ruang yang terhad pada kenderaan. Walau bagaimanapun, kapasiti dan prestasi penjerapan gas bergantung pada jenis and sifat-sifat bahan penjerap. Kajian ini tertumpu kepada kapasiti storan dan prestasi pengeluaran gas asli terjerap (ANG) menggunakan bahan-bahan penjerap komersil yang berlainan jenis dengan menjalankan eksperimen pada suatu sistem storan ANG. Storan secara penjerapan ini dilakukan dalam suatu bejana gas bersaiz 0.5 liter berisi bahan-bahan penjerap di bawah keadaan isotermal dan keadaan dinamik. Bejana ANG tersebut dipam dengan gas metana sehingga 500 psig pada kadar alir yang berlainan dan sistem tersebut pula dinyahpam pada keadaan dinamik dan pada kadar alir yang berbeza-beza. Keputusan eksperimen menunjukkan bahawa kapasiti storan dibawah keadaan isotermal adalah lebih tinggi daripada keadaan dinamik akibat kenaikan suhu yang berterusan semasa pengisian dinamik. Kapasiti storan yang lebih tinggi didapati untuk penjerap yang mempunyai luas permukaan dan isipadu liang mikro yang lebih besar serta ruang antara partikel yang lebih kecil. Penjerap yang mempunyai muatan haba tentu yang tinggi dan haba penjerapan metana yang rendah menunjukkan kenaikan dan penurunan suhu yang rendah semasa penjerapan dan nyahjerapan dan ini membawa kepada kapasiti storan dan pengeluran yang lebih baik. Pengisian dan pengeluaran gas pada kadar alir yang lebih tinggi pula menyebabkan kapasiti storan yang lebih rendah serta ketidakcekapan pengeluaran. Di bawah operasi berkitar, prestasi bahan-bahan penjerap telah merosot apabila strukturnya dirosakkan oleh tekanan storan yang tinggi. Di antara bahan-bahan penjerap yang digunakan, didapati bahawa penjerap karbon teraktif kelapa sawit mempunyai kapasiti storan dan pengeluran yang terbaik iaitu 87.4 *V/V* dan 75.8 *V/V*.

Penyelidik Utama:

Profesor Madya Dr. Hanapi Bin Mat
Encik Zainal Zakaria
Encik Terry George Paou

Email: hbmat@fkkksa.utm.my
No.Tel.: +607-5535590
No. Fax: +607-5581463
Vote No.: 72229

TABLE OF CONTENTS

LIST OF TABLES

LIST OF FIGURES

LIST OF ABBREVIATIONS

Al	-	Aluminum
ANG	-	Adsorbed Natural Gas
CNG	-	Compressed Natural Gas
CO	-	Carbon Monoxide
LEL	-	Lower Explosion Limit
LNG	-	Liquefied Natural Gas
MPa	-	Megapascal
NGV	-	Natural Gas Vehicle
NMHC	-	Non-methane Hydrocarbon
NO_x	-	Oxide of Nitrogen
O	-	Oxygen
ppm	-	Part per million
psi	-	Pound per square inch (Ib_f/in^2)
psia	-	Pound per square inch of absolute pressure
psig	-	Pound per square inch of gauge pressure
Si	-	Silica
STP	-	Standard Temperature and Pressure
upm	-	Unit per million
V/V	-	Volume of Adsorbed Gas per Volume of Solid Adsorbent
V_m/V_s	-	Volume of Stored Methane per Volume of Storage Container

LIST OF APPENDICES

CHAPTER I

INTRODUCTION

1.1 General Background

Natural gas has been increasingly useful and important as fuel for combustion. Lately, natural gas was used promisingly as fuel for the internal combustion engine, i.e., as fuel for vehicle application. In this field, natural gas has advantages over other hydrocarbon fuels because it is more economical, offers a greater reduction in carbon monoxide (CO), nitrogen oxides (NO_x), and non-methane hydrocarbon (NMHC) emissions while having a higher octane numbers – therefore a higher thermal efficiency than gasoline or diesel oil. In other words, it offers a cleaner combustion and a more efficient consumption.

Natural gas has been considered as a potentially attractive fuel for vehicle use. It is cheaper than gasoline and diesel. The wholesale price of natural gas in Malaysia is about RM0.55/liter compared to gasoline and diesel which is RM1.27/liter and RM0.72/liter respectively. The technical feasibility of natural gas vehicles is well established, and these vehicles have a less adverse effect on the environment than liquid-fueled vehicles (Talu. 1992). For example, natural gas can be burned in such a way as to minimize CO and NO_x emissions (Parkyns and Quinn, 1995). CO emissions are reduced by 99% while NO_x are reduced by 30%. Emissions of gases that contribute to global climate change, such as carbon dioxide, are also reduced by about 15%, hydrocarbon emissions are cut by 96% compared to gasoline use and practically no particulates (Mota *et al.*, 1995).

Natural gas consists of about 95% methane, a gas that is unable to be liquefied at ambient temperature by pressurization because of its critical temperature, T_c , is -82.6 ^oC. Since it is a gaseous fuel, its volumetric energy content is low compared with those of liquid fuels (Mota, 1999). In fact, natural gas outscores petroleum-based fuels in every aspect except onboard storage (Talu, 1992). Currently, natural gas is compressed at pressures up to 25 MPa (3600 psi) in order to be stored compactly on-board and dispensed quickly. However, this storage method requires expensive and extensive high-pressure compression technology (Jasionowski *et al.*, 1989).

1.2 Research Background

1.2.1 Introduction

For vehicle application (in NGV technology), natural gas is usually stored in a 50 liter pressurized vessel (cylinder) at a very high pressure which is around 2500 – 3000 psi (17.2 – 20.7 MPa) (Mota *et al.*, 1995) and is called Compressed Natural Gas (CNG). This high pressure, however, causes several drawbacks in the storage system (Elliott and Topaloglu, 1986):

- The energy densities achieved are approximately one quarter that of gasoline. The operational range of the vehicle is limited due to the awkward bulk of high-pressure cylinders which take up valuable cargo or trunk space.
- The fuel supply system compressors are complex and expensive. Three to four compression stages are needed, resulting in high cost of maintenance and energy of operation.
- There is a perception of danger associated with the high-pressure systems as well as some real potential problems, such as cylinder corrosion and the possible explosive release of compressed gas.

These are the main factors why natural gas has not been used widely for vehicle engine (Remick *et al.*, 1984).

A large effort has been invested in the replacement of high-pressure compression by an alternative storage method working at pressures up to 500 psi (3.5 MPa). Besides allowing the use of lighter and safer onboard reservoirs, this upper

limit can be easily achieved with a single-stage compressor or, alternatively, the vehicle can be refueled directly from a high-pressure natural gas pipeline. In this way, a significant decrease in the capital and operating cost of compression stations is achieved (Mota, 1999).

There is a new technology available to answer these difficulties of CNG storage. This technology is called Adsorptive Natural Gas storage or usually called Adsorbed Natural Gas (ANG). ANG storage is a technology in which natural gas is adsorbed by a suitable adsorbent material with high porosity. This storage of natural gas takes place at a relatively low pressure compared to CNG, which is around 500 psi (3.5 MPa), achievable by single-stage compression and can provide nearly the same capacity of CNG (Matranga *et al.*, 1992). When natural gas is charged into a vessel packed with an adsorbent, the energy density stored will be greater than of the same vessel without adsorbent (empty vessel) at the same pressure and therefore, the amount that of natural gas that can be stored is increased. In an empty high-pressure storage tank, gas is forced into the tank - the more gas, the higher pressure. If someone puts some microporous materials into the tank, we can store the same amount of natural gas in the same tank, but at lower pressure (Gubbins and Jiang, 1997). There is a force exerted by carbon atoms inside the pore and this force attracts a lot of gas molecules into the pore so that the amount of gas in the bulk is reduced. As a result, collision between gas molecules in the free space within the tank decreased and therefore, gas pressure is reduced while maintaining a high density of methane in the pores.

Compared to the conventional CNG storage, the ANG storage stored 2/3 (67%) of the amount that could be stored with a vessel without adsorbent but at 1/6 of its pressure (Cook and Horne, 1997). In other words, even though ANG could store less total storable amount of natural gas due to the storage space that is taken up by adsorbent mass, but its storage pressure is 5/6 times (83%) lower than CNG storage. This is illustrated in Figure 1.1 that shows the capacity of methane (g/l) stored in an empty cylinder and the capacity stored in an adsorbent-filled cylinder with an increase in pressure. It is obvious that ANG storage is capable to store more gas at lower pressure than CNG storage. Subsequently, this will allow more gas to be

stored at lower pressure because the ANG vessel can be charged or pressurized with more gas, as the pressure is still low.

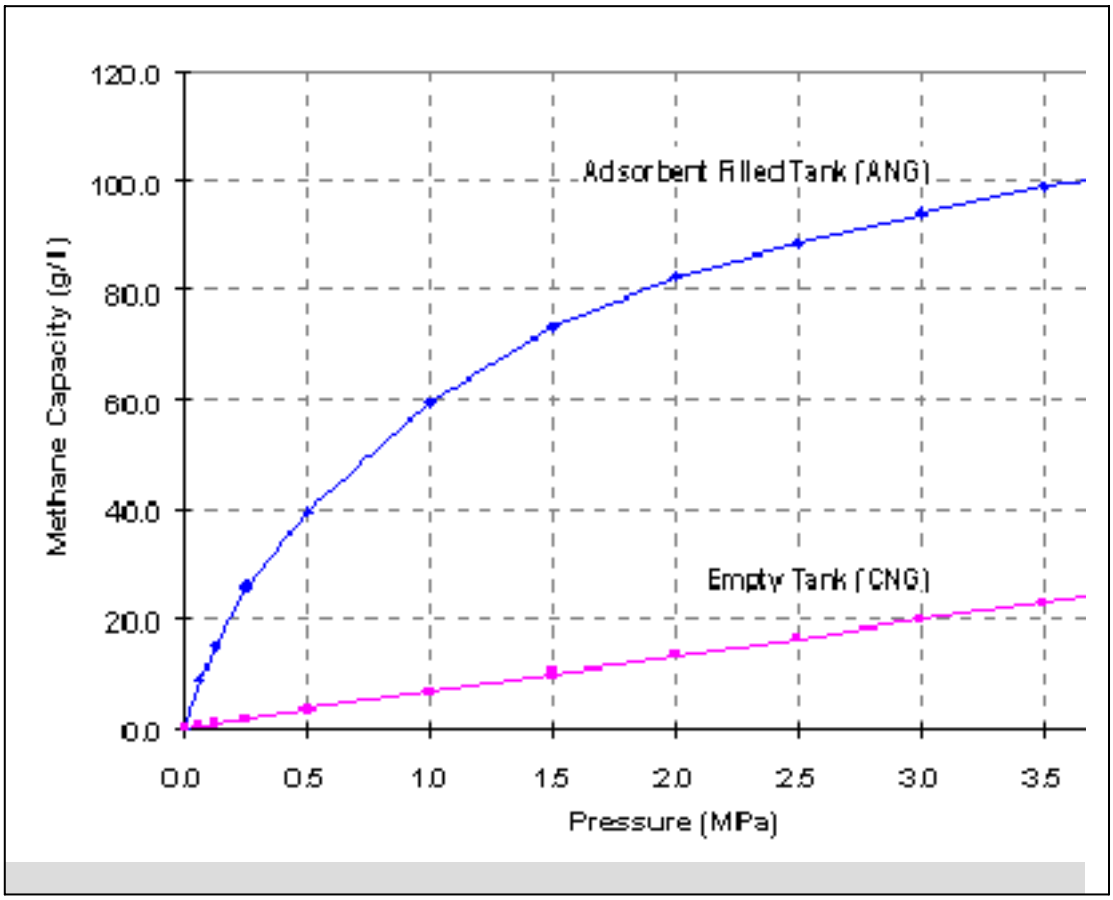

Figure 1.1: Comparison between CNG and ANG storage
(Cook and Horne, 1997)

By using adsorbent in the storage of natural gas, storage size can be reduced without defecting the quantity of the natural gas stored while reducing the pressure inside the storage vessel. This fact will allow usage of a lower pressure compression refilling system in which reducing the compression cost in terms of equipment and operation cost. At least one stage of compression can be reduced, that is, the highest pressure stage. This subsequently will reduce the energy consumed and capital and maintenance cost of the refilling system. Low pressure ANG storage system will also allow the storage vessel to be designed with smaller size and weight, with a lesser material-of-construction cost, as now the pressure is low enough.

ANG system pressures of 500 to 600 psig allow designers to progress from the constraints of cylindrical-shaped containers currently used by CNG vehicles. Conformable tanks, similar to conventional gasoline tank, would not intrude upon or detract from on-board storage space. The capital and the operating cost of compression and refueling equipment also have the potential to be lowered than the current CNG equipment. Moreover, the global warming potential for ANG is also reduced because less energy is required to compress natural gas, resulting in lower carbon dioxide emissions. From a safety and utilization perspective, lower ANG pressure may be more readily accepted compared to CNG (Cook and Horne, 1997).

1.2.2 Previous Research On ANG Storage

Adsorption storage is regarded as the most promising new low-pressure storage for natural gas (Remick and Tiller, 1985). Most research on ANG storage has aimed at the development and evaluation of economical adsorbents with storage capacities comparable to that of CNG. To date, the most promising adsorbents are highly microporous carbons with high packing density (Mota *et al.*, 1997). In addition, other areas of study concerning the ANG storage are the laboratory test of an ANG storage system which includes ANG thermal behavior and management, large scale adsorption experiment, dynamics of ANG system, and demonstration of ANG storage vehicle application.

Chang and Talu (1996) have studied the effect of the heat of adsorption on ANG storage system performance during discharge by performing an ANG performance tests using 35-liter cylinder under dynamic condition. A commercial grade activated carbon was employed and commmercial grade methane was used in the experiment instead of natural gas. The amount of methane adsorbed in the ANG storage is determined at the temperature and pressure range of the practical storage and delivery condition. They reported that in practical application, the gas discharge rate is dictated by the fuel demand. Therefore, it is not possible to operate an ANG system under isothermal conditions in practical. Any finite discharge rate will result in temperature drop. This temperature drop increases to be very substantial as the discharging rate goes higher, resulting in delivery capacity loss. They predicted that under realistic vehicle application, the performance loss is expected to be 15-20%.

Meanwhile, Remick and Tiller (1985) had conducted ANG experiments to assess the magnitude of the impact of the heat of adsorption on storage capacity using a one-liter cylinder. A carbon adsorbent was used for this work and it had a total storage capacity of about 100 volumes per volume (*V/V*) of methane at 500 psi and a delivered capacity of about 80 *V/V* of methane in cycling from 500 psi to atmospheric pressure. The methane adsorption isotherms were performed for this carbon at both 25 ^{o}C and 90 ^{o}C for pressure from vacuum to 500 psi. The cylinder was charge and discharged in slow and rapid rates. The experiment were conducted under condition simulating both a slow fill, where carbon bed temperature would have time to cool down to ambient condition, and a fast fill where the carbon bed temperature rise rapidly. It was determined that rapid filling of an adsorption storage at ambient condition results in only 75% of the storage capacity that can be achieved by a slow fill rate. These quantitative results however, are specific for the carbon used here but nevertheless, the general pattern should hold true.

A more extensive study on ANG storage system was carried out by Sejnoha *et al.* (1996). Their study is focusing on optimisation of activated carbon storage capacity and on performing a large-scale test bench adsorption experiments. The test bench, using 71-liter storage tank, permits simulation of conditions expected in a vehicle, adsorption with thermal management, heavier hydrocarbon filtering from gas stream and re-odorization of desorbed gas. Thermal management systems for cooling on board and at the filling station are described and a model was developed for predicting breakthrough curves at various operating conditions for filter prototype design. They presented the difference between a slow-fill and a fast-fill mode in terms of temperature rise and storage capacity. They concluded that the use of thermal management during a slow-fill has a minimum effect upon increasing storage capacity. During a fast-fill, the temperature rise is significant and leads to storage capacity loss. For as little as 20 ^{o}C of temperature decrease, an increase storage capacity up to 15% can be obtained. The use of thermal management can effectively improve the storage capacity.

Mota *et al.* (1997) have studied various aspects of the dynamics of natural gas adsorption storage systems employing activated carbon. They have addressed the

subject of charging rate of the storage system while given emphasis to thermal effects and hydrodynamics of flow through the carbon bed in order to develop a theoretical tools to provide an accurate description of the dynamics of ANG storage system. In order to study the influence of diffusional resistances, an intraparticle transport equation is added to the computational model. Also, they discussed the discharge process and proposed solutions for reducing the adverse effect of the heat of adsorption on storage capacity including *in situ* thermal energy storage. They concluded that taking vacuum as the initial condition for the charge cycle is unrealistic and a more realistic condition would be certainly the exhaustion pressure used in the discharge cycles. ANG vehicles will have controlled discharge rates which are sufficiently low so that the pressure gradient in the tank can be completely neglected.

Cook and Horne (1997) have developed a high performance, yet low cost microporous adsorbent capable of delivering 150 *V/V* of natural gas from the storage. They have also designed and fabricated a conformable tank to store the fuel and adsorbent and equipped two vehicles with the ANG system to demonstrate their performance. The best performing material developed are derived from coconut shells and peach pits. The ANG tank developed was a 22-cell, rectangular design. The multi-cell tank design aids thermal management of the ANG storage. Both vehicles converted to the ANG system performed very well. Their performance and drivability are equivalent to a comparable gasoline models.

1.3 Problem Statement

Most of ANG studies are employing carbonaceous substances such as activated carbon to be used as adsorbents for ANG storage (Quinn *et al.*, 1994). Nevertheless, highly porous materials such as molecular sieve zeolites and silica gels are also theoretically potential for adsorption of gases. These materials have been used as adsorbents in various chemical process applications such as for drying, separation, and purification process in which these solids preferentially separate substances from the gaseous or liquid phase onto the surfaces of their substrates (Suzuki, 1990; Slejko, 1985). Considering these benefits, then these adsorbents

should also be tested for natural gas adsorption besides currently used activated carbon. Even though highly microporous activated carbon has been reported as the most promisingly potential material as ANG storage adsorbent (Mota *et al.*, 1997), but performance tests should also be imposed on other theoretically potential materials mention above to gauge how far they are reliable as alternatives for activated carbon.

Among the studies of ANG storage in the literature, most of them are regarding the natural gas adsorptive behavior and storage condition, production of an economic carbon adsorbents, and adsorbents storage capacity development, while the viable aspect of this technology is the capability and reliability of the adsorbent-filled storage to discharge sufficient amount of gas for applications under realistic operational condition (Chang and Talu, 1996). In view of this, it is vital to perform ANG tests for both adsorptive charge and desorptive discharge of natural gas on different types of adsorbents in order to know their storage delivery performance with respect to their storage capacity. In addition, it is also equally important to perform the ANG tests under cyclic operation to study the performance of the adsorbents for repetitive application; whether they are reliable for repeated and prolonged operation, as it should be for practical application.

The most important performance measure in ANG storage is the gas delivery performance of the adsorbent (Chang and Talu, 1996). However, not all of the natural gas stored in the ANG storage vessel is deliverable. Past studies have informed us that retention of natural gas occur inside the carbon adsorbent during desorption when it is discharge from the storage for use (Be Vier *et al.*, 1989; Jasionowski *et al.*, 1989; Mota *et al.*, 1995; Remick and Tiller, 1985; Sejnoha *et al.*, 1994). As for pure methane, the dominant component (85-95%) of natural gas, when it is discharge from ANG storage, the storage vessel cools down due to the effect of the heat of desorption. This happens because desorption is an endothermic process. Any finite rate of desorption is accompanied by temperature drop in an ANG storage system. When the temperature of the system decreases during discharge under realistic condition, a larger amount of gas is retained in the storage at depletion pressure than under isothermal condition (Chang and Talu, 1996). The delivery capacity loss due to this effect can be more than 30% of the amount of gas stored at

charging phase (Matranga *et al.*, 1992; Talu, 1992). Therefore, considering this disturbing effect, it is important to run the performance tests of ANG storage system under dynamic condition, a condition where pressure and temperature vary, to determine the actual amount of gas that could be delivered from the adsorbent-filled storage in evaluating their performance for practical application.

1.4 Research Objectives and Scopes

The objective of this study is to develop adsorbent based natural gas storage for vehicle application with special emphasize on determining the storage capacity of different types of commercial adsorbents as adsorption media for Adsorbed Natural Gas (ANG) storage and to evaluate their performance in delivering the stored gas.

This study includes measuring the amount of gas that could be stored and the amount of gas deliverable from the ANG storage, and studying the effect of charge and discharge rate. Eventually, this research would want to figure out the characteristics of a reliable adsorbent, which will leads to a better methane storage capacity and delivery performance. The storage capacity of the commercial adsorbents is measured with pressurization up to 500 psig under isothermal and dynamic condition while the gas delivery performance from the adsorbent-filled storage will be evaluated by discharging from 500 psig to atmospheric pressure under dynamic condition. Under dynamic condition, the ANG storage is charged and discharged at varied flow rates and storage temperature varies naturally. Terms and variables understudies are (1) behavior of storage temperature, (2) profile of storage pressure, (3) the adsorption/desorption characteristics, (4) methane storage and delivery capacity on different adsorbents, (5) dynamic efficiency of methane delivery, (6) effect of charge/discharge flow rates, and (7) cyclic behavior.

1.5 Report Outline

Respective chapter of this report can be generally identified with one of

the objective of research described in section 1.4. This report contains five chapters which each chapter respectively containing its own introduction, descriptions of the relative topics and scopes to achieve the objectives of research and summary. Chapter I basically discussed about the entire project study, which contains general background, research background, problem statement, objectives and scopes of this study, report outline, and summary.

The historical and technical aspects of adsorbed natural gas storage including the fundamental aspects, and operating concept and problems associated with ANG storage are presented in Chapter II. All the materials and methods including equipments, chemicals, and experimental rig used are discussed in Chapter III.

Chapter 4 presents the detailed discussions of experimental results. The discussions include the performance evaluation of various parameters on charging and discharging, storage characteristic evaluation, and cyclic performance evaluation test. The conclusions and recommendations for future study are presented in Chapter V.

1.6 Summary

ANG is a new technology available to answer some difficulties of CNG storage for fleet application. In ANG storage, natural gas is adsorbed by a suitable high porosity adsorbent material packed inside the storage vessel. It takes place at a lower pressure, which is around 500 psi (3.5 MPa). When natural gas is charged into ANG vessel, the energy density stored will be greater than of the CNG vessel at the same pressure, increasing the amount of natural gas that can be stored. Subsequently, this will allow more gas to be stored at lower pressure. In view of this, this research will study on the adsorptive and desorptive performance of different types of commercially available adsorbents in storing and delivering methane for ANG storage application.

CHAPTER II

ADSORBED NATURAL GAS STORAGE

Natural gas is a gaseous mixture of light hydrocarbons which is found underground in sedimentary rock formations, often in the same location as crude oil. It is colorless, odorless fuel that burns cleaner than many other fossil fuels such as coal, gasoline, and diesel. Natural gas consists of mainly methane (85-95%) with a minor amount of ethane, and higher-order hydrocarbon compounds. Natural gas also contains a scant amount of unburned component such as carbon dioxide, nitrogen and sulfur. However, the percentage of natural gas composition is different from one reservoir to another (Parent, 1986). Natural gas composition from Malaysian reservoir is as presented in Table 2.1.

Since natural gas principal component is methane with 85-95% composition, therefore, the characteristics of natural gas are similar to methane. Methane is a colorless and odorless gas with a wide distribution in nature. At room temperature, methane is lighter than air. It melts at –183 °C and boils at –164 °C. Hence, at ambient temperature, methane cannot be liquefied by pressurization (Smith, 1990). This is because the critical temperature of methane which is –82.6°C, is lower than ambient temperature (27 °C). It can be liquefied only by cooling method and natural gas in this form is called Liquefied Natural Gas (LNG). Methane is not very soluble in water. It is combustible, and mixtures of about 5 to 15 percent in air are explosive. Methane is not toxic when inhaled, but it can produce suffocation by reducing the concentration of oxygen inhaled (Shakhashiri, 2000). A trace amount of smelly organic sulphur compounds (tertiary-butyl mercaptan and dimethyl sulfide) is added

to give commercial natural gas a detectable odour. This is done to make gas leaks readily detectable at 20% of lower explosive limit (LEL) (Senatoroff and Forwalter, 1964). An undetected gas leak could result in an explosion or asphyxiation. Natural gas has a specific gravity ranging between 0.60 to 0.65. This characteristic is an advantage in handling natural gas because when natural gas leaks to the atmosphere, it tends to elevate since natural gas is lighter than air.

Table 2.1: Malaysian natural gas composition (Gas Malaysia Sdn. Bhd., 1995)

Natural Gas Component	Volume Percentage	
	Before 1995	After 1995
Methane (CH_4)	84.75	92.73
Ethane (C_2H_6)	10.41	4.07
Propane (C_3H_8)	0.98	0.77
i-butane (C_4H_{10})	0.07	0.08
n-butane (C_5H_{10})	0.04	0.06
Other hydrocarbons (C_{5+})	0.00	0.01
Nitrogen (N_2)	0.39	0.45
Carbon dioxide (CO_2)	3.36	1.83
Total	100.00	100.00
Gross Calorific Value, CV (Kcal/Sm^3)	9.583	9.253
Specific Gravity	0.65	0.61

The principal use of methane is as fuel. The combustion of methane is highly exothermic. Methane requires air to gas ratio of 10:1 to produce a complete combustion (Pritchard *et al.*, 1977). The energy released by the combustion of methane is used directly for heating purposes such as to heat homes and commercial buildings, and to generate electric power. As fuel, natural gas has got advantages over other hydrocarbon fuels because it is more economics, offers a greater reduction in CO, NO_x and NMHC emissions while having a higher octane numbers than gasoline or diesel oil (Stodolsky and Santini, 1993). Therefore, it offers a cleaner combustion and a more efficient consumption.

2.1 Natural Gas Storage

Various approaches can be used to store natural gas, including compression, liquefaction, dissolution, and adsorption. Compression is the currently used fuel storage technique for natural gas vehicle. It is termed as Compressed Natural Gas (CNG). To reach a substantial capacity, very high storage pressures are used and are likely to increase the pressure up to 25 MPa (3600 psi). CNG relies on bulky, high-pressure vessels to store a quantity of natural gas that delivers about one-third (33%) of the range of an equal gasoline under typical operating conditions (Liss *et al.*, 1992). Therefore, the storage tanks are heavy, expensive and unsafe. In addition, this storage method requires expensive multi-stage high-pressure compression facility for refueling (Matranga *et al.*, 1992).

Conventionally, large-scale natural gas storage is by liquefaction, known as Liquefied Natural Gas (LNG). LNG provides nearly two-third (67%) of the range of a comparable volume of gasoline (Liss *et al.*, 1992). In this method, natural gas is cooled to –164 ^{o}C (cryogenic temperature). LNG is liquefied via a cryogenic procedure, and then delivered to some staging area before it is delivered to a vehicle. This method requires an insulated storage vessel to stage the fuel. Thus, the cost of liquefaction, the special insulating vessels required and the potential fire hazard are such as to make it unsuitable for used on a small scale. The LNG cooling requirement is inconvenience to its use as a fuel. Maintaining the cryogenic temperature involves increased insulation and a need for occasional venting of the fuel to the atmosphere, or to a vent recovery system as a means of controlling the fuel temperature. This storage technique is not suitable for vehicle application because it place extreme conditions on the tank for a vehicle (Horstkamp *et al.*, 1997).

Another technique for natural gas storage is the dissolution of natural gas in a solvent species of heavier hydrocarbons, such as ethane and propane. Liquid propane at 20 ^{o}C and 6.9 MPa was reported to hold up to 67% more methane per unit solution compared to CNG at the same pressure (O'Brien and Turnham, 1990). However, due to the change of physical properties of the fuel mixture when the natural gas is depleted, expensive adjustment in the air-fuel mixing mechanism and the ignition

mechanism are required. In addition, lower pressures and higher energy densities of the solutions could be outweighed by cost of the solvents required to make the solutions and the additional energy for cooling if necessary (Horstkamp *et al.*, 1997).

Another alternative to store natural gas especially for vehicle application is the Adsorbed Natural Gas (ANG) storage system at low pressure. ANG storage operates by using a microporous material – an adsorbent – which is loaded into the storage container of the natural gas. When the cylinder is pressurized with natural gas, a large portion of fuel adsorbs on the carbon lowering the storage pressure (Remick and Tiller, 1985). Due to strong enhancement of adsorption potential in the micropores, the density of the adsorbed phase can be higher than that of liquid natural gas. In general, when a storage vessel filled with an adsorbent is used to store natural gas, the storage pressure is reduced to around 500–600 psi. This pressure is relatively low compared to the CNG storage which is around 3000 psi. The ANG storage stored 67% of the total amount storable with the same storage vessel without adsorbent due to the storage space taken up by adsorbent mass but at 1/6 of its pressure (Cook and Horne, 1997). This technology is also known as Low Pressure Adsorbed Natural Gas in which substantial amount of gas is storable at relatively low gas storage pressure.

ANG storage offers a very high potential for exploitation in both vehicle and large-scale applications such as industrial fuel. However, because its actual total equivalent storage density is lower compared to CNG (theoretically 209 *V/V* compared to 240 *V/V* of CNG), a suitable development of the adsorbent is necessary to maximize natural gas uptake per storage volume (Alcaniz *et al.*, 1997). Among the available adsorbent, activated carbons exhibit the largest adsorptive capacity (Parkyns and Quinn, 1995; Cracknell *et al.*, 1993). The key factor for the success of ANG storage is the development of a low cost, high performance adsorbent material (Cook and Horne, 1997). In addition, other areas of research essential to ANG development are simulation of ANG dynamic behavior, experimental ANG performance measurement, feasibility studies and storage concept demonstrations (Talu, 1992)

2.2 Fundamentals of Adsorbed Natural Gas Storage

The foundational study of ANG storage involves the topics of gas adsorption in general, the characteristics of a suitable adsorbent material, the mechanism of natural gas adsorption on the adsorbent and some factors that influence the adsorptivity. The insight on these fundamental subjects will give better understanding regarding the ANG underlying characteristics.

2.2.1 Gas Adsorption

The term *adsorption* is generally used to denote the enrichment of one or more components in an interfacial layer between two bulk phases. In dealing with adsorption at gas/solid interface, it is customary to call the material in the adsorbed state the adsorbate, and to refer to the same species in the bulk gas phase as the adsorptive. The adsorbing solid is called adsorbent (Parfitt and Sing, 1976).

The amount of gas adsorbed, term as x, per gram of solid depends on pressure, p, temperature, T, the specific surface area, S, and the porosity of the adsorbent, and also on the nature of the gas-solid system as shown in Equation 2.1:

$$x = f\,(p,\ T,\ S,\ \text{porosity, system}). \tag{2.1}$$

For a given gas adsorbed on a given solid at a constant temperature, Equation 2.1 simplifies to

$$x = f\,(p)_T\,, \tag{2.2}$$

or if the gas is below its critical temperature, Equation 2.1 simplifies to

$$x = f\,(p/p_o)_T\,, \tag{2.3}$$

where p_o is the saturation vapor pressure of the adsorptive at T.

The nature of the adsorbing surface is a determining factor in adsorption. To be useful as an adsorbent, a solid must present a large surface area per unit mass (up to 1500 m^2/g) (Rodrigues, 1989). This can only be achieved with porous solids such as activated carbon, silica gel, aluminas, and zeolites, which contains many cavities or pores with diameters as small as a fraction of a nanometer. Surfaces of such solids contain sites of particular attraction for adsorbing molecules. If the sites are close together, the adsorbed molecules may interact with one another, if they are sufficiently dispersed, the adsorbed molecules may interact with the sites. Depending upon the strength of the forces binding them to the sites, these adsorbate molecules may be mobile or fixed in its position (Smith *et al.*, 1996).

2.2.1.1 Theory of Gas Adsorption

The surface of a solid has a tendency to attract and to retain molecules of other species (gas or liquid) with which such surface come in contact. This phenomenon of surfaces is termed as adsorption. It denotes the taking up of gases, vapor, or liquid by a surface or interface (Gurdeep, 1977). It is a property of a solid to retain on, or concentrate at its surface, one or more components (atoms, molecules, or ions) from another liquid or gas in contact with the surface. Adsorption is a characteristic surface or interface phenomenon, a fundamental physico-chemical property of solids. Adsorption phenomena are operative in most natural physical, biological, and chemical systems, and adsorption operations employing solids such as activated carbon and synthetic resins are used widely in industrial applications and for purification of waters and wastewaters (Slejko, 1985).

The process of adsorption involves separation of a substance from one phase accompanied by its accumulation or concentration at the surface of another. Adsorption is a spontaneous process. It is accompanied by a decrease in the free energy of the system. The adsorption process involves the loss of degree of freedom of the adsorbate, as it pass into the adsorbed film, there is a decrease in the entropy of the system. As the entropy and free energy decrease in adsorption, the enthalpy of the system decreases. This decrease in enthalpy appears as heat. Hence, the

adsorption process must always be exothermic or heat releasing (Parfitt and Sing, 1976). Adsorption of gas molecules into pores on adsorbent surface will release some amount of heat called *Heat of Adsorption*. In ANG storage context, the heat of methane adsorption is approximately 4 kcal per mole (Golovoy, 1983).

Based on the nature of the forces between the gas and the solid surface, gas phase adsorption are categorize into two types, which are physical adsorption and chemical adsorption. If the physical attraction forces hold the gas molecules to the solid, the adsorption is called physical adsorption (physisorption). Physisorption is a phenomenon where gas or vapor molecules were adsorbed by an adsorbent without any chemical reaction. Physisorption is cause mainly by London Dispersion Forces, a type of Van der Waals Force, which exist between molecules, and the electrostatic forces between adsorbate molecules and the atoms which composes the adsorbent surface. These forces act in a similar way to gravitational forces between planets.

If the chemical forces hold the gas molecules to the surface of the adsorbent, the adsorption is called chemical adsorption (chemisorption). In chemisorption, chemical reaction occurs between gas molecules and adsorbent surface area. Heat of adsorption released via chemisorption is greater than of physisorption. Chemisorption only occur at temperature more than 200 ^{o}C to reach the activation energy requirement to form or break chemical bond during adsorption or desorption process. It involves electron transfer between adsorbent and the adsorbates. The adsorbates will loss its electrons to the adsorbent and became positive ion. Adsorbent, on the other hand, becomes negative ion. With this the adsorbates will get attracted to the adsorbent surface. Reversibly, adsorbates will be desorbed from the adsorbent surface when the adsorbent release ions unto gas molecules.

2.2.1.2 Adsorption Isotherm

The adsorption of a gaseous substance from one phase to the surface of another on a specific system leads to a thermodynamically defined distribution of that gas between the phases when the system reaches equilibrium, that is, when no

further net adsorption occurs (Slejko, 1985). The common manner to depict this distribution is to express the amount of gas adsorbed per unit weight of the adsorbent, as a function of pressure at constant temperature, which is called *Adsorption Isotherm*. Adsorption isotherm is useful for describing adsorption capacity to facilitate evaluation of the feasibility of this process for a given application and for selection of the most appropriate adsorbent. Moreover, the isotherm plays a crucial functional role on predictive modelling procedures for analysis and design of adsorption systems. It is also useful for theoretical evaluation and interpretation of thermodynamics parameters, such as heat of adsorption.

2.2.2 Adsorbent Materials

Adsorbent is a substance that having a molecular structure that allows smaller molecules to penetrate its surface area and be kept inside the pores between its molecules. A large surface area of an adsorbent is a primary determinant for providing large adsorption capacity. Adsorption of natural gas on adsorbent follows pore-filling mechanisms and therefore the adsorption is dependent on the pore shape and volume. A useful adsorbent for ANG storage is a material that has pores of a suitable size to admit, hold, and discharge individual gas molecules.

2.2.2.1 Adsorbents Properties

Adsorbent material can be categorized according to their molecular structure. In general, the molecular structure of an adsorbent can be divided into (a) crystalline and (b) amorphous, solid structure (Webster, 1999). Examples of a crystalline solid are molecular sieve zeolites while carbonaceous material is an amorphous one. The molecular structure of crystalline and carbonaceous solid is shown in Figure 2.1.

Adsorption is a surface phenomenon and therefore, viable adsorbents must be characterized by large surface areas, the majority of which is comprised of internal

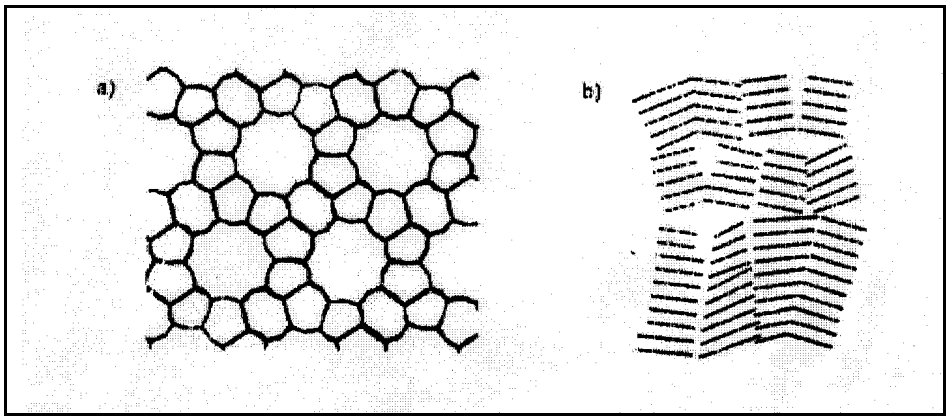

Figure 2.1: Molecular structure of (a) crystalline and (b) amorphous solids (Webster, 1999)

surfaces bounding the extensive pores and capillaries of highly porous solids (Slejko, 1985). A large specific surface area is preferable for providing large adsorption capacity. Larger surface area will allow more contact between gas molecules and adsorbent surface area to give way to more adsorption to take place. For example, activated carbon is one of the most widely used porous adsorbents because of its large surface area and capability of adsorbing a broad range of different types of adsorbates.

The performance characteristics of adsorbents relate in large measure to their intraparticle properties (Slejko, 1985). Surface area and the distribution of area with respect to pore size generally are primary determinants of adsorption capacity. The nature of the intraparticle surface area also markedly affects the types of adsorption interactions for an adsorbent. The effective adsorption capacity depends on the distribution of area or volume with pore size, and the distribution of molecular sizes to be adsorbed. Although not directly affect adsorption capacity, hardness or durability of individual adsorbent particles is an important property to be considered, at least for granular types of adsorbent application. This property largely determines the losses which occur on each adsorption cycle as a result of attrition during handling.

Properties of adsorbents also depend strongly on the manufacturing and activation process. Therefore, adsorbents from different manufacturers often behave

differently even if they are made from the same basic substance (Spang, 1997). Among the most commonly used microporous, high specific area materials in chemical process are alumina, silica gel, zeolites molecular sieves, active carbon, carbon molecular sieves, clays and polymers. The typical physical and adsorptive properties of the most commonly used adsorbent are summarized in Table 2.2 and Table 2.3.

Table 2.2: Physical properties of commonly used adsorbents (Spang, 1997)

Material	**Internal porosity (%)**	**Average pore diameter (nm)**	**Pore volume, micropores (cm^3/g)**	**Pore volume, macropores (cm^3/g)**
Activated carbon	60 - 80	2 - 4	0.30 - 0.50	0.50 - 1.10
Silica gel	40 - 50	2 - 5	0.30 - 0.45	0.05 - 0.10
Activated aluminas	35 - 40	3 - 5	0.40	0.10
Molecular sieves	30 - 40	0.3 – 1.0	0.25 - 0.30	0.30 - 0.40
Polymer resins	40 - 50	9 - 10	0.05 - 0.20	1.2 - 1.5

Table 2.3: Adsorptive properties of commonly used adsorbents (Spang, 1997)

Material	**Bulk Density (kg/m^3)**	**Specific Surface Area (m^2/g)**	**Specific Heat Capacity (kJ/kg.K)**	**Desorption Temperature range (°C)**
Activated carbon	300 - 500	600 - 1500	0.84	100 - 150
Silica gel	400 - 800	600 - 800	0.92	120 - 250
Activated aluminas	700 - 850	100 - 400	0.85 - 1.05	150 - 320
Molecular sieves	600 - 900	500 - 1000	0.95 - 1.05	200 - 300
Polymer resins	300 - 320	550 - 800	0.35	80 - 140

Adsorbents are used for numerous applications in chemical process industries especially for purification and separation of gas or liquid components by adsorption.

Adsorption phenomena are operative in most natural physical, biological, and chemical systems. Adsorption operations employing microporous, high surface area solid adsorbents such as activated carbon, zeolite molecular sieves, alumina, silica gel and synthetic resins are widely used in industrial applications and for purification of water and wastewater (Suzuki, 1990). The typical applications of the most commonly used microporous adsorbents in chemical processes are summarized in Table 2.4.

2.2.2.2 Adsorbents for Natural Gas Storage

Adsorbent that is useful to adsorb the natural gas in ANG storage is a substance that having a molecular structure that will allow methane (dominant component in natural gas) molecules to penetrate its surface area and be kept inside the pores between its molecules, in which pore filling adsorption mechanism takes place. The pore sizes in the adsorbent solid must be of a suitable size to admit, hold, and discharge individual gas molecules. If the pores are too small, the gas cannot be admitted. If they are too large, too many molecules of gas are admitted, and they display the characteristics of gas under pressure: frenzied movement, and constant molecular collisions (Brown, 1995). This means that they cannot be packed as tightly as if they were held nearly immobile in an adsorbent structure. There are some material that fit these characteristics such as activated carbon, zeolites, silica gel and molecular sieves.

Since adsorption of natural gas on adsorbent follows pore filling mechanisms, therefore the adsorption are dependent on the pore shape and are influenced by the properties of the adsorptive and by the adsorbent-adsorbate interactions (Marsh, 1987). The whole of the accessible volume present in micropores may be regarded as adsorption space. The properties of an adsorbent that is suitable for natural gas storage can be summarized in the following four points. The material should have: (1) a high adsorption capacity; (2) a high packing density; (3) a high adsorption/desorption rates; and (4) a ratio between the amount desorbed at depletion

and the amount adsorbed at 3.5 MPa (500 psig), as close as possible to 1 (Parkyns and Quinn, 1995).

Table 2.4: Typical applications of commonly used adsorbents in chemical processes (Suzuki, 1990)

Type of Adsorbent	Typical Application
Alumina	Drying process
Silica Gel:	Drying process
Grade 03	Dehydration of natural gas and industrial gases
Grade 11, 13	Miscellaneous dehydration application where fine particle size is preferred
Grade 40	Liquid and gas dehydration, hydrocarbon recovery
Various Types Zeolites Molecular Sieves:	Gas and liquid separation, drying process
High-strength 3A	Use for cracked gas application for long life and low pressure drop
4A	Use for most gas dehydration application in removing H_2O and CO_2
5A	Pressure swing adsorption of hydrogen purifier
13X	Removal of CO_2 and impurities in butane isomerizers and air pretreatment application
Activated Carbon	Gas and liquid separation, guard beds
Synthetic Resin	Purification of waters and wastewater

Most studies on ANG storage are focusing on development and evaluation upon adsorbent with storage capacity comparable to the CNG storage capacity, if not exceed. In the past study, carbonaceous adsorbent materials have been used mostly as adsorbents for ANG storage (Quinn *et al.*, 1994). The other types of potential

adsorbent rarely employed for ANG storage are molecular sieve zeolites and hydrophobic silica xerogel (Cracknell *et al.*, 1993; Menon, 1997).

According to the research made by the Atlanta Gas Light Adsorbent Research Group (ARLARG) (1997), the best performing materials developed thus far are derived from organic materials including coconut shells and peach pits. These materials have a naturally occurring pore structure that can be optimized for the adsorption of the methane in natural gas. The method of densifying or compacting the adsorbent is also critical to achieving acceptable performance. Proprietary densification techniques were developed during the course of the research to form solid carbon monoliths and briquettes that match the profile of the tank for easy insertion.

A. Activated Carbonaceous Adsorbent

Base on previous study, for ANG storage, adsorbent material made of carbon has been found out to be the best one to store the natural gas molecules compare to the other materials. According to Parkyns and Quinn (1995), microporous activated carbon has emerged to be the best adsorbents for ANG storage. Microporous carbons are effective adsorbents for methane and are superior in this respect to molecular sieve zeolites (Barton *et al.*, 1986 and Cracknell *et al.*, 1993).

Matranga *et al.* (1992) has performed Grand Canonical Monte Carlo (GCMC) calculations to stimulate the adsorption of natural gas on carbon. In the GCMC simulations, the natural gas was modeled as pure methane adsorbed on parallel planes of graphite which is optimized for ANG storage. Micropores of the activated carbons are modeled as having the shape of an infinite slit enclosed between two parallel basic atom planes of graphite. Primary micropore filling takes place in very narrow slit-shape pores. The simulation predicts that the theoretical maximum storage capacity of carbon for methane at 3.4 MPa (500 psi) is 209 V_m/V_s for monolithic carbon and 146 V_m/V_s for pelletized carbon. These figures for ANG may be compared to 240 V_m/V_s for CNG at 3000 psi. The delivered capacity of carbon is

less than the storage capacity because carbon retains some gas at the exhaustion pressure. The maximum delivered capacity of ANG is 195 V_m/V_s for monolithic carbon and 137 V_m/V_s for pelletized carbon, compared to 216 V_m/V_s for CNG. However, in spite of the simulated capacities obtained, the highest experimental values obtained to date are 86 V_m/V_s for granular AX-21 activated carbon and 125 V_m/V_s for a monolithic carbon (Quinn, 1990).

Activated carbon is a crude form of graphite. From a chemist's perspective, activated carbon is an imperfect form of graphite. This imperfect structure results in a high degree of porosity and more than million-fold range of pore sizes. Porosity is what distinguishes activated carbon from other carbon substances and makes it "activated". The graphite structure gives the carbon its very large surface area which allows the carbon to adsorb a wide range of compounds. Figure 2.2 shows the pore structure of an activated carbon.

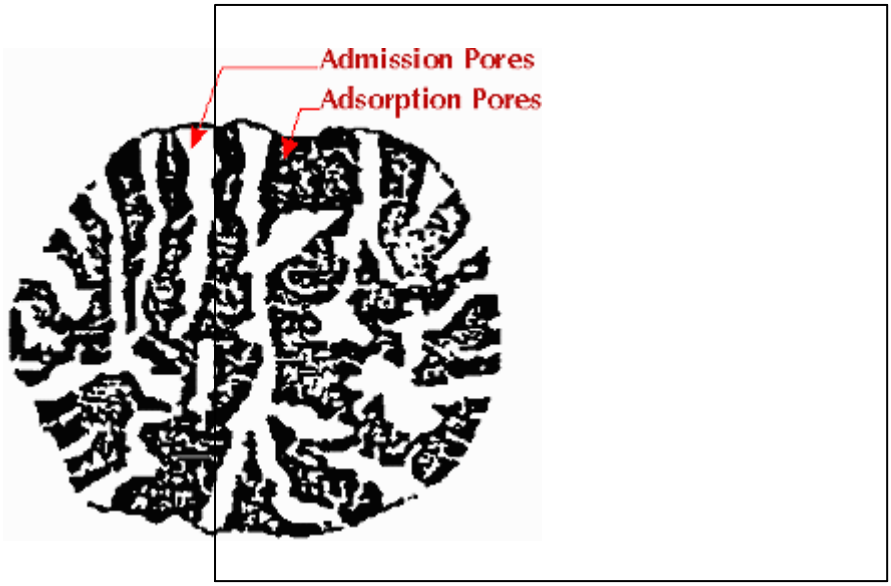

Figure 2.2: Pore structure of activated carbon (Brown, 1995)

Activated carbon of a high surface area is highly porous and has a range of pores with different shapes and size. Pores within an adsorbent are classified based on effective width of pore. Base on IUPAC standard, pores are categorized into 3 categories according to their effective width (Sing *et al.*, 1985):

1. Pores with widths not exceeding 2 nm are called micropores.
2. Pores with widths within 2 and 50 nm are called mesopores.
3. Pores with width more than 50 nm are called macropores.

The micropores represent at least 95% of the active internal sorptive area of the carbon (Jonas, 1987). The macropores and the mesopores play the role to conduct the adsorbate gases to the active site in the micropores. If an activated carbon contained only micropores, the probability of obtaining a high efficiency in adsorptive behavior of the carbon would be low because high pressures are required to force the gaseous fluid through a small diameter. Thus, the presence of the macropores is sufficient to permit easy entry of the gas molecules, from which they migrate by momentum and diffusion through the mesopores, and finally to the micropores where they are strongly bound by the London dispersion forces in a physical adsorption bond (Jonas, 1987).

Activated carbon is made from many substances containing high carbon content such as coal, coconut shells, and wood. The raw material has a very large influence on the characteristics and performance of activated carbon. These raw materials must be activated before being used as adsorbent. Activation process is needed to improve and enhance the porosity of the material. Activated carbons are produced in three main forms, which are in granular, pelletized, and powdered forms as shown in Figures 2.3, 2.4 and 2.5. Granular activated carbon is an irregular shaped particles with sizes ranging from 0.2 to 0.5 mm. This type is used both in liquid and gas phase application. Powder activated carbon is a pulverized carbon with size predominantly less than 0.18 mm (US Mesh 80). These are mainly used in liquid phase applications and for flue gas treatment. Pelletized activated carbon is extruded and cylindrical shaped with diameters from 0.8 to 5 mm. These are mainly used for gas phase applications because of their low pressure drop, high mechanical strength and low dust content. However, adsorbents in the form of powder adsorb more gas than of granules. This is due to the presence in granules of a non-adsorbing binder which partly decreases their porosity and, hence, their adsorption capacity. When the adsorbent is compacted from granules to powder form, i.e., when the bulk density is increased, the storage capacity is improved (Malbrunot *et al.*, 1996).

Figure 2.3: Granular activated carbon (Chemiviron, 1998)

Figure 2.4: Powder activated carbon (Chemiviron, 1998)

Figure 2.5: Pelleted activated carbon (Chemiviron, 1998)

Figure 2.6 shows a view of a packed bed activated carbon while Figure 2.7 and Figure 2.8 show a microscopic view of it. A bed of an activated carbon is consisted of carbon granule, void fraction and pores with different shapes and sizes. The volume void fractions of a packed bed of activated carbon granules are the spaces between granules. The different types of pores are the macro-, meso-, and the micropore system of the carbon which was developed as a result of the activation process.

The storage capacity and delivery performances of the activated carbonaceous solids employed as adsorbents for ANG storage as reported in the literature are summarized in Table 2.5.

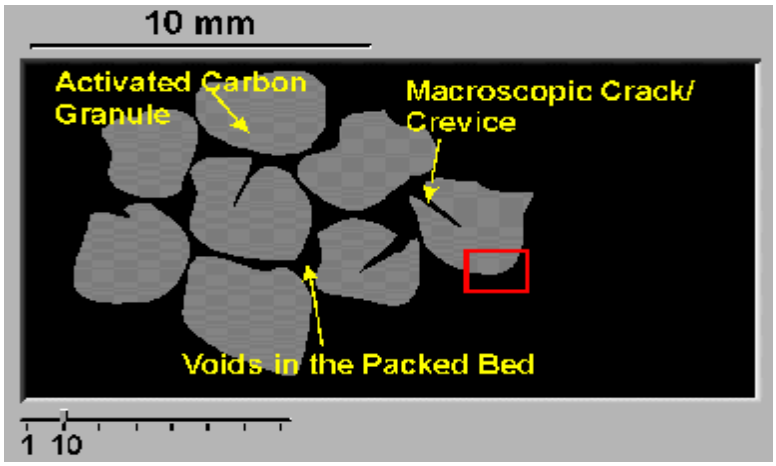

Figure 2.6: View of activated carbon packed bed (Chemiviron, 1998)

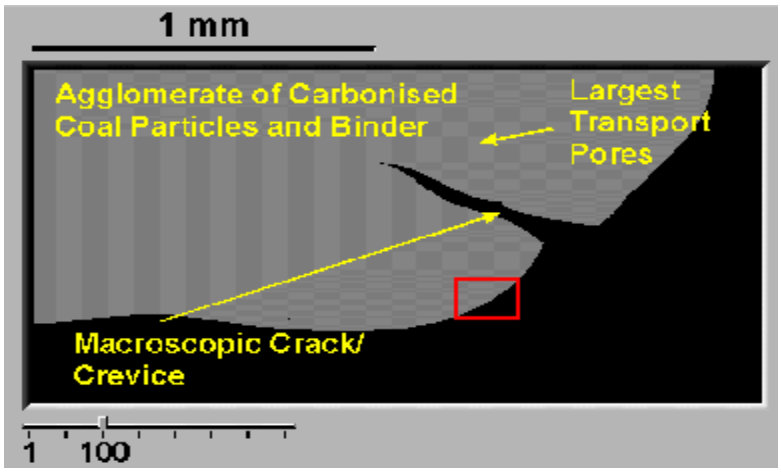

Figure 2.7: Zooming 1:10 of the above packed carbon (Chemiviron, 1998)

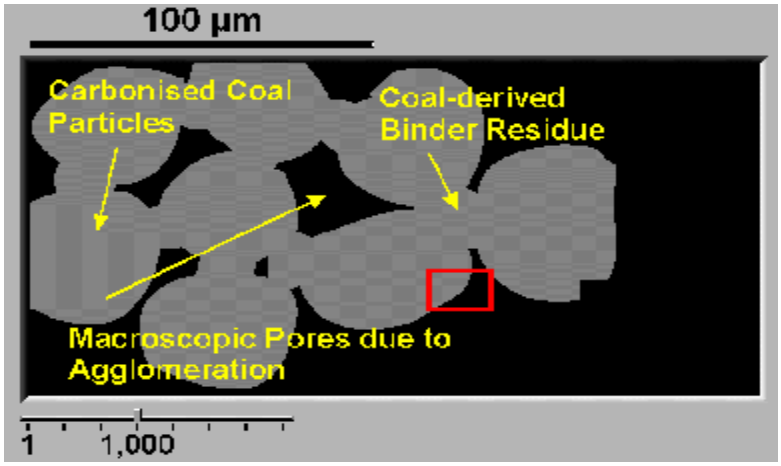

Figure 2.8: Zooming 1:100 of the above packed carbon (Chemiviron, 1998)

Table 2.5: Storage and delivery performance of carbonaceous adsorbent in literature

ADSORBENT	PERFORMANCE		REFERENCES
	Storage Capacity (V_m/V_s)	**Delivery Capacity (V_m/V_s)**	
BPL Commercial Activated Carbon	72	-	Abadi *et al.* (1995)
Pelletized Carbon from Oxidized IBC-106 Coal	83	-	Abadi *et al.* (1995)
Peach Pit and Coconut Shells derived Activated Carbon	-	164 at 500 psig 143 at 600 psig	Cook and Horne (1997)
Activated Carbon Fiber (ACF) from CO_2 activation	163	143 at 500 psig	Alcaniz *et al.* (1997)
KOH activation MCB-48M Carbon Powder	174	161 at 500 psig	Chen *et al.* (1997)
AX-21 Commercial Activated Carbon: *Granule* *Mixture with polymeric binder*	 101 144	 - -	Sejnoha *et al.* (1994)
CNS Commercial Activated Carbon: *Granule* *Mixture with polymeric binder*	 82 103	 - -	Sejnoha *et al.* (1994)
G126 Activated Carbon	100	80 at 500 psig	Remick And Tiller (1985)
PVDC derived Carbon	92.2	68 at 500 psig	Elliott and Topaloglu (1986)

B. Zeolites Adsorbent

There have been a number of experimental studies of the feasibility of using already existing materials for methane storage. Among these materials are zeolites (Cracknell *et al.*, 1993; Jiang *et al.*, 1994). The zeolites structures contain (-Si-O-Al-) linkages that form surface pores of uniform diameter and enclose regular internal cavities and channels of discrete sizes and shapes, depending on the chemical composition and crystal structure of the specific zeolites involved. Its significance as commercial adsorbent depend on the fact that in each of the crystals containing interconnecting cavities of uniform size, separated by narrower openings, or pores, of equal uniformity (Trent, 1995). Pore sizes range from about 2 to 4.3 angstroms.

Zeolites are crystalline hydrated aluminosilicates, of the alkali and alkaline earth metals. Their crystalline framework is arranged in an interconnecting lattice structure. The arrangement of these elements in a zeolites crystal creates a porous framework silicate structure with interconnecting channels of various sizes. This structure allows zeolites to perform gas adsorption, which is the ability to selectively adsorb specific gas molecules consistently within a broad range of chemical and physical environments.

The adsorption functions of zeolites are accomplished when gas molecules of different sizes are allowed to pass through the channels, and depending upon the size of the channel are separated, in a process known as molecular sieving. The ability of activated zeolites to adsorb many gases on a selective basis is in part determined by the size of the channels ranging from 2.5 to 4.3Å (0.25 to 0.43 nm) in diameter (according to zeolite type) (Trent, 1995). Specific channel size enables zeolites to act as molecular gas sieves and selectively adsorb such gases as ammonia, hydrogen sulfide, carbon dioxide, sulfur dioxide, water vapor, oxygen, nitrogen, and others.

Zeolites are predictably potential for natural gas adsorption due to the availability and ability of the microporous interconnecting channels of discrete sizes and shapes within its structure. Zeolites have micropores with dimensions that are comparable to the dimensions of methane molecules (Well, 1998). The size of these channels is around 0.25 to 0.43 nm and can be up to 0.95 nm while the size of

methane molecule is 0.32 nm (Trent, 1995; Elliott and Topaloglu, 1986). This fact shows that zeolites are capable for methane adsorption in which methane molecules could penetrate through its surface and fill the microporous channels within zeolites substrates.

A work by Cracknell *et al.* (1993) has established a comparison discussion for both zeolite (assumed to have cylindrical pores) and carbon (assumed to have slit pores) for the advantage of storing methane from Grand Canonical Monte Carlo (GCMC) simulation for different pore sizes at 213 and 274 K have been also discussed. Their results suggested that an optimized pores of porous carbon is a more suitable material for adsorptive storage of methane than an optimised zeolite pores. The best pore size to use depends on the operating conditions of the system. They found that for a storage pressure of 3.4 MPa (500 psi) at 274 K the model slit carbon pore yields 166 g/l (methane adsorbed) compared to 53.1 g/l for the zeolite. Reduction in temperature does allow a greater amount of methane to be adsorptively stored for a given pressure.

C. Silica-Gel Adsorbent

Hydrophobic adsorbents having a high surface area on a volumetric basis are potential candidate materials for ANG storage. Silica xerogel adsorbents are hydrophobically porous but have a low surface area. However, this property can be modified using several methods to increase the surface area in order to produce synthesized hydrophobic silica xerogels adsorbent with a good adsorptivity. Certain treatments made on silica xerogels will improve its microporosity. In turn, this will produce high surface area adsorbents that are useful for adsorptive natural gas storage. Already a study being made in the literature concerning this subject where silica xerogel adsorbents are treated and synthesized from tetraethoxysilane (TEOS) by systematically varying selected sol-gel processing parameters (Menon, 1997). The synthesized silica xerogel adsorbents are said to be potential materials for vehicular natural gas storage.

2.2.3 Mechanism of Natural Gas (Methane) Adsorptive Storage

Intermolecular attraction in the smallest pores result in adsorption forces. This attraction is a type of Van der Waals force called London Dispersion Force. The adsorption forces works like gravity, but on molecular scale. They cause precipitation, in which adsorbates are removed from vapor stream. To develop a strong adsorption force, either the distance between the adsorbent platelets and the adsorbates must be decreased (by reducing its pore size), or the number of atoms in the solid structure must be increased (by raising the density of the carbon).

In a conventional high-pressure storage tank, such as a propane tank used for cooking, gas is forced into the tank - the more gas, the more pressure. If someone puts some microporous materials into the tank, we can store the same amount of natural gas in the same tank, but at lower pressure (Gubbins and Jiang, 1997). Using the Connection Machine CM-2 at Pittsburgh, Gubbins and Jiang simulated how parallel layers of carbon atoms can adsorb methane atoms. There is a force exerted by the carbon atoms inside the pore and this force attracts a lot of gas molecules into the pore so that the amount of gas in the bulk is reduced. As a result, the pressure of the tank can be kept low while maintaining high density of methane in the pores.

The optimal pore size that Gubbins and Jiang discovered is the width between two methane molecules. After the first layers of methane atoms line up along the pore's sides, carbon's attractive forces fall off rapidly. Thus, the adsorbed methane that are not in the contact layer on the wall will be much less tightly adsorbed because he forces will be much weaker. A rough analogy might be iron fillings attracted to the pole of a magnet. The first one or two layers will be tightly bound to the surface, and subsequent layers will be more loosely bound and less dense.

The hexagonal structure of graphite (Figure 2.9), with carbon atoms at the vertices of the hexagon, provides a surface for the adsorption of methane atoms (magenta). Because the potential energy of the hexagon centers is lower than the outer edges, they are favored adsorption sites for methane. At low temperature (left side), methane adsorbs at centers of alternate hexagons, similar to eggs filling an egg

carton. At increased pressure (right side), the methane pack more closely and no longer sit over the hexagon centers.

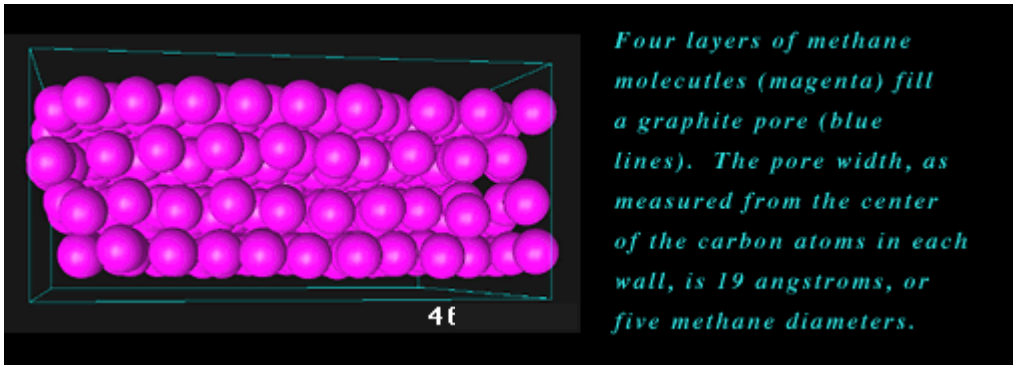

Figure 2.9: Methane adsorption on a graphite surface (Gubbins and Jiang, 1997)

2.2.4 Factors Influencing The Adsorption Capacity of Natural Gas

The adsorption capacity of natural gas on an adsorbent depend upon several factors such as the properties of adsorbent and adsorbate, the adsorbent surface area and pores, temperature of the adsorption process and packing density of the adsorbent loading into the ANG vessel.

2.2.4.1 Natural Properties of Adsorbent and Adsorbate

Gaseous compound with higher molecular weight is easier to be adsorbed compared to compound with lower molecular weight. This is due to molecule with heavier molecular weight possesses greater Van der Waals force. In the natural gas composition, heavier hydrocarbons such as propane to heptane are adsorbed easier than methane and ethane (Mota, 1999). Meanwhile, for the adsorbent that is prepared from different raw material and methods of production will show different adsorption

behavior (Spang, 1997). Activated carbonaceous adsorbent, having greater measure of surface area and better porosity, will give higher storage capacity.

2.2.4.2 Adsorbent Surface Area and Pores

Efficiency of an adsorbent to adsorb gas depends on its surface area. Surface area, in turn, depends on the pore size. Macropores did not play important role in adsorption. They only serve as to give route for gas molecules to reach smaller pores that are micropores. Micropores, mainly formed during activation process, are very important for natural gas adsorption. This is because micropores structure is the most effective area to store gas molecules such as natural gas, which mostly consist of methane. Micropores typically range from less than 2 nm while methane molecule size is 0.32 nm (Elliot and Topaloglu, 1986). Therefore, possibility for all methane to be adsorbed is high. Generally, microporous activated carbon is having typical surface area range from 600 m^2/g to 1200 m^2/g (Rodrigues *et al.*, 1989). Van der Waals force of the micropores is greater than of the mesopores and macropores. In addition, larger surface area will allow more contact between gas molecules and adsorbent surface area to give way to more adsorption to take place, in other words, more surface area, more pores.

2.2.4.3 Adsorption Temperature

Adsorption is a process that is temperature sensitive. Adsorption capacity decreases when temperature rises. When natural gas is charged into an adsorbent-filled container, substantial amount of heat is releases. When this happens, capacity of natural gas adsorbed will decrease (Remick and Tiller, 1985). Adsorption capacity can be determined through equilibrium between adsorption rate and desorption rate. Decrement of adsorption capacity with temperature rise can be explained by Le Chateleir principle. Adsorption reaction can be written as follows:

$$A + S \rightleftharpoons A - S + \text{heat} \qquad (2.4)$$

Above is the reaction for adsorption and desorption where A is adsorbate (natural gas) and S is adsorbent surface. When natural gas is adsorbed, heat of adsorption is released. When heat increases, reaction system will transfer the equilibrium to the left side and causing more gas molecules not to be adsorbed and subsequently reduces adsorption capacity.

2.2.4.4 Packing Density of Adsorbent

Packing density is defined as the mass of settled material per unit volume of storage space (Remick and Tiller, 1985). It is one of the critical parameters associated with the adsorbent storage of the natural gas. Though the adsorbents may indicate a high adsorbency on a mass basis, the low packing density means that much of the potential advantage is lost and the volumetric energy densities are still low. A carbon adsorbent with a mediocre surface area but a high packing density may actually store more methane, when loaded into a cylinder, than a high surface area carbon with a low packing density. For example, CECA carbon has a surface area of 1030 m^2/g and a packing density of about 0.56 g/cm^3. Nuchar WV-B, on the other hand, has a surface area of about 1600 m^2/g but a packing density of only 0.30 g/cm^3. When both carbons were loaded into a 1-liter cylinder and pressurized with methane to 3.6 MPa, the CECA carbon delivered 51.4 grams when discharged to atmospheric pressure while the Nuchar carbon only delivered 41.1 grams (Remick and Tiller, 1985).

The impact of both surface area and packing density can be best seen in Figure 2.10. In this diagram, the individual lines represent carbons with the same specific adsorption of methane at 5400 psig and are labeled 0.165, 0.15, 0.100, and 0.085 grams of methane per gram of carbon substrate. Point S1 represents the total grams of methane stored at 5000 psig in a 1-liter cylinder filled with a composite of 90% Amoco GX-32 and 10% Saran, point S2 is for the 50/50 composite, S3 is the

data point for the 25% GX-32 and 75% Saran composite, and point S4 is for 100% Saran. Furthermore, Barton et al. (1984) have proposed that it may be possible to obtain a packing density as high as 1.0 g/cm^3 for the Saran carbon. This point is plotted as S in the figure.

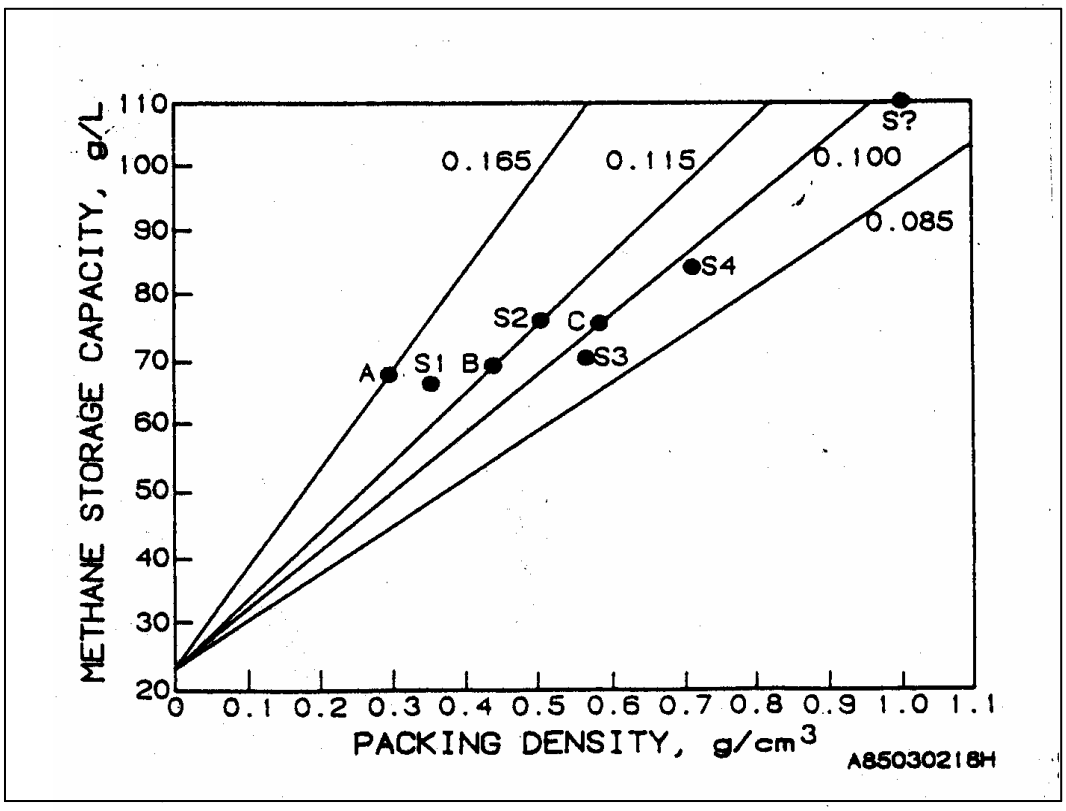

Figure 2.10: Impact of packing density on adsorption and methane storage capacity (Remick and Tiller, 1985)

2.3 Concept of ANG Storage Operation

ANG storage operation is sorted into charging and discharging phase which make up a complete cycle of gas filling and emptying process of an adsorbent-filled storage. Charging phase represents the pressurization of the ANG storage from atmospheric pressure to the storage pressure of 500 psig in which the natural gas is charged into the storage container while the discharging phase represents the

depressurization of the storage from 500 psig back to the atmospheric pressure to remove the stored gas. ANG storage operates by enhancing the amount of gas stored when a large portion of gas adsorbs on the adsorbent and markedly improve the storage capacity at lower pressure. The ANG storage amount is measured with two capacity measures, which are the storage capacity and the delivery capacity. In the literature, ANG capacity measurements have been carried out by performing natural gas charging and discharging test on an adsorbent-filled pressurized vessel of different scales and experimental variations.

2.3.1 ANG Storage Model

ANG storage is modeled as series of consecutive cycles. Series of consecutive cycles means that the charging and discharging process of the natural gas from ANG storage is done repeatedly. Every cycle involves two steps. The first step is the filling of gas with a fixed composition gas mixture followed by the second step which is the discharging of gas at constant molar flow rate until the original storage pressure is achieved (Mota, 1999). Figure 2.11 shows schematic of the cycle. The two steps of this cycle series, which are filling phase and discharging phase of natural gas from storage, occur at P_1 (initial pressure inside container before charging, 1 atm) and P_2 (charging pressure of natural gas into storage, 3.5 atm).

2.3.1.1 Charge (filling) Phase

Charging is the process of pressurizing the ANG storage with natural gas for the purpose of storing it. Adsorption of natural gas on adsorbent packed inside the storage vessel will be accompanied by temperature rise as the heat of adsorption is released. Figure 2.12 shows adsorption isotherm of methane by activated carbon versus temperature. The adsorption isotherm shows amount of methane adsorbed at different temperature (0^o, 23^o, 45 ^{o}C). Amount of methane adsorbed at 45 ^{o}C is the

lowest. This means that adsorption capacity will reduce with temperature elevation. Charging of the natural gas into ANG storage can be achieved by several ways.

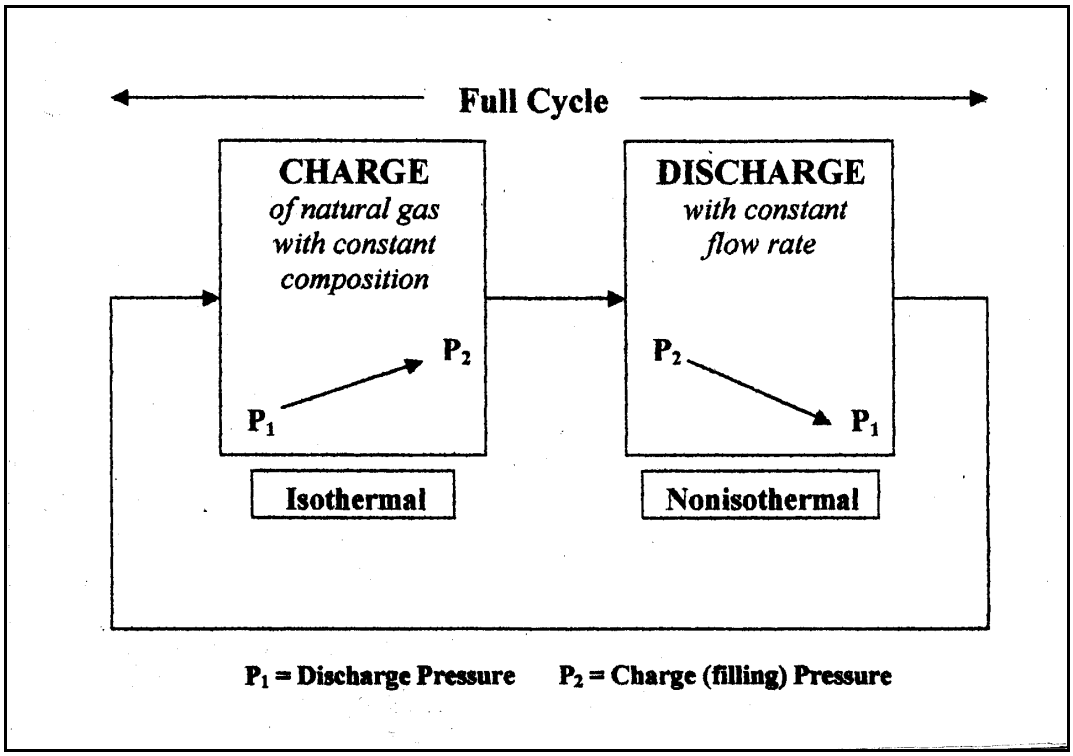

Figure 2.11: Simulation of ANG storage charge and discharge cycle (Mota, 1999)

Usually, filling method that can minimize adsorption heat will be preferred. This is because adsorption capacity of natural gas will decrease when heat of adsorption increase, causing less amount of gas to be stored (Chang and Talu, 1996). For fast filling at refueling station, the most economic way is by installing recycle loop. This loop is fixed outside the storage tank and it removes heat of adsorption by transferring the heat to the surroundings through a heat exchanger (Be Veir *et al.*, 1989; Jasionowski *et al.*, 1992). Another method that can be utilized is the refueling process done overnight so that the time is enough for heat of adsorption to dissipate (Parkyns and Quinn, 1995; Chang and Talu, 1996). However, the second method requires a long period of charging. Both methods increasing natural gas charging rate at isothermal condition. At this state, the pressure inside the container is assumed uniform.

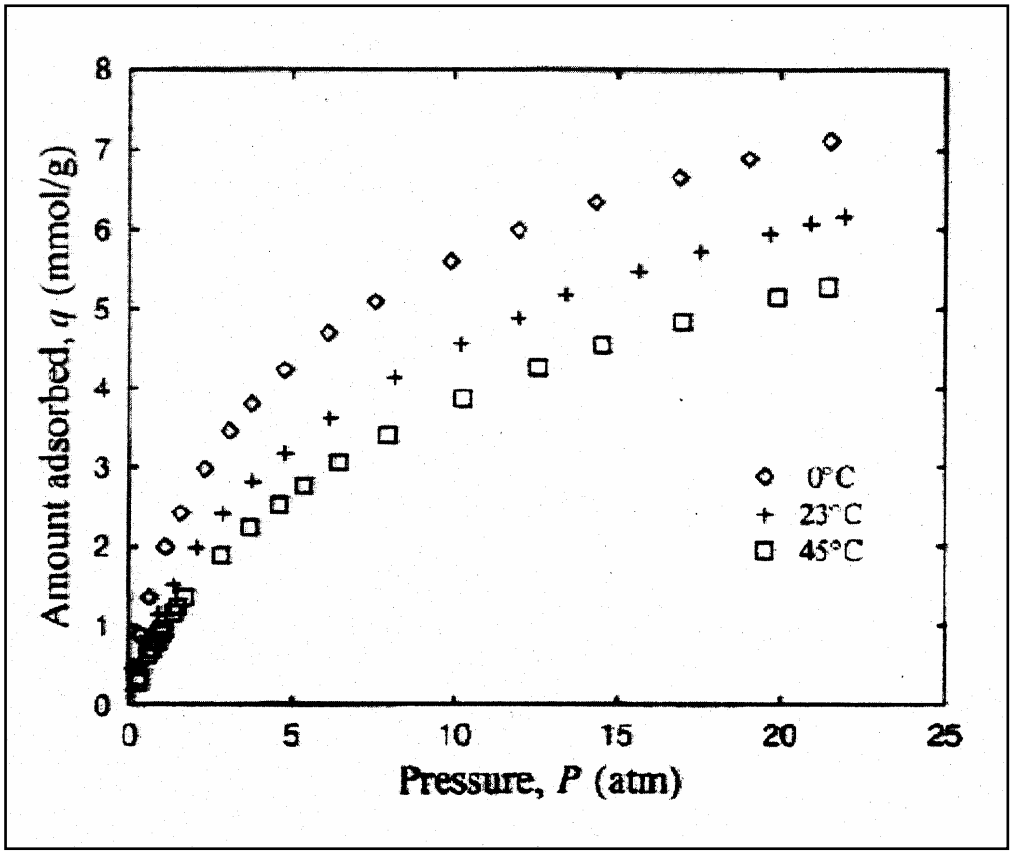

Figure 2.12: Methane adsorption isotherm on activated carbon (Chang and Talu, 1996)

2.3.1.2 Discharge Phase

Discharging of the natural gas from its storage container is actually a depressurization of natural gas unto depletion pressure, which is the minimum pressure to discharge the gas from the ANG container, normally at 14.7 psig under natural condition. For actual vehicular application of ANG storage system, discharge flow rate will be determined by the engine power demand. During this phase, some assumptions are made (Mota, 1999):

- Pressure inside container is uniform.
- Instantaneous equilibrium between compressed and adsorbed gas.
- Difference between particles is negligible.

- Temperature of gas and particles is uniform along cylinder (container).

From the literature, it was found out that the heat consumed for desorption is only partially replaced by the wall thermal capacity and by the heat transferred from the surrounding (Chang and Talu, 1996). Consequently, drastic temperature fall occurs inside the storage vessel as the heat of the system is used up for desorption process. This phenomenon is more dominants at the center part of the cylindrical container.

Theoretically, as the storage container is always being refueled with the same gas mixture (fixed composition), the storage system will approach a steady-state cycle after it operates for an extended period of time. At this state, charge capacity will be equal to the discharge capacity, i.e., the natural gas stored are fully deliverable for use during discharge (Mota, 1999). At steady-state cycle, amount of species *i* discharged is defined in Equation 2.5.

$$Q_i = z_i \, Q^{(\infty)} \tag{2.5}$$

where,

Q_i = amount of species *i* discharge

$Q^{(\infty)}$ = total amount of gas delivered at steady state

z_i = mole fraction of species *i* supplied

The discharge performance of the ANG storage system is determined from the *dynamic efficiency* of gas delivery. Dynamic efficiency is the ratio of the amount of gas discharged under dynamic (real) condition over that at isothermal condition as shown in Equation 2.6:

$$\text{Dynamic efficiency, } \eta = \frac{Q_i \text{ at dynamic condition}}{Q_i \text{ at isothermal condition}} \tag{2.6}$$

Several cycles are necessary before cyclic steady state is reached starting from the first cycle with an empty cylinder. The steady state condition is achieved when the

amount of gas discharged equal with the amount of gas charged to the container. There is a drastic reduction in the net delivery capacity of natural gas with cyclic operation. The leveling off of delivered capacity was observed when the cyclic testing was prolonged sufficiently (Parkyn and Quinn, 1995). The loss in the net deliverable capacity is 10% more when operates at non-isothermal condition (Mota, 1999).

When the discharge rate of the natural gas is held constant (constant molar flow rate), discharge duration (period) decreases with cycle number due to the reduction in the storage capacity causes by gradual filling of micropore volume with higher molecular weight hydrocarbon (Mota, 1999). Heavier species tends to remain adsorbed at depletion pressure during discharge phase. This impact of composition also occurs for other carbonaceous adsorbent and other mixture of natural gas composition.

2.3.2 ANG Storage Operation Principle

Gas storage by adsorption is carried out by using the micropores of the microporous adsorbent to enhance the density of the stored gas. The first thing to consider in performing this method is that if the introduction of the adsorbent is beneficial when compare with compressed gas. Figure 2.13 schematically shows this matter. The amount adsorbed increases with increasing storage pressure, and so does the amount stored by compression. If the storage pressure is higher than p_C, then compression is better than adsorption. However, at lower pressures, adsorption is better than compression and the introduction of adsorbent can markedly improve the capacity. It is in this pressure range that adsorbed gas has its advantage.

The second thing to consider is the capacity. If only the storage capacity is concerned, then the capacity is the amount adsorbed at a certain pressure converted to an appropriate unit. Figure 2.14 shows four storage capacities V_{S1}, V_{S2}, V_{S3} and V_{S4} at two different pressures, p_S and p_D and two temperatures T_L and T_H. However, in most cases such as vehicular applications, where the gas is adsorbed to storage and

then desorbed for use, the most relevant parameter is the delivered capacity that will determine the fuel supply and the energy produced.

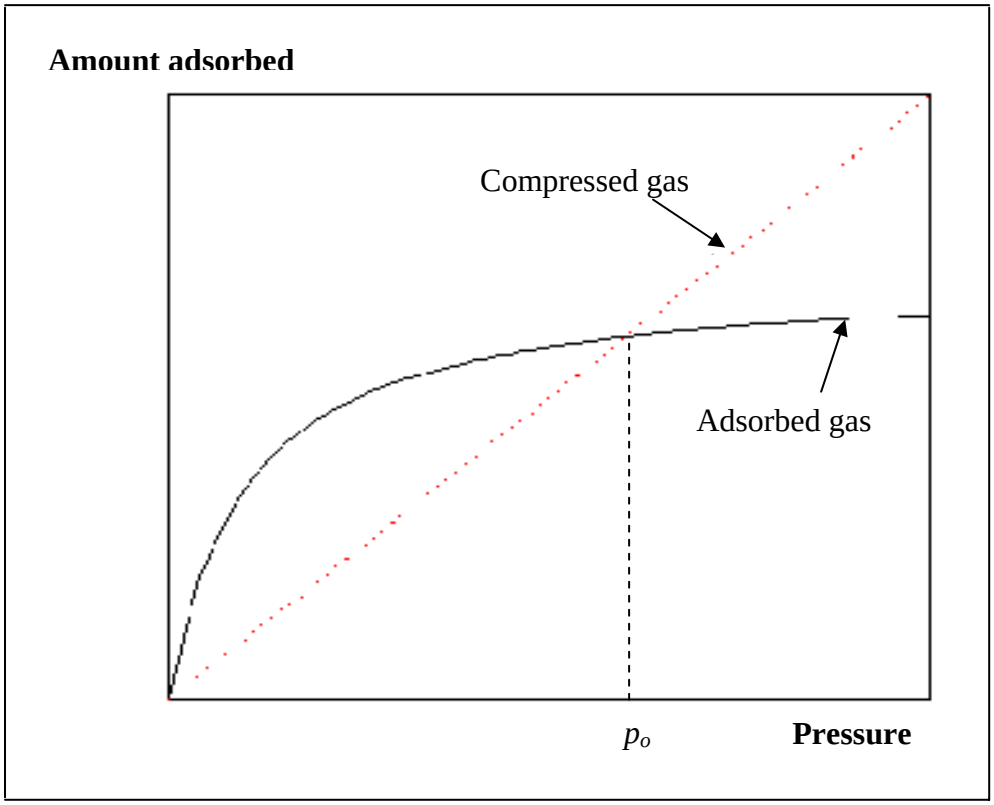

Figure 2.13: Methane adsorption storage versus compression storage (Cook and Horne, 1997)

Generally, if the storage capacity at the storage condition is V_S and is V_D at the delivery condition, then the delivered capacity is the difference between V_S and V_D as shown in Equation 2.7:

$$V_{DEL} = V_S - V_D \tag{2.7}$$

where,

V_{DEL} = delivered capacity

V_S = storage capacity at the storage condition

V_D = storage capacity at the delivery condition

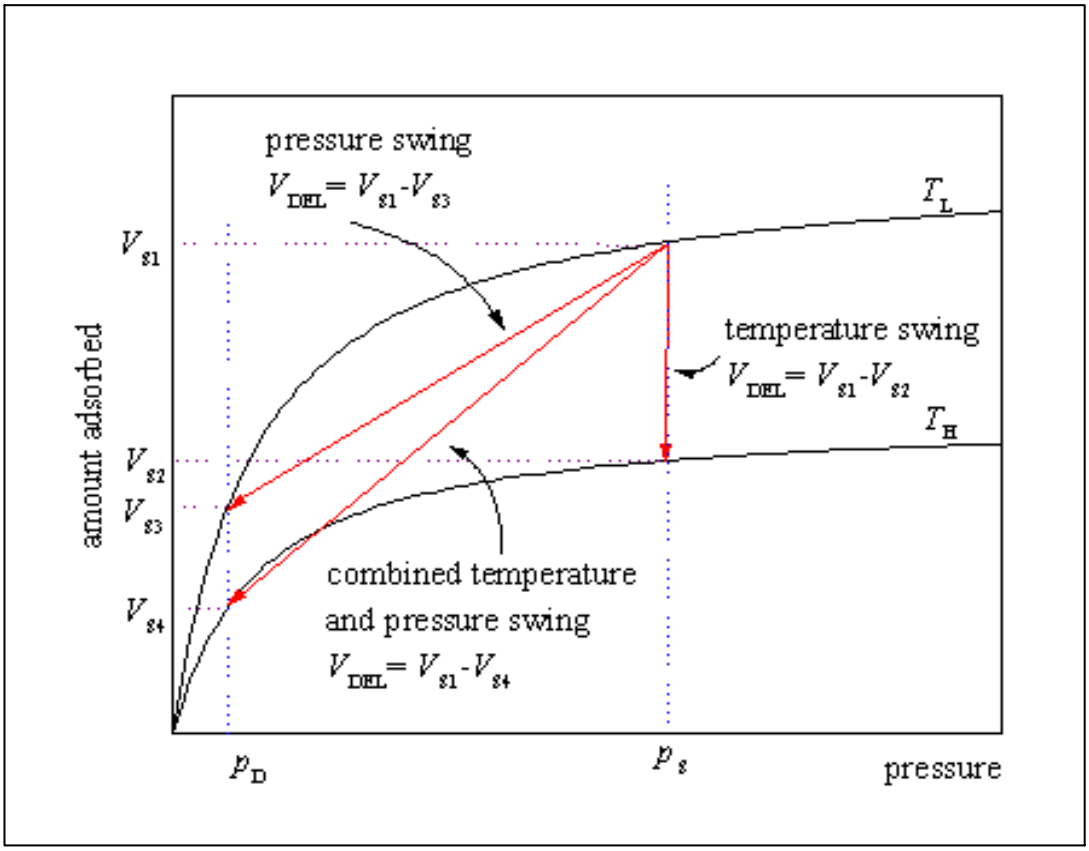

Figure 2.14: Different methods of methane desorption
(Cook and Horne, 1997)

Suppose that the gas is adsorbed in the adsorbent at temperature T_L and pressure p_S, then there are a few theoretical ways to deliver the adsorbed gas:

1. Pressure swing desorption. The system is kept at the temperature T_L, but the pressure is lowered to p_D to allow the delivery of the adsorbed gas. In this case, the delivered capacity will be the storage capacity at p_S minus the storage capacity at p_D, i.e.,
   $V_{DEL} = V_{S1} - V_{S3}$.

2. Temperature swing desorption. In this case, the pressure of the system is kept at p_S, but the system is heated to a higher temperature T_H to deliver the adsorbed gas. The delivered capacity now is $V_{DEL} = V_{S1} - V_{S2}$.

3. Combined temperature and pressure swing desorption. The pressure is lowered to p_D and the system is heated to a higher temperature T_H to deliver the adsorbed gas and the delivered capacity is $V_{DEL} = V_{S1}-V_{S4}$. The combined process gives the highest capacity. However, the second method is probably not practical in vehicular application while the combination method is yet to be reported in the research papers.

2.3.3 ANG Performance Indicator

The capability and performance of ANG storage is measured in two capacity indicators, which are the storage capacity and the delivery capacity. The storage capacity is a measure of the amount of gas that could be stored in the adsorbent-filled cylinder while the delivery capacity depicted the amount of gas that is deliverable from the storage during discharge. The amount of gas deliverable from the storage during discharge is always lesser than the amount storable due to the retention of some amount of gas which result from factors such as heat of desorption and natural gas composition.

2.3.3.1 Storage Capacity

On mass basis, ANG storage capacity can be expressed as molar storage capacity (Malbrunot *et al.*, 1996). The volume, V of a storage container filled with adsorbent is having the form of powder, pellet or granules. The adsorbent is normally packed and its *weight per unit volume of container* is called bulk density, ρ_b. When gas is introduced into V at pressure P, a part is adsorbed while other fills the whole accessible volume, V_d, which is the free volume (void space). V_d is the difference between V of the container and the volume V_s of the solid adsorbent. V_s is defined as mass of the adsorbent divided by the real density of the adsorbent (measured by using helium densitometer) shown in Equation 2.8.

$$V_s = m_s/\rho_s \tag{2.8}$$

where,

m_s = amount of adsorbent in V

ρ_s = real density of the adsorbent

Therefore, the amount of non-adsorbed gas inside the container is defined by Equation 2.9.

$$\rho_g V_d = \rho_g (V - m_s/\rho_s) \tag{2.9}$$

where,

ρ_g = molar gas density at P and T considered

The total amount of gas, M, contained in the volume V is the storage capacity of the container is shown in Equation 2.10.

$$M = m_s m_a + \rho_g (V - m_s/\rho_s) \tag{2.10}$$

where,

m_a = amount of gas adsorbed by adsorbent (mole/gram of adsorbent)

If the volume V is taken as a unity of volume, i.e., $V = 1$, the mass of solid adsorbent, m_s in the container becomes

$$m_s = \rho_b \text{ x } 1 = \rho_b \tag{2.11}$$

Then, M becomes a ‘specific storage capacity’, M_s which is the molar storage capacity per unit volume (mole/unit volume) of a container as shown in Equation 2.12.

$$M_s = \rho_b m_a + \rho_g (1 - \rho_b/\rho_s) \tag{2.12}$$

This definition reveals the importance of adsorbent compactness. The first term is the storage capacity of an adsorbent due to gas adsorption. The second term is the storage capacity due to gas compression.

There are two other capacities commonly used in discussion of gas storage. One is the volumetric capacity and the other is the gravimetric capacity (Cook and Horne, 1997). The volumetric capacity is defined as the amount of gas adsorbed either in mass or in volume divided by the total volume occupied by the adsorbent and the adsorbed gas, or in other words, the volume of the container. Because the gas is adsorbed in the solid, the volume of the adsorbent can be regarded as the total volume provided that the container is fully loaded with adsorbent. For ease of comparison, the volume of the adsorbed gas is commonly converted to the volume at a reference point. The standard reference point of temperature and pressure (STP) is 1 bar and 15° C (Smith, 1990). The volumetric storage capacity is defined by Equation 2.13.

$$V = \frac{volume\ of\ \ adsorbed\ \ gas\ converted\ to\ STP}{volume\ of\ \ solid\ \ adsorbent} \tag{2.13}$$

The volumetric capacity is more important in situations where space is limited, such as in a car. Similarly, the gravimetric capacities are often defined as the weight percentage of the adsorbed gas to the total weight of the system, including the weight of the gas as shown in Equation 2.14.

$$V = \frac{weight\ of\ \ adsorbed\ \ gas}{weight\ of\ \ solid\ \ adsorbent + weight\ of\ \ adsorbed\ \ gas} \tag{2.14}$$

The gravimetric capacity is more important in cases where weight of the system is the first priority. In some cases both capacities may need to achieve a certain target.

The natural gas storage target is 150 *V/V* at the following conditions: storage pressure 34 bar (500 psi), delivery pressure 1 bar (atmospheric pressure) and at 25 °C (Nelson, 1993). This volumetric capacity is equivalent to about 136 *V/V* at STP. This target was chosen because it was reasonable and reachable from detailed

experimental studies of methane storage in activated carbons and theoretical analysis. However, this capacity is still difficult to be reached by commercially available adsorbents at the stated storage and delivery conditions.

2.3.3.2 Delivery Capacity

The most commonly used indicator of the ANG storage delivery performance is volume ratio which is defined as *V/V* that is volume of gas discharge at ambient condition over volume of the storage container (Chang and Talu, 1996). This indicator is also known as V_m/V_s in which subscript m refers to methane delivered and subscript s refers to the storage container. The overall dynamic performance of ANG storage is measured by dynamic efficiency. Dynamic efficiency is the ratio of the amount of methane delivered under dynamic conditions over that at isothermal conditions as shown in Equation 2.15.

$$\eta = \frac{Dynamic\,V/V}{Isothermal\,V/V} \tag{2.15}$$

A value of unity of η (η = 1.0) is only achievable at an infinitely slow rate of discharge. The lowest value of η will be at adiabatic conditions.

2.3.4 ANG Performance Measurement

In studying the effect of the heat of adsorption on ANG storage system performance during discharge, Chang and Talu (1996) have carried out the performance tests under dynamic condition. Technical grade methane (99%) was used in the experiment instead of natural gas. The majority of tests were performed with the ANG test system shown in Figure 2.15. The apparatus consist of two main parts: (1) the control unit, and (2) the test cylinder. Charge/discharge rates and pressure were varied in the control unit, which also include a gas meter and

thermocouples display. The test cylinder is equipped with thermocouples distributed throughout its volume and thermocouple pads in the outside surface.

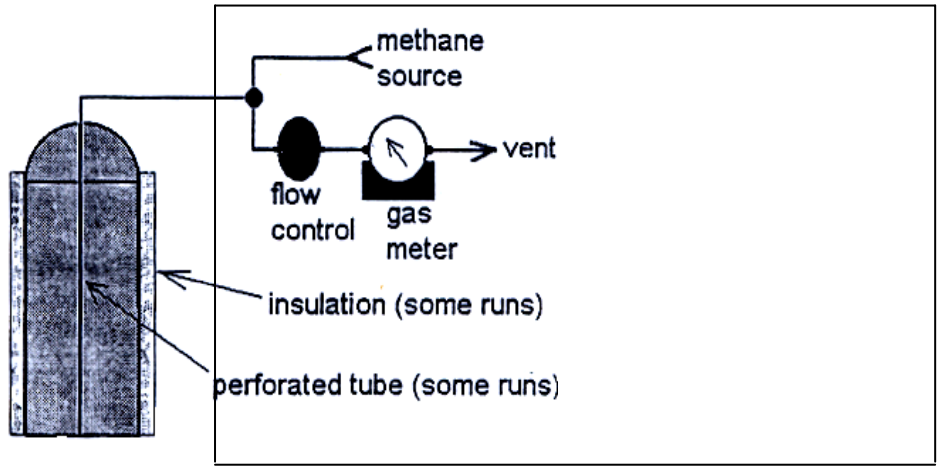

Figure 2.15: Schematic of dynamic ANG test system
(Chang and Talu, 1996)

"Real" cylinder was used in this work to prevent any bias in the dynamic response of the system. Commercial-size ANG cylinders were obtained from G-Tec Company. These were regular carbon-steel propane cylinders filled with an activated carbon adsorbent.

The main experimental variation was the discharge flow rate. It was varied between 1 and 15 l/min at ambient condition, 6-7 l/min corresponds to the demand rate per cylinder of a subcompact car with 4 cylinders travelling at cruising speed. Experimental procedure involved slow 'overnight' charge, where the cylinder was brought to 21 bar of methane pressure and until uniform ambient temperature is achieved. A fixed, controlled rate of discharge followed. The experiments were stopped when the pressure dropped below 1.66 bar when the cylinder was 'depleted'. The experiment stopped at this pressure since it is not possible to control the discharge at lower pressure. A pressure differential of 0.66 bar above the atmospheric pressure also seems to be reasonable during the operation of a vehicle to force the flow of natural gas from the storage cylinder to the engine. A substantial amount of residual methane remains in the cylinder at depletion. The pressure, the

amount of gas output and all thermocouple readings were recorded as function of time during discharge. Experiment lasted from 60 to 1200 minutes (20 hours).

After the discharge cycle, the cylinder was closed and left to warm-up to ambient temperature. A final pressure was recorded when the temperature was uniform, which provided a check of experimental accuracy by the overall material balance. The difference between the amount of methane in the cylinder after warm-up and the initial amount at charge condition should equal to the total gas output measured during the discharge cycle. The amount was calculated by the isotherm relation and the known packing density.

The performance result of this experiment which employing a moderate quality of commercial activated carbon is about 60 *V/V* for the isothermal run. The highest measured efficiency of methane delivery is 0.95 at 1.04 l/min of discharge rate with the lowest temperature drop of 5.7 ^{o}C while the lowest efficiency is 0.75 at 15.01 l/min with the highest temperature drop 25.7 ^{o}C. The capacity loss is due to the effect of heat of desorption which causes cooling during desorption.

Elliott and Topaloglu (1986) have performed a test on materials that intended to be used as adsorbent for ANG storage packed into 1-liter capacity pressurized vessel. The adsorbent-filled container was charged with commercial grade methane (99%) followed by discharging phase for several cycles. Amount of gas stored and delivered were determined. The parameters recorded during the testing are charge and discharge time, test pressure, volume of gas stored and volume of gas delivered from the storage. The adsorbent undergoing the charge/discharge cycle with methane at pressure between 14.7 psig (atmospheric pressure, which is the initial vessel pressure) until 300-500 psig (target storage pressure). The performance test is done by analysis upon the adsorbent packing density, adsorbent composition, volume of gas storable inside the container, which comprises of the amount adsorbed in the adsorbent and amount stored the free-space inside the container. The amount of gas stored/delivered was measured based on its mass per volume of container (g/l) and on its volume at STP per volume of container (l/l). Analysis was also done on the ratio of the amount of deliverable gas from storage towards the amount of gas charged in to see the delivery capability of the adsorbents.

The results of the storage capacities and delivery performance of these adsorbent materials are shown in Table 2.6 and Table 2.7. Table 2.6 shows the adsorption parameters and the storage capacities of three types of adsorbents tested after charging with methane at 500 psig. The storage capacities of the adsorbent-filled vessel are measured in both gravimetric (g/l) and volumetric (l/l) units. Table 2.7 shows the charge/discharge period and the delivery capacity of the three adsorbents after charge/discharge cycle between atmospheric pressure and 300 or 500 psig. The storage capacity is compared with delivery capacity in term of delivery to capacity ratio.

Table 2.6: Methane stored with different adsorbents (Elliott and Topaloglu, 1986)

ADSORBENT	BPL	AX-21	PVDC Carbon
Packing Density (kg/l)	0.51	0.30	0.93
Volume			
❑ Carbon	23.20	13.60	42.30
❑ Micropore	17.30	16.40	35.20
❑ Macropore	23.30	36.70	15.50
❑ Void	36.20	33.30	7.00
Methane Stored at 500 psi (g/l)			
❑ Adsorbed	35.70	47.40	90.20
❑ Voids and free space	14.60	17.20	5.50
Total Mass	50.30	64.60	95.70
Total Volume	75.90	97.50	144.40

Table 2.7: Cycling test results with pure methane (Elliott and Topaloglu, 1986)

ADSORBENT	BPL	AX-21	PVDC Carbon
Cycles	12	20	20
Fill Time (min)	15	15	15
Empty Time (min)	105	105	105
Pressure (psi)	300	300	500
(a) Methane Contained in vessel (g/l)	45.6	43.0	92.2
(b) Methane Delivered (g/l)	32.4	38.1	68.0
Ratio b/a	0.71	0.87	0.74

Remick and Tiller (1985) had conducted experiments at Institute of Gas Technology (IGT) to assess the magnitude of the impact of the heat of adsorption on storage capacity. A carbon was chosen for this work which had a total storage capacity of about 100 volumes per volume of methane at 3.44 MPa (500 psi) and a delivered capacity of about 80 volumes per volume of methane in cycling from 3.44 MPa to atmospheric pressure, which was previously tested. This carbon was obtained from North American Inc. of Columbus, Ohio, and was designated G216. The methane adsorption isotherms were performed for this carbon at both 25 ^{o}C and 90 ^{o}C for pressure from vacuum to 3.44 MPa (500 psi).

A one-liter stainless steel cylinder having an external diameter of 8.9 cm and a wall thickness of 0.53 cm was filled with 410 grams of activated carbon. A fine wire thermocouple was then positioned in the center of the bed while a second thermocouple was mounted on the external surface area of the cylinder. The cylinder was evacuated from all gases using a two-stage vacuum pump. Then it was charged with methane from a manifold maintained at 3.44 MPa (500 psia). The cylinder remained attached to the manifold until thermal equilibrium with the surroundings was achieved. Once achieved, at about 25 ^{o}C, the cylinder was disconnected from the manifold and connected to a low-pressure regulator and a wet test meter. The contents of the cylinder were then exhausted and bled off through the wet test meter. The temperatures of the carbon bed and of the cylinder wall were closely recorded. The cylinder was allowed to remain attached to the wet test meter until the internal (carbon bed) rose to ambient temperature before which it was fall some degrees below. The volume of gas exhausted from the cylinder was determined after corrections were made for methane in the connecting tubes.

The main experimental variations were the charge and discharge flow rate. The cylinder was charge in slow and rapid filling rates. The same modes were carried out for discharging phase. For slow fill, the cylinder was slowly opened to the methane pressure manifold whereas for quick fill, the cylinder was steadily opened to the pressure manifold and filled rapidly for only 5 minutes and then isolated. For slow discharge, methane contained in the cylinder was slowly decompressed out through the regulating valve and slowly bled through the wet test meter to be

measured. On the other hand, for fast discharge, the valve of the cylinder was fully opened and the methane rapidly exhausted through the meter.

For slow charge and discharge rate, the delivery capacity of the adsorbent-filled vessel is 75 liters and this represents 75 volumes per volume of container. This is the maximum delivered capacity that could be achieved with this carbon under these experimental conditions. The temperature drop of 20 ^{o}C occurs for this run. For a fast charge run, the temperature within the carbon bed inside the vessel rose rapidly within few minutes and reaching a peak of 107 ^{o}C. When the storage is discharge slowly, 56.7 liters of methane were exhausted from the cylinder. This lower value of discharge is due to the sensitivity of the adsorption isotherm to temperature. Finally, for the fast discharge depressurization, after a slow filling process, as the gas was exhausted rapidly from the cylinder, the temperature fell by more than 60 degrees in about 120 seconds. However, the volume of gas delivered is 66.0 liters within 60 seconds, which is 88% of the deliverable capacity under slow discharge despite the fact that the bed temperature fell to near -40 ^{o}C.

The experiment described above were conducted under condition simulating both a slow fill, where carbon bed temperature would have time to cool down to ambient condition, and a fast fill where the carbon bed temperature rise rapidly. It was determined that rapid filling of an adsorption storage at ambient condition results in only 75% of the storage capacity that can be achieved by a slow fill rate. These quantitative results are specific for the carbon used here but however, the general pattern should hold true.

2.4. Problems in ANG Storage Operation

Some operating problems have been identified in ANG storage technology as addressed in the literature. There are three main problems that could deteriorate the ANG storage and delivery capacity which are the presence of heavier hydrocarbon compounds in the natural gas composition, the effect of heat of adsorption and the consequence of the adsorption isotherm shape during gas uptake and delivery.

2.4.1 Natural Gas Composition

The adsorptive capacity of an adsorbent will decrease when ANG storage operates for an extended period of time. This is due to the nature of natural gas composition. Apart from methane, natural gas also contains ethane, nitrogen and minor amount of alkanes from $C_3 - C_7$. In addition, carbon dioxide might exist in a small amount (0.04 to 1.00 molar %), as well as water vapor (75-180 ppm) and sulfur-containing compound at the ppm level (Parkyns and Quinn, 1995).

These heavy hydrocarbon species, with heavier molecular weight, are actually adsorbed stronger compared to methane, especially at low pressure. This behavior is shown in Figure 2.16. This figure shows the adsorption isotherm for each hydrocarbon in the natural gas at 25 ^{o}C on activated carbon. These hydrocarbons are methane, ethane, propane, butane and pentane. It can be seen that methane is the least adsorbed species while pentane is the most adsorbed one by an activated carbon. This shows that heavier hydrocarbon is easier to be adsorbed than the lighter hydrocarbon.

When heavier hydrocarbons enter the storage system during refilling, the container will be filled with heavier species than methane. They adsorbed preferentially and decrease the amount of gas that can actually be delivered by the storage system because methane, which has the highest volume percent, is least adsorbed. During discharge cycle, these heavy hydrocarbons are not preferentially desorbed and will always tend to accumulate in the storage container during the charge and discharge cycle operation (Sejnoha *et al.*, 1994).

However, the presence of these heavy hydrocarbons in the natural gas composition is not necessarily critical to the ANG storage system. According to Talu (1993), introducing an additive into the natural gas stream can increase amount of storage capacity. Additive is added to the natural gas stream during refilling of gas into the storage. Storage capacity will increase when additive causes the amount of gas adsorbed or stored at outlet pressure is more than during refilling at charge pressure.

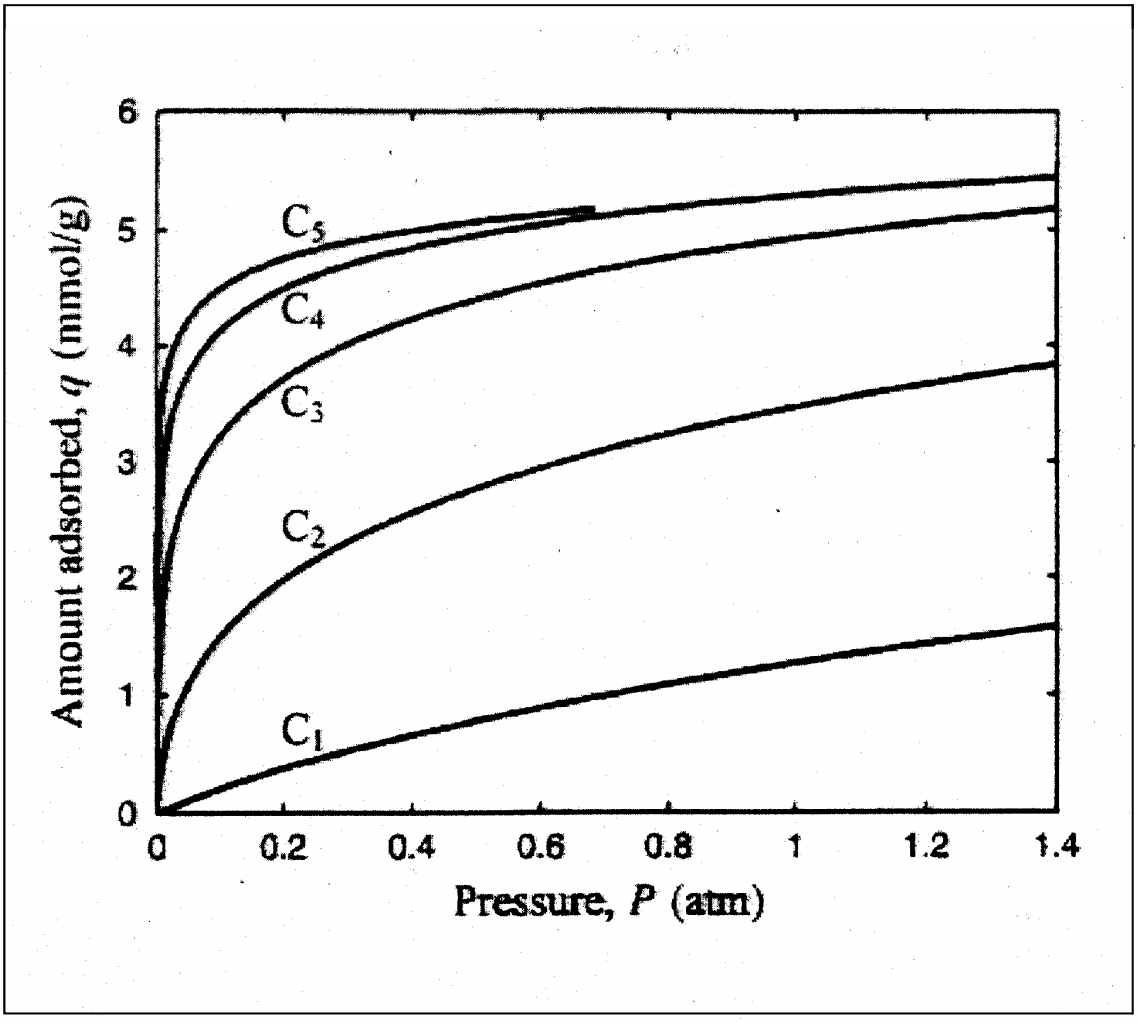

Figure 2.16: Adsorption isotherm for every hydrocarbon component by an activated carbon at 25 ^{o}C (Mota, 1999)

Apart from the concept introduced by Talu, there are also studies being made to determine economic method to reduce the heavy hydrocarbon species from entering the ANG storage system. An effective method to overcome this problem is by installing filtering unit at the refueling station (Sejnoha *et al.*, 1994) or installed at the front part of the storage where the natural gas goes in and out (Cook *et al.*, 1999). Therefore, based on these facts, this is not a critical problem for mobile ANG application because it can be solved.

2.4.2. Heat of Adsorption

Adsorption is an exothermic process. Any finite rate of adsorption or desorption is accompanied by temperature changes in an ANG storage system. The heat of adsorption has a detrimental effect on performance during both charge and discharge cycles. However, although the temperature increase during the charge cycle is important, it is not considered critical for mobile ANG applications due to two reasons: (1) the charge cycle will be normally performed in a fuel-station where the necessary hardware can be built to remove the released heat of adsorption if a "fast" charge is necessary; and (2) the highest perceived potential for mobile ANG is for fleet vehicles to be charged at central site over a long period of time (i.e., overnight) which provide enough time for "slow" charge to dissipate the heat of adsorption to the surroundings (Chang and Talu, 1996).

Contrary to the charge cycle, the rate of discharge is dictated by the energy demand of the application. Discharge time cannot be widely varied to moderate the impact of cooling during the use of ANG cylinders. It is also not feasible to include excessive hardware to moderate the temperature drop in a mobile application. Study on impact of the heat of adsorption during ANG discharge, play a crucial role in determining the feasibility of mobile applications.

As natural gas is discharge from an ANG system, the vessel cools down due to the heat of desorption. As a result, a larger amount of gas is retained in the system at the depletion pressure compared to the isothermal operation, as shown in Figure 2.17. At any finite rate of discharge, the amount of gas delivered under dynamic condition is always lower than isothermal operation. According to Chang and Talu (1996), the loss in dynamic efficiency of the ANG storage performance at dynamic condition is corresponding to 25% loss of the capacity that could be achieved for isothermal operation due to cooling during desorption.

Figure 2.18 and 2.19 show the axial and radial temperature profile of the ANG storage vessel during discharge. Figure 2.18 illustrates the axial temperature data at the centerline of the cylinder at which the largest temperature drop occurs. Obviously, the temperature variation is not so evident in the axial direction.

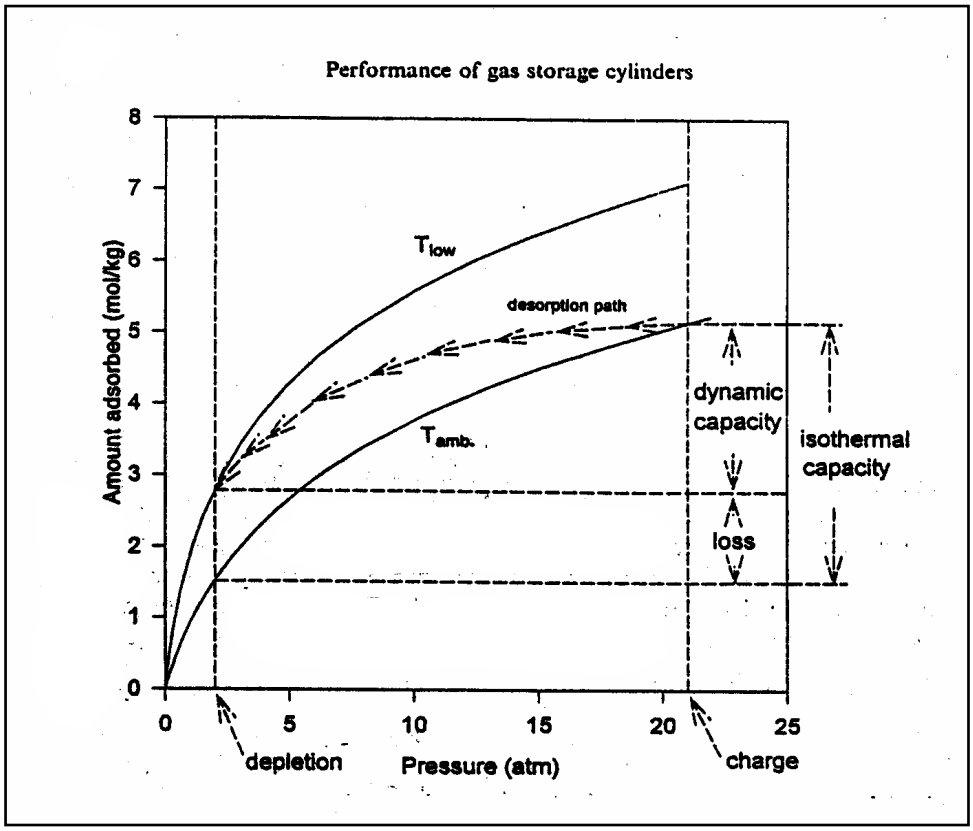

Figure 2.17: Illustration of the impact of heat of adsorption on capacity during discharge (Chang and Talu, 1996)

Figure 2.19 which illustrates the radial temperature distribution with time, is an evident illustration of the impact of heat of adsorption on ANG discharge. A drastic temperature fall occurs inside the storage vessel in radial direction. From the figure, it can be seen that this phenomenon is more dominant at the center part of the cylinder. This temperature fall happens because the heat of the system is used for desorption process. The result of large temperature drop is a higher of methane retained in the cylinder at depletion. Figure 2.20 shows the profiles of residual methane left in the cylinder at depletion as a percentage of the amount at charge conditions. The shapes of the profiles are reversibly related to the temperature gradient across the cylinder radius shown in Figure 2.19. The retention of methane is higher at the center of the cylinder in which lower temperature field occurs.

Using extensive experimental data collected with real ANG cylinders and a fairly simple model, Chang and Talu have demonstrated that it is not possible to operate an ANG system under isothermal conditions. Any finite discharging rate will

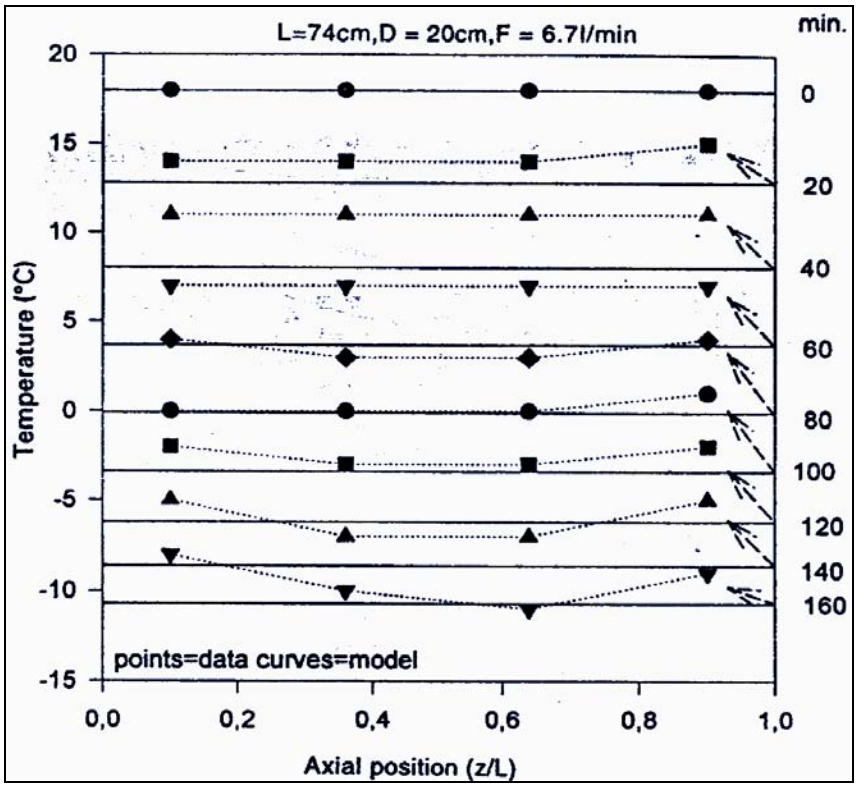

Figure 2.18: Axial temperature profile at the center of an ANG cylinder during discharge (Chang and Talu, 1996)

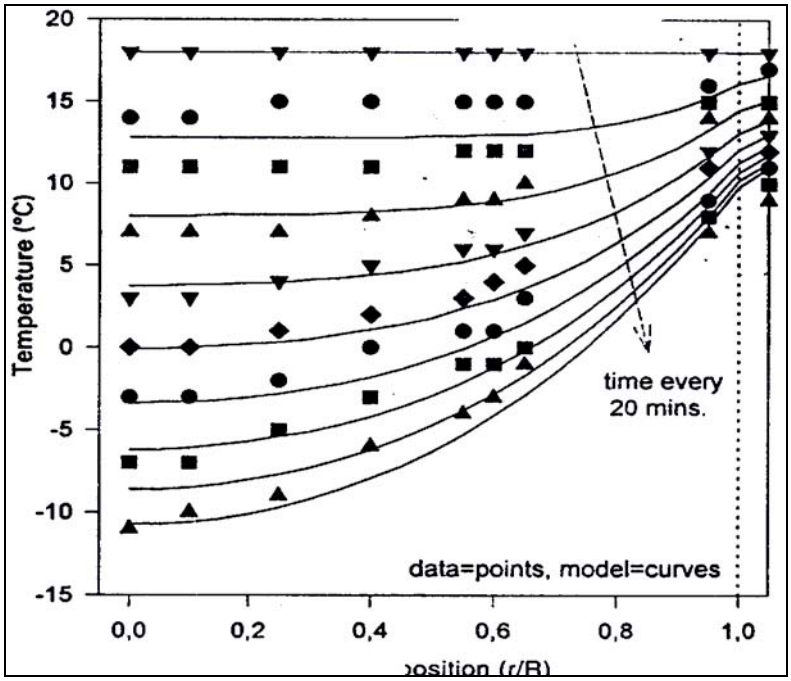

Figure 2.19: Radial temperature profile in an ANG cylinder during discharge (Chang and Talu, 1996)

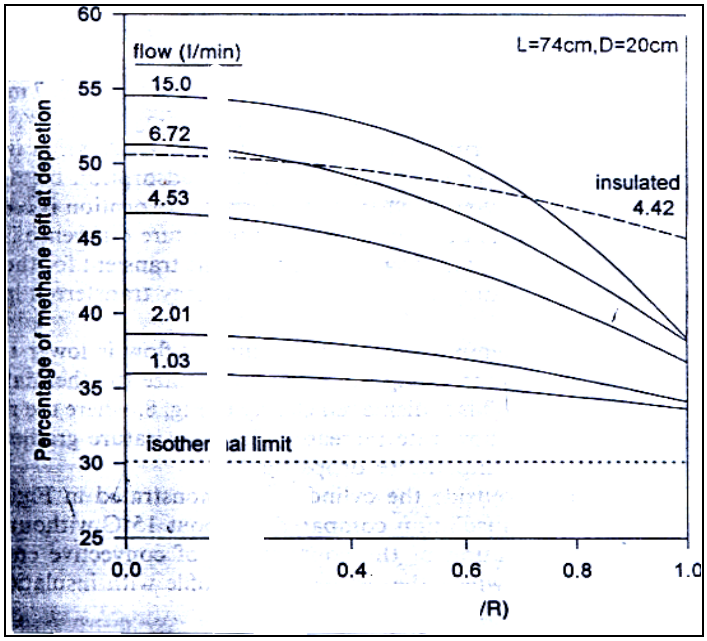

Figure 2.20: Radial profile of residual amount of methane left in ANG cylinder at depletion (Chang and Talu, 1996)

result in temperature drop. At the smallest controllable discharge rate, the observed temperature drop is about 5 ^{o}C, resulting in an 8% loss of capacity. The temperature drop can be very substantial and it is greater at the higher demand rate of discharge. Under realistic conditions of a vehicle application, the dynamic loss is expected to be 15-20%.

At the other extreme, the ANG discharge is not an adiabatic operation. The thermal capacity of the cylinder wall is an important energy source and external convective heat transfer can supply significant amount of energy. The main obstacle in utilizing these energy sources is the poor thermal conductivity of packed carbon adsorbent. Chang and Talu have introduced a simple yet effective remedy to increase energy transfer to the central region of ANG cylinder. This was accomplished by a perforated tube inserted at the centerline, which acts as a collector for the exiting gas. Unlike other suggested remedies to moderate the impact of the heat of adsorption, the tube insert does not significantly reduce precious storage space, it is easy and inexpensive to implement, and it moderates the temperature drop under any ambient condition. The dynamic loss is reduced from 22 to 12% with the tube insert at the most pertinent flow condition. This represents a 40% reduction in loss.

2.4.3 Isotherm Shape

The relationship at ambient temperature between the amount of natural gas uptake on adsorbent and pressure prevents the system from responding linearly to pressure. This situation is represented by characteristic isotherm as shown in Figure 2.21. This figure shows that at relatively low pressures there is initially a rapid increase in the adsorption of natural gas. The isotherm begins to level off between 3 and 4 MPa, beyond which there would be only a gradual increase in storage capacity due partly to further adsorption and to compression of the gas itself.

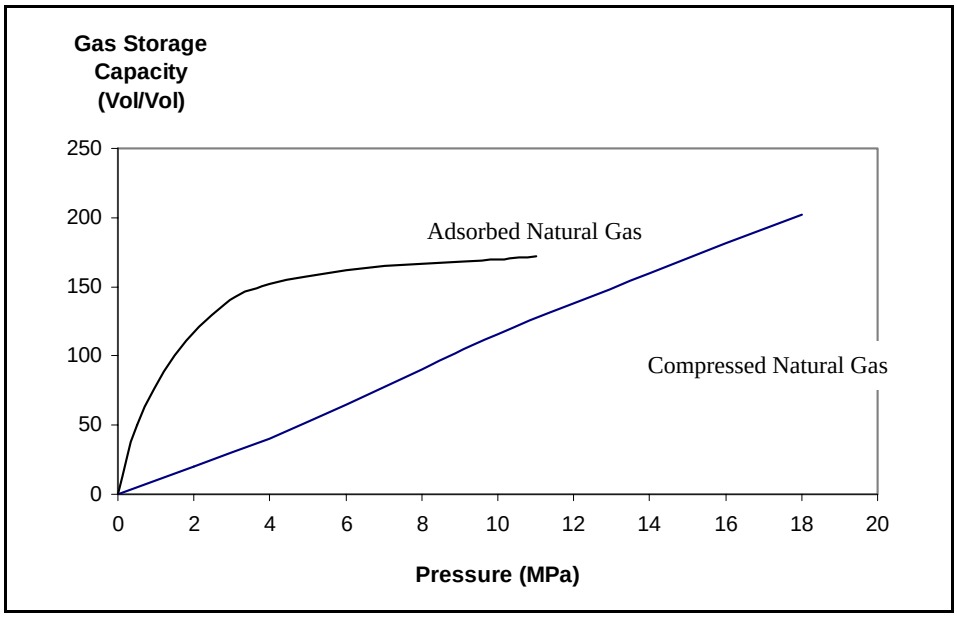

Figure 2.21: Characteristic of natural gas adsorption isotherm and compression storage (Komodromos *et al.*, 1992)

It is clear that at low pressure, the adsorbed system shows a substantial enhancement of gas storage over CNG. Since for ANG, most of the gas storage occurs below 3.5 MPa, this pressure defines the practical operating pressure, at which point the storage is equivalent to a CNG system at 13-14 MPa (Mota *et al.*, 1995 and Komodromos *et al.*, 1992). For a compression storage system, removal of the first 10% of the fuel results in about the same pressure drops as removal of the last 10%. However, this is not the case with adsorption system where the greatest pressure drop occurs with the removal of the first 10% of the fuel and where as much as 15-18% of the fuel still remains in storage at atmospheric pressure (Remick and

Tiller, 1985). This situation related to the phenomena of adsorption itself, so no suggestions can be proposed at this point. Only a small modification is expected for the limits of the system that can be established, and this will absolutely refers for only a specific adsorbents.

Subsequently, the consequence of the isotherm shape and the unfeasibility of lowering the discharge pressure below atmospheric pressure cause loss in gas delivery capacity during discharge due to the residual amount of gas left at depletion. This amount can be as high as 30% of the amount stored at charge conditions. Also, this residual percentage can increase due to the temperature drop in the storage at depletion (Mota *et al.*, 1997). However, an effective thermal management of the process can decrease the residual amount left at depletion.

2.5 Summary

Adsorbent that is useful to adsorb the natural gas in ANG storage is a substance that having a molecular structure that will allow smaller molecules to penetrate its surface area and be kept inside the pores between its molecules, in which pore filling adsorption mechanism takes place. The pore sizes in the adsorbent solid must be of a suitable size to admit, hold, and discharge individual gas molecules. Base on previous study, adsorbent material made of carbon has been found out to be the best to store natural gas molecules compared to the other materials. Nevertheless, some other types of adsorbents such as zeolites and silica gel are predictably potential for natural gas adsorption due to the availability of the microporous channels within their structure. ANG storage operation is modeled as series of consecutive cycles where charging of gas with a fixed composition and discharging of gas at constant molar flow rate back to the original storage pressure is done repeatedly. ANG storage performances are measured according to its storage capacity and delivery capacity. The performance measure must be carried out at dynamic-atmospheric condition in order to identify the practical reliability of this storage. According to the literature studies, there are three main implementation problems of ANG storage, which are the impact of natural gas heavier hydrocarbon

components, the effect of heat of adsorption and the isotherm shape of natural gas adsorption. All factors reduce the delivery amount of natural gas from the storage during discharge.

CHAPTER III

MATERIALS AND METHODS

The adsorptive storage test is carried out using 0.5 liter adsorbent-filled pressurized vessel. The different type of adsorbents tested is packed into the vessel at different packing densities depending on their individual density. The whole ANG storage-testing rig is consists of the ANG vessel and the measuring and controlling unit. The ANG test is divided into two parts which are isothermal adsorption and dynamic adsorption/desorption. In isothermal adsorption, the ANG vessel is charged with methane up to few level of storage pressure until reaching 500 psig. At each pressure level, the ANG storage is isolated to achieve thermal equilibrium with surroundings. For dynamic adsorption, the system is continuously charged with methane until 500 psig at varied flow rates. The ANG system is then discharge right after thermal equilibrium is achieved at varied flow rates to release the stored gas.

3.1 Materials

The materials used in this study are comprises of different type of commercial grade adsorbents among which are Darco® activated carbon (termed as Darco AC), palm shell-derived activated carbon (termed as palm shell AC), 13X molecular sieve zeolites (termed as MS zeolites) and silica gel with different particle sizes, and commercial grade methane gas with 99.5% purity. The usage of virtually pure methane in this study instead of the actual natural gas is because the natural gas

is multi-compositional which consisted of dominantly methane, small portions of ethane and other heavier hydrocarbon compounds from C_4-C_7. These heavier-than-methane hydrocarbons can decrease amount of gas deliverable from ANG storage as discussed in Chapter II, page 52 and eventually reducing ANG delivery efficiency unless a filtering unit is installed to prevent these compounds from entering the ANG storage as suggested by Sejnoha *et al.* (1994) and Cook *et al.* (1999). Unfortunately, this unit is not available in this work. Therefore, to prevent further inefficiency of gas delivery besides the unavoidable thermal problem as discussed previously, commercial grade methane is used in the place of natural gas since it is its principle component. In addition, compressed air is also used for system test. The surface (physical) and thermal properties of the adsorbents are listed in Table 3.1 and Table 3.2 respectively. The surface properties of the adsorbents are obtained through volumetric adsorption analysis using Micromeritics ASAP 2010 apparatus. The summary report of the adsorbents surface analysis is shown in Appendix A. The composition and the thermal properties of the commercial grade methane are listed in Table 3.3 and Table 3.4 respectively.

Table 3.1: Surface properties of adsorbent materials used in ANG testing

Adsorbent	Particle Size (MESH)	Average Pore Diameter (Å)	Micropore Volume (cm^3/g)	BET Surface Area (m^2/g)
Darco® AC (granular)	20-40	49.75	0.131	651.69
Palm Shell AC (granular)	99	19.80	0.214	1012.39
13X MS Zeolites (powder)	100	19.78	0.149	435.90
13X MS Zeolites (beads)	4-8	26.14	0.135	407.99
Silica Gel (powder)	70-230	62.17	0.097	500.00

Table 3.2: Adsorbents thermal properties (Menon, 1997)

Adsorbent	Heat Capacity (J/g. K)	Heat of Methane Adsorption (Kcal/mol)
Darco® AC	0.70	4.00
Palm Shell AC	0.70	4.00
13X MS Zeolites	1.95	3.90
Silica Gel	2.2	3.28

Table 3.3: Composition of methane used in ANG testing (Meser Gas Company)

Composition	Volumetric Fraction
Methane (CH_4)	99.5 %
Oxygen (O_2)	100 ppm
Nitrogen (N_2)	600 ppm
Hydrogen (H_2)	2000 ppm
Non-methane Hydrocarbon (NMHC)	1500 ppm

Table 3.4: Properties of methane (Friend, 1989)

Flammable Range in Air	5-15% of mole fraction
Ignition Temperature	538 ^oC
Specific Gravity	0.55
Vapor Density at 1 atm	1.342 g/L
Heat Capacity, C_p at STP (0 ^oC, 1 atm)	2.134 J/g. K
Thermal Conductivity, λ at STP	0.0306 W/m ^oC
Standard Enthalpy, ΔH_o	803 kJ/mol
Upper Calorific Value	55.67 MJ/kg
Lower Calorific Value	50.17 MJ/kg
Critical Pressure, P_c	671.5 psi
Critical Temperature, T_c	-82.6 ^oC

3.2. Experimental Set-up

The experimental set-up in this work is consisted of the ANG storage vessel used to perform the adsorptive storage, the measuring and controlling equipment, the configuration of ANG system and the gravimetric data of the adsorbents loaded into the ANG vessel. These headings describe the designation of the adsorptive storage experiment.

3.2.1 Lab-scale ANG Test Vessel

The ANG vessel used to conduct ANG adsorption test is a 500-cm^3 lab-scale stainless steel pressurized gas cell as shown schematically Figure 3.1. This

pressurized cell is specially made for this purpose. It is manufactured from stainless steel type 316 L. The top cover of the cell is a flanged type cap to withstand high pressure and is airtight. It will be opened and closed when replacing the adsorbent. The specification of the test vessel is tabulated in Table 3.5.

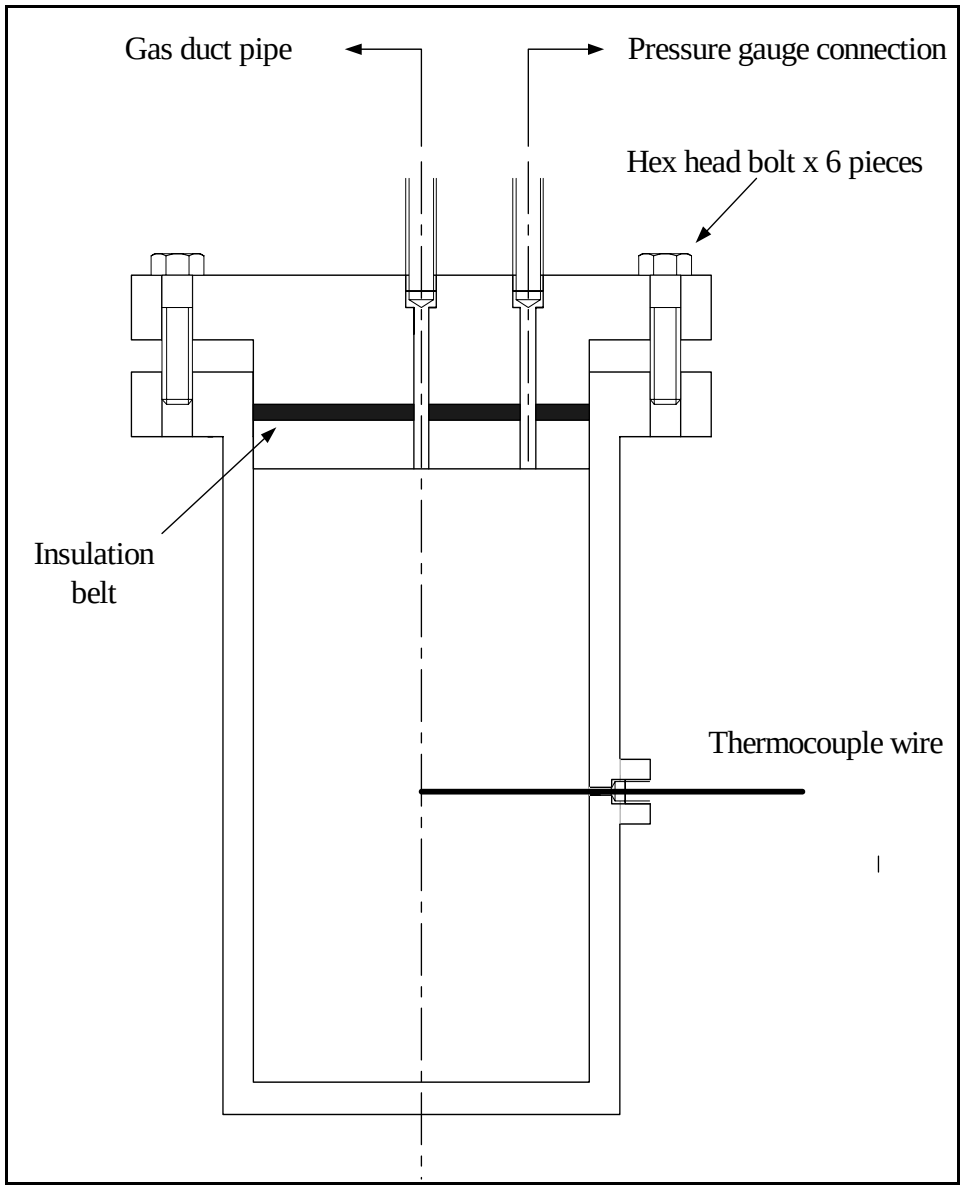

Figure 3.1: Schematic diagram of ANG pressurized gas vessel

Table 3.5: ANG vessel specification

TYPE	Natural Gas Pressurized Vessel	
MATERIAL OF CONSRUCTION	Stainless Steel Type 316 L	
DESIGN CODE	ASME Section VIII	
DESIGN PRESSURE	Up to 600 psig	
DESIGN TEMPERATURE	Up to 100 ^{o}C	
WATER CAPACITY (VOLUME)	500 cm^3 0.5 liter	
DIMENSION	**INTERNAL HEIGHT**	13 cm
	INTERNAL DIAMETER	7 cm
	WALL THICKNESS	0.4 cm
PRODUCT STORAGE	Methane/Natural Gas	

The ANG cell is installed with a pressure gauge and a temperature probe and is connected to methane supply using 1/4 inch stainless steel tubing. The temperature probe is installed at the center of the adsorbent bed within the cell in order to get the storage temperature reading. Temperature probe is not installed in other locations within the vessel internal perimeter such as along the axial direction or along the radial direction from the center to the vessel wall because the size of this ANG cell is sufficiently small that the axial and the radial temperature gradients are insignificant. These assumptions are made based on the work carried out by Chang and Talu (1996) in which they performed ANG storage performance test using a cylinder with length of 74 cm and 10 cm radius. According to their results, the highest temperature variation along the 74 cm axial direction is only 3 ^{o}C and they concluded that it is insignificant. Therefore, since length of the ANG vessel used in this study is only 13 cm (about 82% shorter), then the axial temperature gradient should be much smaller and much more insignificant. On the other hand, from their results, it is observed that in the radial direction of 10 cm distance, the temperature gradient only significantly occurred beyond 4 cm of the cylinder radius after 100 minutes of discharge (about 1 ^{o}C at 4 cm radius). Since radius of the vessel used in this study is only 3.5 cm while the longest discharging time taken for this ANG system to reach depletion pressure is well below 100 minutes, it can be safely assumed that the radial temperature

variation is negligible. Therefore, the central temperature point is considered to be sufficient to represent the overall ANG temperature reading.

3.2.2 Measuring and Controlling Equipment

The measuring devices used for this ANG storage testing are temperature probes (–60^{o} to 100 ^{o}C), pressure gauges (0 to 600 psig, 0 to 8 psig), wet test meter (0 to 1000 liter), natural gas flow meters (0 to 10 l/min, 0 to 18 l/min) and electronic balance (0.00 to 6200.00 g). The controlling equipment used are plug valves, needle valves, 3-way valve, multi-stage gas cylinder pressure regulator (500 to 3000 psig), and two-stage on-line pressure regulator (14.7 to 6000 psig). In addition, a vacuum pump is also needed in this experiment to evacuate the ANG cell before any gas charging is performed. The list and function of all equipment are summarized in Table 3.6.

3.2.3 Experimental Rig

The configuration of the ANG storage-testing rig is shown in Figure 3.2 and illustrated schematically in Figure 3.3. It consists of the ANG test cell and the controlling unit. The adsorbent-filled cell is attached with a pressure gauge, temperature probe, and connected to methane supply and controlling section using 1/4 inches stainless steel tubing. Needle valve and plug valve is installed at the inlet and outlet of the cell to allow or stop gas flow in and out of the cell. The ANG cell is placed on the electronic balance so that the weight of gas uptake can be measured continuously. The controlling and measuring unit is consists of multi-stage cylinder regulator, charge flow meter, 3-way valve, 2-stage on-line pressure regulator, discharge flow meter, and wet test meter. A pressure gauge is also installed just after the on-line pressure regulator in order to indicate the pressure of the system after regulations.

Table 3.6: Measuring and controlling equipment

ITEM	OPERATING RANGE	FUNCTION
Temperature probe	-60^{o} to 100 ^{o}C	To measure the temperature of the gas inside the cell.
Pressure gauges	0 to 600 psig and 0 to 8 psig	To measure the internal pressure of the test cell. To measure the system pressure after regulations.
Natural gas flow meters	0 to 10 l/min and 0 to 18 l/min	To measure gas charged flow rate To measure gas discharged flow rate
Wet type gas meter	0.0-1000.0 *l*	To measure the total amount of gas discharge.
3-way valve	-	To change flow direction.
Plug valve	-	To open/close gas flow abruptly.
Needle valve	-	To open/close gas flow gradually.
Metering valve	-	To regulate gas flow.
Multi-stage gas cylinder regulator	500 to 3000 psig	To step down gas supply pressure to the operating pressure.
Two-stage on-line regulator	14.7 to 6000 psig	To step down gas storage pressure to the working pressure of wet test meter.
Vacuum pump	-760 to 0 mm Hg	To evacuate the test cell before methane charging.
Electronic balance	0.00-6200.00 g	To measure the weight of the adsorbent and to detect weight changes during adsorption/desorption.

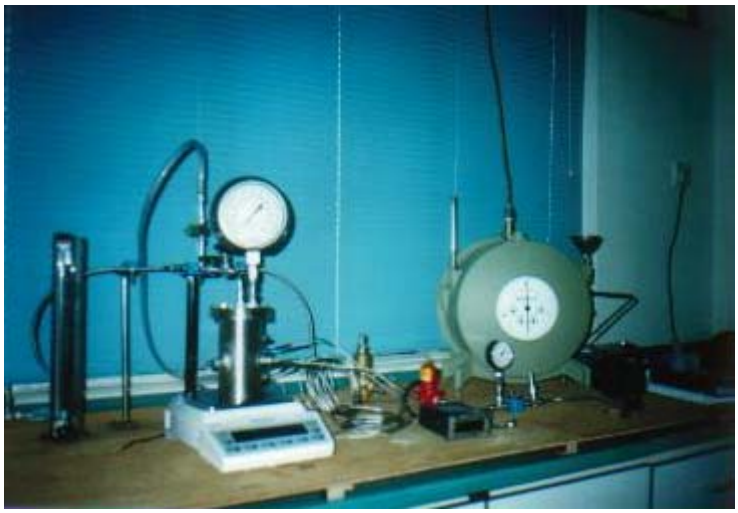

Figure 3.2: The ANG storage experimental rig

3.2.4 Adsorbent Loading

In this experimental work, for every set of adsorbent loading into the ANG vessel, the weight of each adsorbent loaded varies from one to another depending on loading compactness, particle size and mass of a particular type of adsorbent. These differences lead to differences in the packing density, which is the mass of the adsorbent particle per unit volume of the storage space. Table 3.7 below shows the value of the adsorbent loading weight into the vessel, the packing density and also the true density of the adsorbent tested. Values of the adsorbents true density are obtained from the literatures (Perry, 1984; Slejko, 1985). The adsorbents are loaded into the ANG vessel by conventional method in which they are pressed into the vessel as pack as possible by applying appropriate force. This technique is elaborated further in the following section of experimental procedure.

Table 3.7: Loading weight and densities of adsorbents

Adsorbent	Weight loaded (g)	Packing density, ρ_b (g/cm^3)	True density, ρ_s (g/cm^3)
Darco® Activated Carbon	180.75	0.36	n/a
Palm Shell Activated Carbon	251.50	0.50	0.79
13X Molecular Sieves (powder)	266.27	0.53	0.92
13X Molecular Sieves (beads)	125.30	0.25	0.92
Silica Gel	255.32	0.51	0.85

3.3 Experimental Description

Different types of commercial grade adsorbent were selected to test their adsorptive and desorptive performance as adsorbent media for ANG storage. At an initial stage, the weight of an empty ANG cell with its connections is measured using the electronic balance. Prior to loading the adsorbents into the cell, they are heated in an oven to remove volatile compounds within the adsorbent pores. The adsorbent is then loaded into the ANG test cell using a conventional method. In this simple

technique, the adsorbent particles are packed inside the ANG cell by pressing them on using a flat object with a size comparable to the cell opening. This simple technique is used since the adsorbents employed are in granular or powdered form and it is not practical either to effectively pack these forms of particles for a high packing density. Meanwhile the appropriate packing methods describe in the literature (Cook and Horne, 1997; Sejnoha *et al.*, 1995; Mota *et al.*, 1997) is not viable under this fairly simple experimental set-up since it requires a certain apparatus and a need for adsorbent solidification which are costly. Subsequent to the adsorbent loading, the weight of the cell is measured to obtain the amount of adsorbent packed inside. The packing density of the adsorbent is calculated based on its weight and the volume occupied inside the cell.

The ANG storage performance test on different type of adsorbents is divided into two parts which are isothermal adsorption, and dynamic adsorption/desorption. In isothermal adsorption, the ANG storage was isolated upon every extent of pressurization and was allowed to achieve thermal equilibrium with the surrounding so that the heat of adsorption generated during methane adsorption would be dissipated upon the charging of a certain amount of the gas. On the other hand, under dynamic condition methane is continuously charged into the adsorbent-filled vessel until gas charging is stopped at 500 psig. Under this condition, no opportunity is given for the heat of adsorption to be dissipated to the surrounding.

In the isothermal adsorption, the adsorbent-filled vessel is charged with methane at a considerably slow flow rate of 1-2 l/min up to at least six levels of storage pressure, namely, from 0 psig to 50, 100, 200, 300, 400, 500 psig. Upon the completion of every level of pressurization, the gas supply into the ANG storage is then stopped until the storage temperature return to room temperature at approximately 30 ^{o}C to let the system achieve thermal equilibrium with the surroundings. After thermal equilibrium is achieved, the amount of gas within the vessel at every pressure level is measured on electronic balance to obtain adsorption isotherm for the adsorbent. In the dynamic adsorption, the system is charged with methane until 500 psig at a varied flow rate to simulate slow (1.0 l/min), typical (6.0 l/min), and fast (10.0 l/min) rates. During this process, the behavior of temperature and amount of gas uptake is closely observed and are recorded with time. After the

ANG system has reached thermal equilibrium with surrounding at 500 psig, it is then depressurized to discharge the stored gas. Discharging process is also carried out at different flow rates, which are 1.0 l/min to represent a slow rate, 6.0 l/min to represent typical rate, and 10.0 l/min for fast discharge. These values are taken based on the literature resources in which 0.01 kg/min (equivalent to 1.5 l/min) is taken as a slow rate (Sejnoha *et al.*, 1995) while 6-7 l/min is a typical fuel flow rate corresponds to the demand rate per cylinder on a subcompact car with 4 cylinders traveling at cruising speed (Chang and Talu, 1992). This amount of flow rate is taken to simulate a practical demand of fuel delivery from mobile ANG storage. However, the value for fast rate is taken only as a flow rate that is higher than the typical value due to experimental restrictions since the ANG vessel is fabricated only to laboratory scale with small volumetric capacity. The volume of gas exhausted is measured via wet test meter while temperature and pressure change is closely observed and recorded. After that, a new adsorbent of the same type is loaded into the ANG cell and the entire dynamic run is repeated for a moderate charge/discharge flow rate. Finally, the whole procedure is repeated again for a fast flow rate.

Upon the completion of ANG testing on this type of adsorbent, the entire isothermal and dynamic adsorption/desorption process is repeated for different type of adsorbents. From here onwards, all testing is carried out at a single value of charge and discharge rate, that is, 1.0 l/min in which flow rate is designated as a fixed parameter while the type of adsorbent is designated as variable. Other values of flow rate are not used because flow rate variation is already applied for the previous type of adsorbent and it is enough to illustrate the effect of flow rate on the ANG storage performance. This is justified by the fact that performance changes due to flow rate are caused by the amount of gas charged into the ANG storage regardless of the type of adsorbent used (Mota *et al.*, 1995). The value of 1.0 l/min is used because it simulates a slow gas flow rate as explained earlier. A slow rate is necessary to minimize temperature change during charging and discharging so that higher storage and delivery capacity could be achieved since adsorption and desorption is temperature sensitive. In addition, the dynamic adsorption/desorption test was also carried out under cyclic operation for 3 cycles for each type of adsorbent to evaluate their performances under repetitive application.

3.3.1 Experimental Procedure

The experimental procedures taken in this work are consisted of three parts which are pre-adsorption, isothermal adsorption and dynamic adsorption/desorption. The pre-adsorption part involves preparation of the adsorbents and the ANG system, and weights measurement before the adsorption tests. The isothermal adsorption procedure is the instructions regarding the isothermal adsorption test on selected type of adsorbents while the dynamic adsorption/desorption procedure is regarding the charge and discharge process under cyclic test, varied charging and discharging rates and for different type of adsorbents.

3.3.1.1 Pre-adsorption

1. Heat the adsorbent in oven for approximately 3 to 4 hours at 110 ^{o}C to remove the volatile compounds trapped within the adsorbents pores before they are used in the adsorption test.
2. Measure the weight of the empty ANG cell on the electronic balance.
3. Load the adsorbent into the cell by filling the ANG cell with the adsorbent particles layer by layer until the entire accessible cell volume is filled with adsorbent mass. Each layer should be about one inch thick. For every layer, press the adsorbent particle as compact as possible by applying appropriate force using a flat-ended object such as the flat end of a bottle or steel of a comparable size to the vessel opening (about 5-6 cm in diameter) so that the adsorbent particle is distributed and packed evenly. The intensity of force applied during pressing must be appropriate to avoid the adsorbent particles from being damaged by excessive force. After the ANG cell is filled with adsorbent mass, cover the whole opening diameter of the cell with a very fine lattice before replacing the cell cap to prevent the adsorbent particle from being sucked out during vacuuming process.
4. Measure the weight of the adsorbent-filled cell.
5. Calculate the packing density of the adsorbent bed within the ANG cell.

6. Evacuate the adsorbent-filled cell from air using vacuum pump until –14.7 psig or 0 atm. Measure the weight of the evacuated filled-cell again.

3.3.1.2 Isothermal Adsorption

1. Charge the evacuated adsorbent-filled cell with methane slowly until 0 psig (1 atm) and let the system reach thermal equilibrium with surrounding at room temperature (typically at 27 ^{o}C).
2. After thermal equilibrium is achieved, check the storage pressure again. It must be at 0 psig at thermal equilibrium. If lower than that, recharge the storage cell slowly until the desired pressure is achieved at thermal equilibrium. If the pressure is higher than 0 psig, discharge the storage slowly until the pressure fall to 0 psig. The cell must be recharged or discharged slowly at a slowest controllable flow rate to minimize temperature change since thermal equilibrium has already been achieved. After temperature has stabilized at 27 ^{o}C, measure the weight of the charged cell.
3. Charge the adsorbent-filled cell at considerably slow flow rate of 1-2 l/min until 50 psig.
4. After the storage pressure has reached 50 psig, stop the gas flow and isolated the system to reach thermal equilibrium with surrounding at 27 ^{o}C.
5. After thermal equilibrium is reached, record the weight of the storage and record the pressure reading at this level as the first point of the adsorption isotherm.
6. Repeat step (3) to (5) for pressurization until 100, 200, 300, 400 and finally 500 psig which is the target storage pressure.
7. Plot the amount of gas adsorbed within the adsorbent bed (in gram/liter of storage volume) versus pressure level to establish the adsorption isotherm of methane on the adsorbent.
8. Repeat the entire isothermal adsorption process for other types of adsorbent.

3.3.1.3 Dynamic Adsorption/Desorption

1. Charge the evacuated adsorbent-filled cell slowly with methane until 0 psig (1 atm) and let the system reach thermal equilibrium with surrounding at 27 ^{o}C.
2. After thermal equilibrium is achieved, check the storage pressure again. It must be at 0 psig at thermal equilibrium. If lower than that, recharge the storage cell slowly until the desired pressure is achieved at thermal equilibrium. If the pressure is higher than 0 psig, discharge the storage slowly until the pressure fall to 0 psig. The cell must be recharged or discharged slowly at a slowest controllable flow rate to minimize temperature change since thermal equilibrium has already been achieved. After temperature has stabilized at 27 ^{o}C, measure the weight of the charged cell.
3. Record the weight of the charged cell at 0 psig.
4. Charge the adsorbent-filled cell again from 0 until 500 psig (about 3.5 atm) at a slow charge flow rate of 1 l/min. During this process, the storage temperature is observed and recorded closely along with the weight of gas uptake and pressure level with time. For slow charge, all readings are taken every 5 minutes.
5. After the pressure has reached 500 psig, stop the methane supply and record the final temperature and the weight of the storage cell to determine amount of gas stored at 500 psig under dynamic condition.
6. Let the ANG system achieve thermal equilibrium with surrounding.
7. Discharge the stored methane from 500 psig until 0 psig (1 atm) at slow rate of 1.0 l/min by opening the valves of the ANG cell gradually and carefully adjusting the knob at the flow meter. During this phase, the storage temperature, volume of gas discharged and pressure level are recorded with time for every 10 seconds for delivery of the first 50% of the gas. Recording time distance can be extended appropriately for the rest of the gas delivery.
8. Record the total volume of gas deliverable from the adsorbent-filled storage shown by the wet test meter and the final temperature reading at 0 psig, which is the lowest depressurization level.
9. Repeat the entire dynamic adsorption/desorption process for 3 cycles at the same charge/discharged flow rate. Ensure that the weight of the adsorbent

loaded in the ANG cell is consistent with its value in the previous run to maintain consistent packing density.

10. Repeat the entire dynamic adsorption/desorption process with a new adsorbent at charge/discharge flow rates of 6.0 l/min and 10.0 l/min respectively to simulate a moderate and fast charge/discharge flow rates. Ensure that the weight of adsorbent loaded is consistent with the preceding run to maintain consistent packing density.
11. Repeat the entire dynamic adsorption/desorption process for different type of adsorbent at charge/discharge rate of 1.0 l/min.

CHAPTER IV

RESULTS AND DISCUSSION

The results of methane adsorptive storage are discussed in terms of parametric study which describes the behavior of pressure and temperature of the ANG system alongside gas uptake into the ANG storage during charging and alongside gas delivery from the storage during discharging. The resultant parametric behaviors are influenced by the difference of physical properties of different types of material and by charge/discharge flow rates. Apart from the parametric study, characteristics of the ANG storage during charge/discharge operation are also discussed. This includes the characteristic of adsorption isotherm on different types of adsorbent material during isothermal charging and the characteristic of gas uptake and delivery during dynamic charging/discharging. To study the reliability of the adsorbents for prolonged application, their storage and delivery performances under cyclic operation are also studied in terms of capacity consistency and delivery ratio.

4.1 Parametric Study

Behavior of the storage pressure and of the temperature of the adsorbent-filled storage (or the temperature of adsorbent bed, since the whole storage is filled with adsorbent mass) varies with the amount of gas charged into and discharged from the ANG storage. The storage capacities achieved differ on different type of adsorbent and with different degree of surface area and micropore volume of the

adsorbent. However, the efficiency of gas delivery from the adsorbents-filled storage during discharge is very much dependent on adsorbent bed temperature behavior during discharge. The temperature behavior in turn, are varies depending on the thermodynamic properties of the adsorbent such as heat capacity and heats of methane adsorption/desorption. Besides that, the rate of gas charge into and discharge from the adsorbent-filled vessel also has effect on the storage capacity and delivery performance of the adsorbent. Faster charging rate causes higher temperature rise while faster discharging rate causes greater temperature fall which in turn deteriorate both the storage capacity and the delivery efficiency obtained.

4.1.1 Charging Phase

Charging the adsorbent-filled storage from 0 to 500 psig results in pressure and temperature elevation within the ANG vessel. The storage pressure build up is proportional to the amount of gas charged into the vessel while the temperature rise is the result of heat of adsorption generated during methane adsorption. The storage capacity on different type of adsorbents is determine by the surface area, micropore volume and packing density of the adsorbent. Meanwhile, the extent of temperature rise on individual adsorbent, which will also affect their storage capacity, is influence by their thermodynamic properties. Similarly, the extent of temperature rise due to charging velocity affects the adsorbents performance in adsorbing the gas.

4.1.1.1 Results of Different Type of Adsorbents

The ANG storage capacities employing different type of commercial adsorbents tested in this work are listed in Table 4.1. The table indicates amount of methane stored in the ANG vessel under isothermal and under dynamic condition charging at 1.0 l/min of gas flow rate. All capacities shown in the table are the amount of gas uptake between 0 and 500 psig. The unit gram per liter (*g/l*) in the table is used to indicate storage capacity in terms of weight while unit liter per liter

(*l/l*) indicates in terms of volume. Usually, unit *l/l* is alternatively written as *V/V* or V_m/V_s which stands for volume of methane per volume of storage.

Table 4.1: Storage capacity of different type of commercial adsorbents tested

Adsorbent	**Storage Capacity between 0 and 500 psig**				
	Isothermal		Dynamic (at 1 *l/min*)		
	g/l	*l/l*	*g/l*	*l/l*	Charging time
Palm Shell AC	58.23	87.35	57.16	85.74	157 minutes
Darco© AC	38.00	57.00	36.64	54.96	105 minutes
13X MS Zeolites (powder)	34.58	51.87	31.96	47.94	86 minutes
13X MS Zeolites (beads)	-	-	24.18	36.27	65 minutes
Silica Gel	28.50	42.75	28.00	42.00	70 minutes

The test results of ANG storage capacity employing granular palm shell AC is 87.35 *l/l* at 500 psig under isothermal condition, which is considered as the maximum storage capacity achievable under this experimental condition. Under dynamic run, at gas flow rate of 1.0 l/min, it yields 85.74 *l/l* in which it exhibits about 2% less of gas uptake. The other adsorbents tested are also showing a similar behavior during their dynamic adsorption that leads to reduction of their storage capacities compared to their isothermal capacities. Darco AC yield storage capacity of 57.00 *l/l* under isothermal condition and shows 4% of capacity loss, yielding 54.96 *l/l* under dynamic condition. Respectively, MS zeolites (powder) and silica gel show 8% and 2% reduction of their storage capacity, yielding 47.94 *l/l* and 42.00 *l/l* correspondingly.

Apparently, the amount of gas uptake under dynamic adsorption is lower than under isothermal adsorption at the same pressure. Difference between this two capacities is due to the continuous temperature rise occurred during dynamic charging, which is detriment to gas adsorption, as shown in Figure 4.1. This figure illustrates the temperature behavior of the ANG storage charged under isothermal and dynamic condition employing palm shell AC. There is a significant temperature rise takes place during dynamic charging in which the adsorbent bed temperature rises from room temperature of 27 ^{o}C to 42 ^{o}C during the first 26% of gas uptake

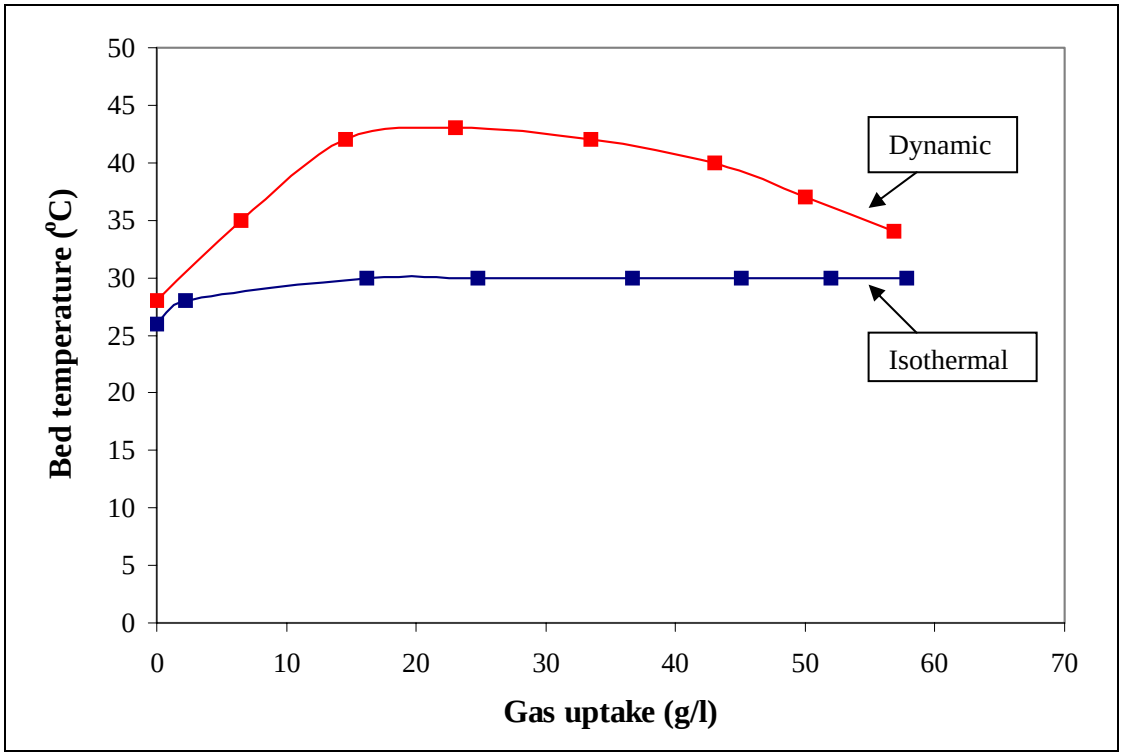

Figure 4.1: Temperature behavior during adsorption

while during isothermal charge, the bed temperature rises slightly from room temperature of 26 ^{o}C to 30 ^{o}C during the first 28% of gas uptake. The bed temperature for dynamic charge then reaches maximum value of 43 ^{o}C corresponding to 41% of gas uptake and thereafter, it begins to fall gradually to the final temperature of 34 ^{o}C as gas uptake ended at 500 psig due to environmental cooling. When the temperature reaches its maximum rise, it reflects that gas adsorption begins to gradually decrease while gas compression begins to gradually contribute to the increment of gas uptake within the adsorbent-filled vessel. As adsorption reduces, the heat of adsorption generated decreases thus lowering the temperature gradient between the storage system and the surroundings as the heat dissipating to the surroundings while heat generation decreasing. Meanwhile under isothermal charging, the bed temperature is kept constant at 30 ^{o}C for the next 72% of gas uptake.

Since adsorption is an exothermic process, continuous temperature rise during dynamic adsorption causes capacity loss because adsorption is inversely proportional to temperature (Suzuki, 1990). Under dynamic charging, methane is

continuously charged into the adsorbent-filled vessel. Consequently, storage pressure continuously builds up along with the substantial increase of the temperature with gas uptake as a result of heat of adsorption generated when methane adsorbs on the adsorbent substrate. Under isothermal charging, however, since the ANG storage was isolated upon every extent of pressurization, the system is allowed to achieve thermal equilibrium with the surrounding. Hence, the heat of adsorption generated during methane adsorption is allowed to dissipate upon the charging of a certain amount of gas and thus allowing more gas to be adsorbed on the adsorbent substrate rather than being stored as compressed gas. The amount of gas stored in adsorbed state under dynamic condition is less than under isothermal condition because as the temperature rises, proportion of gas charged into the vessel tends to remain compressed rather than being adsorbed (Mota, 1997). In other words, the storage capacity measured at 500 psig under dynamic condition is consist of more compressed gas than under isothermal condition. If we let the heat generated during dynamic adsorption to dissipate upon achieving 500 psig, which will take some time, then in the end the final pressure will decrease below 500 psig as further adsorption takes place at lower temperature (Komodromos *et al.*, 1992).

From Table 4.1, in page 78, we can see that the storage capacities for Darco AC are lower than of palm shell AC although both adsorbents are derived from the same type of material, namely carbonaceous substance. The isothermal capacity of Darco AC is 57.00 *l/l* compared to 87.35 *l/l* for palm shell AC where it stores 35% less gas while the dynamic capacity of Darco AC is 54.96 *l/l* compared to 85.74 *l/l* for palm shell AC in which it stores 36% less gas. This capacity difference is due to the smaller surface area that Darco AC had, which is 651.69 m^2/g compared to palm shell AC which is 1012.39 m^2/g. Still, other reasons could be because of the difference in microporosity and particle size between these two carbons. As shown in Table 3.1 in Chapter III, page 62, Darco AC has micropore volume of 0.131 cm^3/g and particle size of 40 MESH compared to that of palm shell AC which are 0.214 cm^3/g and 99 MESH respectively. Conclusively, Darco AC has a smaller value of surface area and micropore volume but a larger particle size compare to palm shell AC. Adsorbent with larger surface area allows more contact between gas molecules and its surface to give way for more adsorption into the micropores (Marsh, 1987). Although an adsorbent posses macropore, it could not increase methane density

during adsorption because gaseous molecules behave as compressed gas within this region and therefore, macropores can be regarded as void volume (Quinn and MacDonald, 1992). This fact leads to the importance of micropore volume available over the adsorbent surface area. A larger micropore volume will increase methane density stored within this structure. In addition, adsorbent particle size is also an important criteria for better storage because a larger particle size create more void volume between particles within the ANG vessel (Cracknell *et al.*, 1993; Menon, 1997).

Isothermal storage capacity for other type of non-carbonaceous adsorbent like MS zeolites and silica gel (both powder) are lower than of the activated carbons, which are 51.87 *l/l* and 42.75 *l/l* respectively compare to 87.35 *l/l* for palm shell AC and 57.00 *l/l* for Darco AC. Mathematically, with reference to palm shell AC which has the highest storage capacity, MS zeolites and silica gel store 41% and 51% less gas correspondingly. Conclusively, carbon-based adsorbent has a superior capability for methane adsorptive storage than non-carbonaceous adsorbent. This confirms results reported in the literature that, up to date, porous carbon is superior to other materials as a medium for the adsorptive storage of methane (Cracknell *et al.*, 1993; Parkyns and Quinn, 1995).

Another adsorbent tested for methane adsorption is the 13X MS zeolites with particle size of 4-8 MESH. This adsorbent is the same as the previous MS zeolites but having a much larger particle size. From the result in Table 4.1, obviously this adsorbent yield a poor storage capacity, leave alone its delivery capacity. Relatively, its storage capacity is only 76% of the equivalent zeolites. This result demonstrates the importance of particle size, because larger particle size leads to storage capacity loss due to larger void volume resulted when the adsorbent is loaded inside the storage vessel. Although methane molecules did partly adsorbed on the adsorbent substrate, but majority of the gas fills the larger void volume since this region is more accessible than the micropores.

The time taken to charge the adsorbent-filled vessel from 0 to 500 psig varies from one adsorbent to another as shown in Table 4.1 in page 78. Palm shell AC took the longest charging time of 157 minutes followed by Darco AC which took 105

minutes, powder MS zeolites which took 86 minutes, silica gel which took 70 minutes while beads MS zeolites took the shortest time, which is 65 minutes. The duration taken to finish charging at 500 psig is related to the amount of gas storable by the adsorbents. As shown in Table 4.1, palm shell AC yields the highest storage capacities among all adsorbents tested and as a result, it took a longer to time to be charged while on the contrary, the beads MS zeolites which is capable of the lowest storage capacity, took the shortest charging time accordingly. Adsorbent that is capable of a higher storage capacity reflects higher microporosity and higher packing density (means smaller void volume) compared to adsorbent that has lower storage capacity (Komodromos *et al.*, 1994). As this adsorbent is charged, a larger proportion of gas adsorbs on its substrate than the lower-capacity adsorbent thus lowering the rate of storage pressure elevation. For adsorbent that has lower microporosity and lower packing density (larger void volume), larger proportion of gas is compressed compared to the previous adsorbent. When higher proportion of gas is compressed, the rate of pressure elevation is higher. Therefore, adsorbent with higher storage capacity, took longer charging time to reach 500 psig because the rate of pressure elevation is lower compared to adsorbent with lower capacity to reach the same pressure in which more gas is compressed resulting in faster pressure elevation.

The overall results of the storage capacities obtained in this study are not so convincing when compared to the target capacity for natural gas storage defined in the literature. The adsorbed natural gas storage target is 150 *V/V* at storage pressure of 34 bar (500 psig), delivery pressure at 1 bar (atmospheric pressure or 0 psig) and at 25 °C as deduced from detailed experimental studies and from theoretical analysis in the literature (Nelson, 1993). Except for palm shell AC that achieved 58% of the target capacity, the rest of the adsorbents yield less than half of the target. Darco AC could only achieve 38% while MS zeolites (powder) yield 35% and silica gel yield 28% of the target capacity. However, the results achieved in this work are subjected to experimental error, and restrictions such as packing density (compactness) of the adsorbents loaded inside the vessel and thermal management during experiment that are not being considered in this study. These two aspects are beyond the scope of this study. With reference to Table 3.7 in Chapter III, page 69, the highest adsorbent packing density achieved in this work is only 0.53 g/cm^3 where as the ideal value would be 0.90 to 1.00 g/cm^3 as reported in the literature (Remick and Tiller, 1985;

Elliott and Topaloglu, 1986). If these matters are improved, the results achieved could be better.

Increasing the compactness of the adsorbent mass loaded per volume of the vessel will reduce interparticle void volume within the storage (Remick and Tiller, 1985). However, ideal packing density is not used in this study because it requires solidification of the adsorbent using certain densification technique. This process requires certain polymeric binder, mechanical tools and also expertise to carry out the process, which are unavailable and unfeasible for this study. Nevertheless, a high packing density can be obtained by proprietary technique to form a solid adsorbent briquette. In this technique, granular adsorbent is mixed with an aqueous solution of a polymeric binder. The mixture is then pressed into a mold of desired geometrical shape to form a solid briquette under mechanical pressure varying between 100 and 300 MPa and then dried (Cook and Horne, 1997). The briquette formed is mechanically strong and resistant to abrasion.

If the ANG storage temperature could be managed in such a way so that heat of adsorption generated during charging is dissipated to the surrounding, then gas adsorption in the ANG vessel could be increased. This can be done by installing heat exchanger system within the ANG storage such as TES heat management system (Jasionowski *et al.*, 1992), or by cooling the gas before it enters the storage vessel (Sejnoha *et al.*, 1995).

The ANG storage pressure elevates exponentially with the amount of gas uptake during charging. Figure 4.2 illustrates the ANG pressure profile versus gas uptake and time under dynamic charging until 500 psig. The figure shows that the pressure elevates slowly as the gas is charged in during the first 25% of gas uptake corresponds to 9% of total pressurization (that is until 500 psig) in 25 minutes. Pressure elevation increases to 32% during the next 25% of gas uptake in 35 minutes of charging. During the next 50% of gas uptake, pressure build up in the ANG storage is more rapidly where it represents 68% of the total pressurization which takes 97 minutes. Apparently, the pressure curve shown that the pressure increases from a lower to higher rate and time taken for gas uptake had increased. In other words, the rate of gas stored within the adsorbent-filled vessel has decreased as

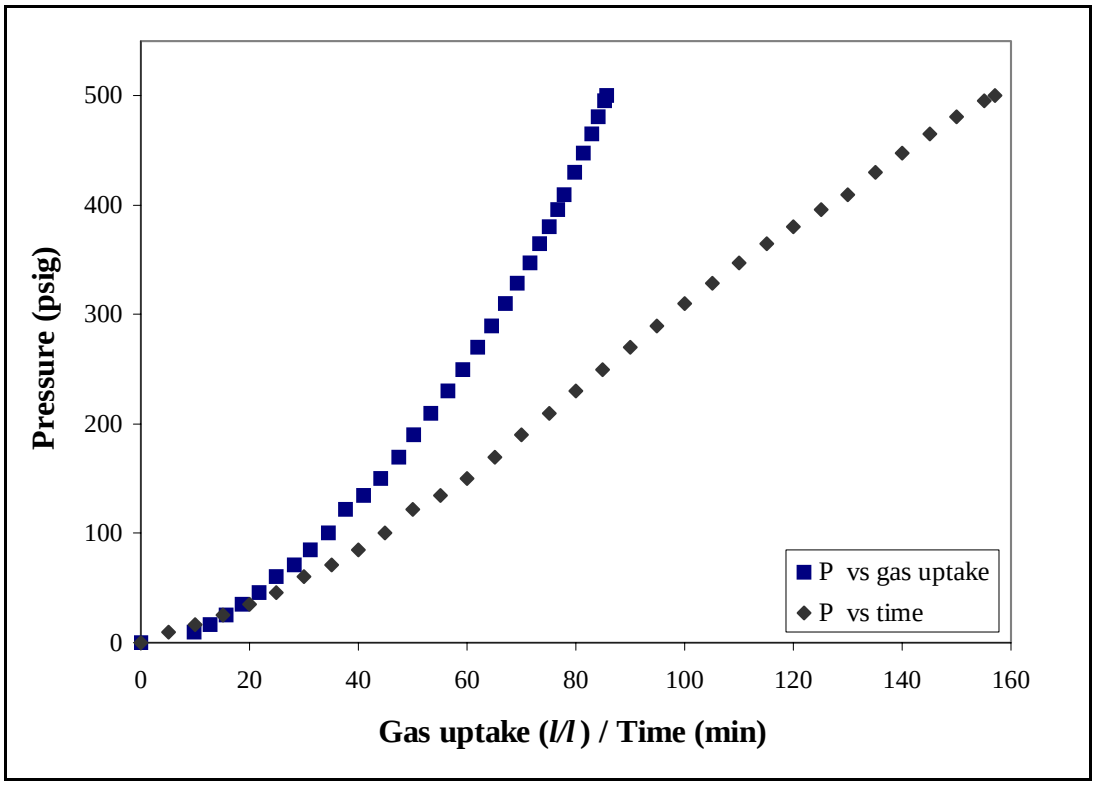

Figure 4.2: ANG storage pressure vs. gas uptake, bed temperature and time during dynamic charge using palm shell AC

pressure increases. In Figure 4.2, the time taken to finish charging the ANG storage until 500 psig is 157 minutes and is obviously too long. However, this long charging time is subjected to the slow rate of 1.0 l/min which is used purposely to minimize temperature rise during charge. In practical application such vehicular fuel storage, fast flow rate (for example, >10 l/min) should be used to hasten the charging duration. However, the refueling system need to be equipped with heat exchanger facility to remove the very substantial amount of heat of adsorption generated during fast charge.

The exponential pressure elevation in the ANG storage is in such a way because during the early stage of charging, most of the gas molecules charged into the vessel are adsorbed into the adsorbent micropores and therefore, the pressure build up in the vessel are slow although substantial amount of gas has been charged. When gas molecules adsorbed into a very much smaller space in the micropore, they were subjugated to the force exerted by the adsorbent surface. This force attracts a lot

of gas molecules into the pore so that the amount of gas in the bulk is reduced. As a result, collision between gas molecules in the free space within the vessel decreased and therefore, rate of pressure build up is slow (Gubbins and Jiang, 1997). However, when the amount of gas molecule charged into the vessel increased with further charging, the adsorbent micropores are more and more occupied and consequently, part of the gas molecules begins to occupy a larger pores and interparticle voids, thus causing more collisions of gas molecules that contributed to a higher rate of pressure elevation. The rate of gas uptake apparently had decreased because when adsorption sites are getting occupied, more and more gas is stored as compressed gas rather than being adsorbed. Since it is the adsorbed gas that is contributing to greater amount of gas rather than the compressed gas, therefore the instantaneous amount of gas uptake is getting lesser and lesser (Malbrunot *et al.*, 1996; Quinn and MacDonald, 1992).

The temperature profiles of different type of adsorbents during charge are shown in Figure 4.3. Apparently, their profile are quite similar to each other. However, the extents of temperature rise are different among the adsorbents. Charging at 1.0 l/min, the bed temperature of palm shell AC adsorbent rises to a maximum value of 43 ^{o}C while for Darco AC and MS zeolites, their temperature rises to 39 ^{o}C. Silica gel shows a much lower extent of temperature rise which is 31 ^{o}C. These differences are due to the difference of heat capacity and heat of methane adsorption for different material. Material such as silica gels is having a higher heat capacity and lower methane heat of adsorption than any other adsorbents (Menon, 1997). Activated carbons and MS zeolites generally are having a nearly common range of heat of adsorption but lower heat capacities than silica gel (Menon, 1997).

4.1.1.2 Effect of Charge Flow Rate

The rate of gas charge into the adsorbent-filled vessel has effect on the storage capacity of the ANG storage. During the adsorption tests on palm shell AC adsorbent at different flow rates, it was observed that a slower gas charging rate yields a higher gas uptake into the adsorbent-filled storage and a faster charging rate

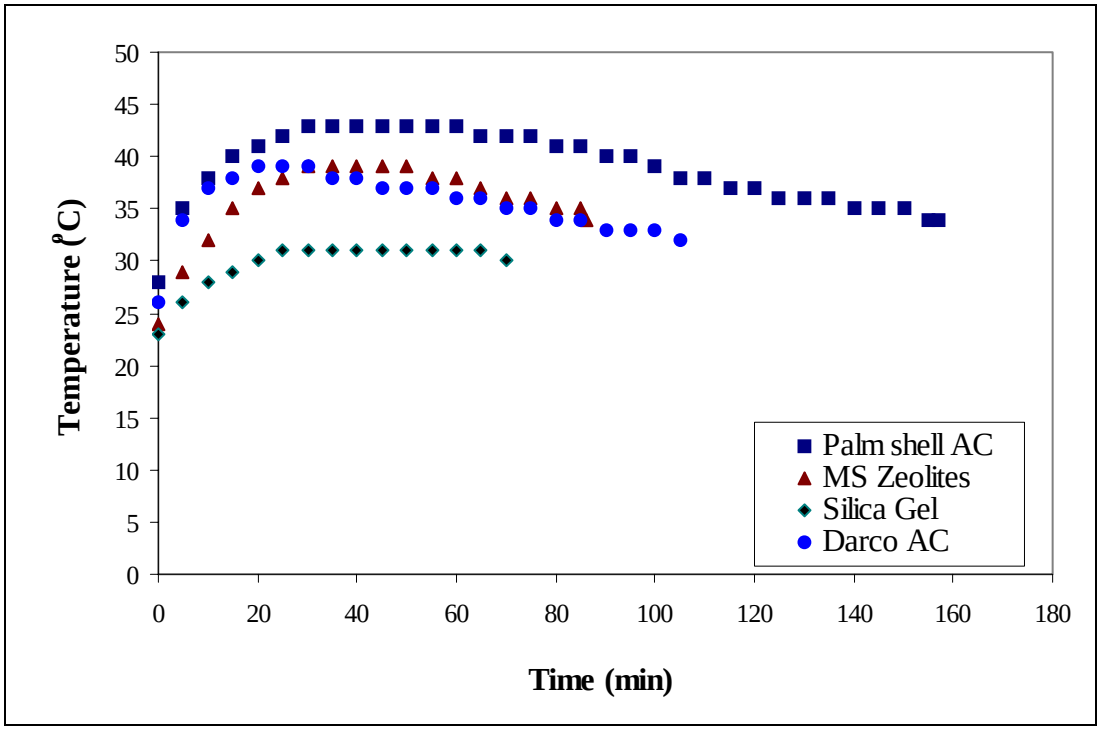

Figure 4.3: Adsorbents bed temperature profiles during charge at 1 l/min

yield a lower gas uptake. Table 4.2 shows the ANG dynamic storage capacity obtained when charging at different flow rates. When charging at 1.0 l/min, gas uptake into the ANG vessel measured is 57.16 g/l compare to 51.18 g/l at 6.0 l/min and 42.76 g/l at 10.0 l/min. The amount of gas uptake at different flow rates is affected by the storage temperature behavior during charging. This fact is shown in Figure 4.4. From the figure, a slow charge at 1.0 l/min causes bed temperature to rise 15 ^{o}C from room temperature corresponds to the first 30% of gas uptake while when charging at 6.0 l/min, the storage temperature rise 23 ^{o}C for the first 30% of gas uptake and fast charging at 10.0 l/min cause the temperature to rise 31 ^{o}C during the first 30% of gas

Table 4.2: Storage capacity of palm shell AC at different flow rates

Flow rates	Storage Capacity at 500 psig		Charging time (min)
	g/l	*l/l*	
1.0 l/min	57.16	85.74	157
6.0 l/min	51.18	76.77	34
10.0 l/min	48.76	73.14	20

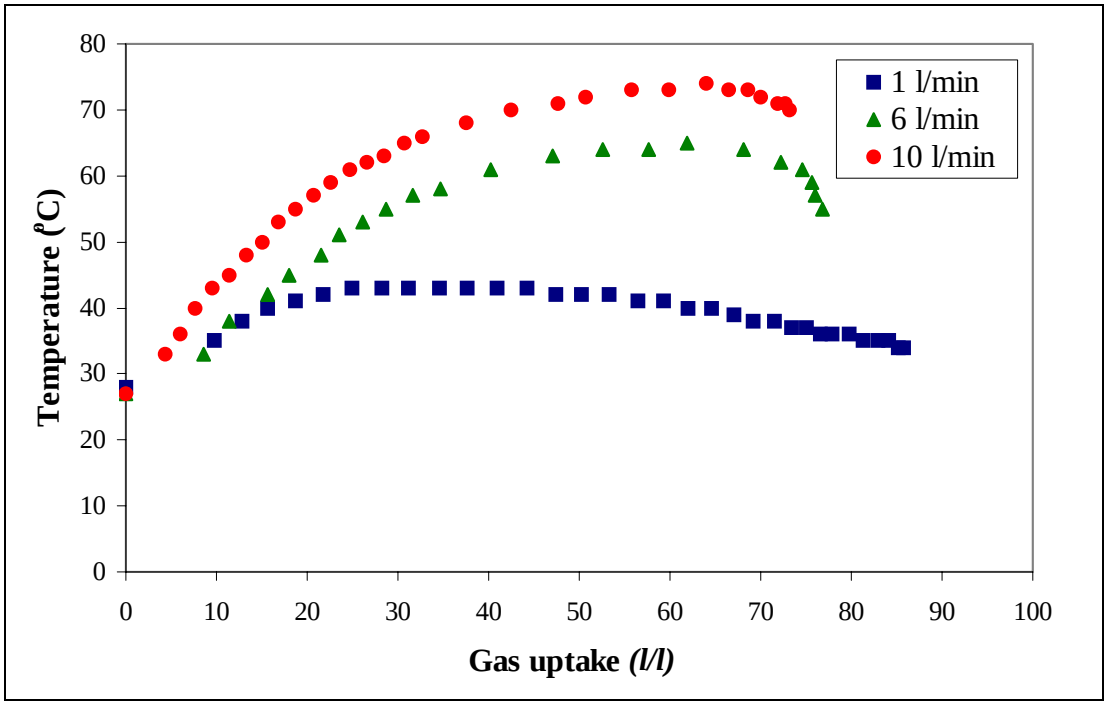

Figure 4.4: Effect of charging rate on gas uptake using palm shell AC

uptake. Furthermore, the storage temperature under 1.0 l/min of charging rate remains constant for the next 20% of gas uptake before it gradually fall to 34 ^{o}C during the next 50% of gas uptake. However, for the charging at 6.0 l/min the temperature continue to rise to the maximum value of 65 ^{o}C during the next 50% of gas uptake while for the charging at 10.0 l/min temperature rises to the maximum value of 74 ^{o}C during the next 57% of gas uptake. Thereafter, the temperature begin to fall to 55 ^{o}C during the final 20% of gas uptake and to 70 ^{o}C during the final 13% of gas uptake for the charging at 6.0 and 10.0 l/min respectively. Obviously, the figure shows that charging at slower rate yield a higher storage capacity. Charging at 1.0 l/min yields 85.74 *l/l* of total gas uptake, charging at 6.0 l/min yields 76.77 *l/l* and charging at 10.0 l/min yields 73.14 *l/l*. The extents of temperature rise influence the storage capacity obtained.

Temperature of the adsorbent bed within the vessel increase exponentially with the rate of gas charged into the vessel. This is due to the heat of adsorption released when methane adsorbed on adsorbent substrate (Remick and Tiller, 1985). The shape of temperature elevation curve is depending on the charging rate. The

temperature changes are barely evident in the first 5-10 minutes during slow charge but for fast charge, adsorbent bed temperature rise rapidly to a maximum value before it decreases faintly as a result of environmental cooling. This phenomenon is shown in Figure 4.5 for methane adsorption on palm shell AC at different charge flow rates. A higher gas flow rate yield a higher temperature rise within the adsorbent bed during charge. Under fast charging rate of 10.0 l/min, the ANG storage indicates a maximum temperature rise of 47 ^{o}C from room temperature of 28 ^{o}C in 15 minutes while at 6.0 l/min of gas flow rate, bed temperature rises 38 ^{o}C in 20 minutes compare to the maximum 16 ^{o}C of temperature rise in 30 minutes under slow flow rate of 1.0 l/min. Since gas adsorption itself is an exothermic process and because pressure builds up quite significantly inside the ANG vessel during charging, we can understand that the more rapid gas is charged in, the higher the temperature rises because greater amount of heat of adsorption is generated per mole of gas charged into the vessel, resulting in lower storage capacity obtainable. Meanwhile, under slow charging rate of 1.0 l/min, bed temperature remains constant at 43 ^{o}C for about 30 minutes before it drops to 34 ^{o}C in a much longer duration due to environmental cooling. This behavior happens because temperature rise during charging at slow rate is limited by the longer duration of charging which permits the heat generated to dissipate before gas uptake finishes at target pressure of 500 psig (Sejnoha *et al.*, 1995). The total charging time taken to reach 500 psig at 1 l/min, 6 l/min and 10 l/min is 157 minutes, 34 minutes and 20 minutes respectively. The time taken at slow rate of 1 l/min is about 4.6 times longer than at typical flow rate of 6 l/min and 7.8 times longer than at fast flow rate of 10 l/min.

4.1.2 Discharging Phase

Discharging the ANG storage from 500 psig to atmospheric pressure results in pressure and temperature fall within the ANG vessel. The fall of storage pressure is from a rapid to slow rate along with constant rate of gas removal while the temperature is falling drastically with depressurization as a result of heat of desorption and partly due to pressure drop. The delivery capacity of adsorbents, in

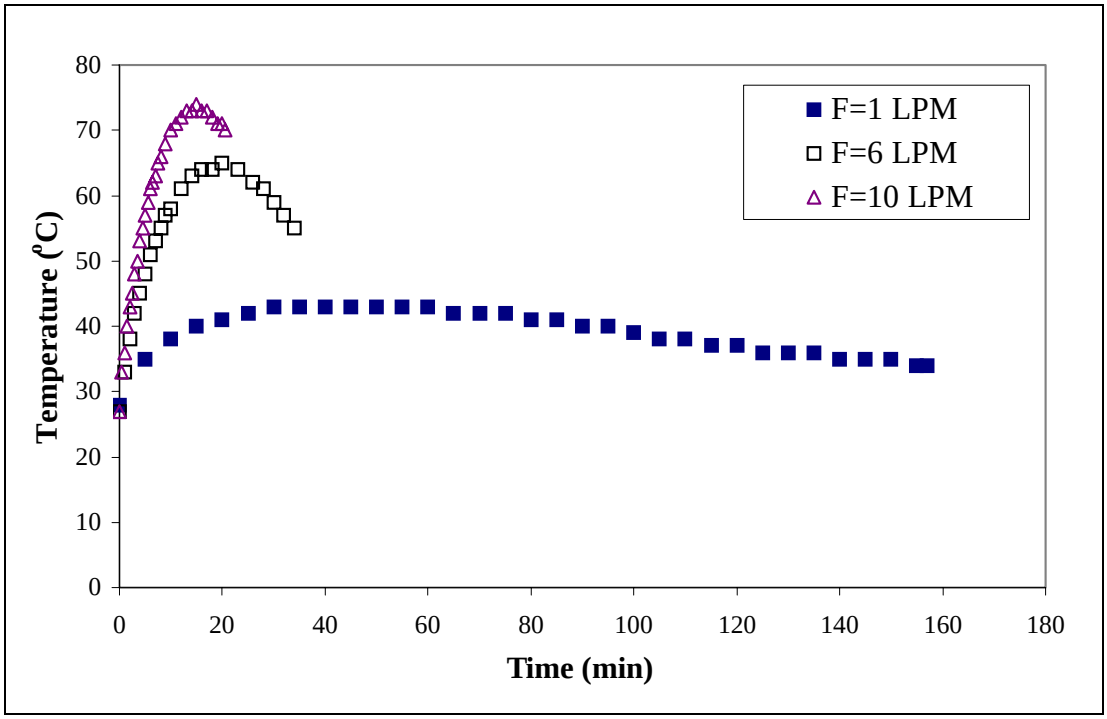

Figure 4.5: Palm shell AC adsorbent bed temperature profiles during charging at different flow rates

term of their dynamic efficiency in delivering the stored gas, is determine by the extent temperature fall during discharge. This temperature behavior in turn, is governed by the adsorbent heat capacity and heats of methane desorption. Likewise, the extent of temperature fall is also influence by the rate of discharge.

4.1.2.1 Results of Different Type of Adsorbents

From the experimental results, it was observed that the amount of methane deliverable from the ANG storage is always lower than its storage capacity. Table 4.3 shows the gas delivery performance of the adsorbents tested in this study. From the table, the delivery capacity of palm shell AC is 75.8 *l/l* compared to its isothermal storage capacity, which is 87.35 *l/l*. Similarly, Darco AC, MS zeolites and silica gel also yield a delivery capacity that is lower than their storage capacity. Darco AC delivers 49.6 *l/l* of the 57.0 *l/l* gas stored, MS zeolites delivers 46.0 *l/l* of the 51.9 *l/l* and silica gel delivers 40.6 *l/l* of the 42.8 *l/l*. Technically, the delivery performance

of an adsorbent employed for ANG storage is measured by its dynamic efficiency, η. The dynamic efficiency, or in other words, ratio of gas delivered over gas stored for palm shell AC is 87%, for Darco AC, 87%, MS zeolites, 89% and silica gel, 95%.

Table 4.3: Gas delivery performance of different type of commercial adsorbents

Adsorbent	Storage capacity at 500 psig	Delivery capacity at 1 l/min, 0 psig	Dynamic efficiency, η
Palm shell AC	87.4 *l/l*	75.8 *l/l*	0.87
Darco© AC	57.0 *l/l*	49.6 *l/l*	0.87
MS zeolites (powder)	51.9 *l/l*	46.0 *l/l*	0.89
Silica gel	42.8 *l/l*	40.6 *l/l*	0.95

The capacity loss in all of the above is due to the effect of heat of desorption. While methane adsorption is an exothermic process, desorption of the gas from adsorbent substrate is a reverse process. Desorption is an endothermic process and substantial amount of heat is required to desorb the adsorbed gas (Chang and Talu, 1996). To accomplish this, the gas molecules cunsume the heat available within the storage system and subsequently causing the system temperature to drop. When temperature drops, as part of methane molecules is discharged, the remaining gas however, tends to remain adsorbed because adsorption increases when temperature decreases. More ever, when the heat available within the storage system is used up by the molecules that had desorbed earlier, consequently the remaining gas molecules do not have enough energy to liberate themselves from the adsorbent substrate (Mota *et al.*, 1997). As a result, substantial amount of gas remains within the ANG storage at depletion.

From Table 4.3, it is clearly seen that dynamic efficiency for palm shell AC and Darco AC is identical, that is 0.87 because the two adsorbent are derived from the same substance. MS zeolites exhibits dynamic efficiency of 0.89, which is quite close to the previous two carbonaceous adsorbents but silica gel obviously have a much higher efficiency than the rest, that is 0.95. The dynamic efficiency of gas delivery from the adsorbents-filled storage is related to the temperature profile during discharge. Palm shell AC has a lower dynamic efficiency because its temperature

falls is more significant than of the others. On the contrary, we can see that silica gel yields a higher efficiency because it exhibits lesser temperature drop compared to other adsorbents. This behavior will be discussed further in the following paragraphs. Note that palm shell AC and Darco AC yield a lower efficiency compared to MS zeolites and silica gel even though they have a higher delivery capacities because dynamic efficiency does not represent the storage or delivery capacities but it is a measure of how efficient an adsorbent could deliver the gas stored. Therefore, dynamic efficiency is only useful to measure reliability of an adsorbent-filled storage to supply the stored gas. To determine the capability of an ANG storage, the important measure is the storage capacity.

Figure 4.6 shows the temperature profiles of the adsorbents during discharge. The figure shows that temperature profiles of the different type of adsorbents exhibit a trend that quite similar to each other, especially between palm shell AC and Darco AC. However, the extents of temperature fall are different for among the adsorbents. As shown in Figure 4.6, palm shell AC bed temperature fall as low as –14 ^{o}C from 30 ^{o}C during slow discharge. Darco AC bed temperature fall from 29 to –10 ^{o}C while for zeolites and silica gel, temperature falls from 30 ^{o}C to –3 ^{o}C and from 30 ^{o}C to 9 ^{o}C respectively. From these values, obviously silica gel has the least temperature fall among the above while palm shell AC shows the greatest. The temperature curves shown that after reaching their minimum temperature at depletion, the storage temperature for all of the adsorbents gradually returns to ambient temperature in a relatively very much longer period of time to naturally reaching thermal equilibrium with surrounding. The shape of the temperature curves shows that the rate of temperature fall during discharge is much greater than the rate of temperature recovery to return to ambient temperature. This is because temperature fall during gas relief is due to endothermic desorption effect and assisted by intense pressure drop where as the subsequent temperature recovery is drive solely by natural heat transfer from the surroundings. Temperature drops substantially during endothermic desorption when the ANG system is brought down to atmospheric pressure (Chang and Talu, 1996) but slowly recovering from depletion level to ambient condition as a results of external convective heat transfer into the ANG system (Komodromos *et al.*, 1992).

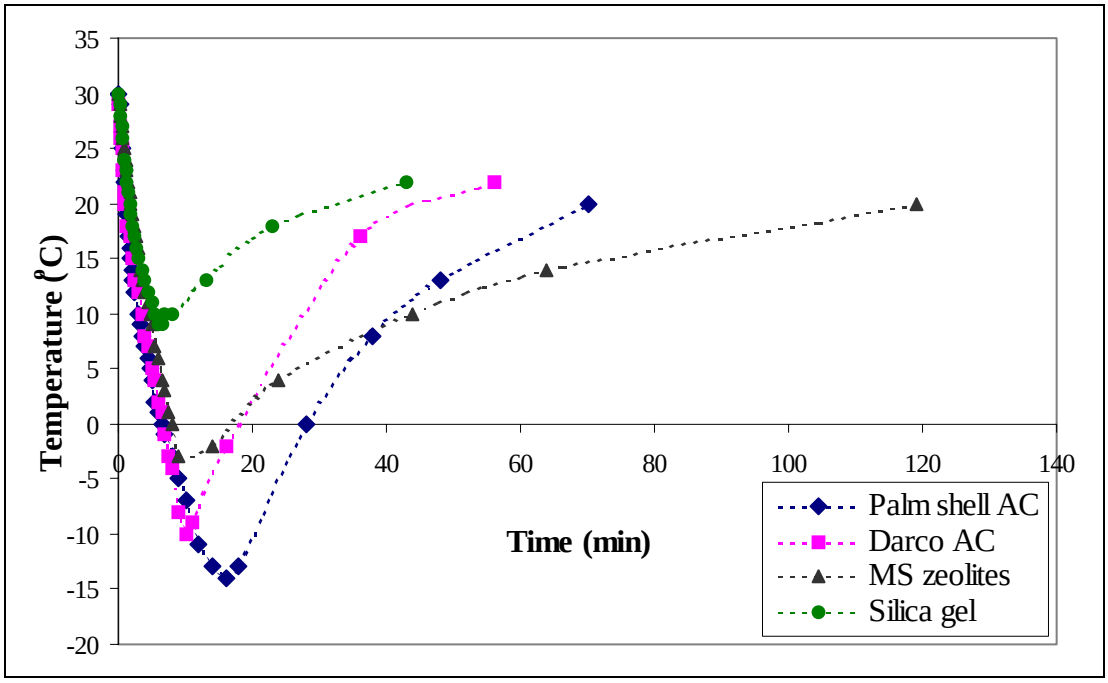

Figure 4.6: Adsorbents bed temperature profiles during discharge at 1 l/min

The difference in the extents of temperature fall among different type of adsorbents can be explained from the difference in the heat capacity of the adsorbents. Different adsorbent materials are having different values of heat capacity. Carbons is reported to have a low heat capacity of 0.7 J/g.K (Otto, 1981). During adsorption, there can be a substantial increase on the adsorbent temperature as well as a substantial decrease during desorption for adsorbent with low heat capacity (Menon, 1997). For this reason, the extent of temperature drop for carbonaceous adsorbents, namely palm shell AC and Darco AC is higher than the non-carbonaceous adsorbents such as MS zeolites and silica gel. Meanwhile, silica gels have a higher heat capacity of 2.2 J/g.K (Otto, 1981). Hence, this type of adsorbent exhibits a lesser decrease of temperature during discharge and consequently, yields a higher delivery efficiency than the other type of adsorbents. For that reason, in terms of thermal property, silica gel is a better adsorbent than carbonaceous adsorbent.

Another factor that causes the difference of extents of temperature fall is the difference in storage capacity of the adsorbents. From Table 4.3 in page 90, clearly palm shell AC has the highest storage capacity among all of the adsorbents tested

while silica gel yields the lowest storage capacity. Adsorbent that have capability to store greater amount of gas generates greater amount of heat during adsorption and in turn consumes greater amount of heat per mole of gas released during desorption compared to adsorbent that has a lower adsorption capacities. As a result, greater temperature fall occurred for higher-capacity adsorbent than the lower-capacity adsorbent during desorption. For that reason, palm shell AC yields greatest temperature fall while silica gel yields the least temperature fall among the adsorbents tested. In Figure 4.6, apparently the order of the amount of temperature drop follows the order of storage and delivery capacities in which palm shell AC with highest capacities exhibits greatest temperature fall followed by Darco AC, MS zeolites and lastly silica gel with the lowest capacities and least temperature drop.

Bed temperature fall with gas exhaustion happens due to the effect of the heat of desorption. Under natural desorption process, where no heat is resupplied to desorb the gas, methane molecules consume heat available within the ANG storage system. The heat released during adsorption is substituted with the sensible heat from the adsorbent bed and the vessel wall as the gas exiting the ANG vessel. When this phenomenon occurs, the system temperature falls substantially besides that which partly due to pressure drop when gas is discharged. When temperature falls within the vessel, natural heat convection begins to take place outside the vessel wall from the surroundings due to temperature difference and subsequently, heat is transferred into the adsorbent bed by conduction at the inner side of the vessel wall (Chang and Talu, 1996). However, since the temperature falls of the adsorbents bed shown in Figure 4.6 are rapid, seemingly the rate of sensible heat consummation is much higher than the rates of both convective heat transfer from surrounding and conductive heat transfer through the vessel wall and adsorbent bed. Heat consummation is governed by the rate of gas exhaustion (Chang and Talu, 1996) which is in this case is faster than the rate of heat transfer into the system. Heat consumed during discharge is only partially compensated by heat transfer from the surroundings at immediate time (Mota *et al.*, 1997). In addition, this matter could be also due to low thermal conductivity of the adsorbent bed.

The pressure history of the ANG storage during discharge is somewhat reverse of the charging phase. Figure 4.7 shows behavior of storage pressure with

time during dynamic discharge from 500 to 0 psig or atmospheric pressure at 1.0 l/min. With constant flow rate, storage pressure decreased exponentially with time when the system is brought down to its depletion (the lowest depressurization level) as the gas stored within the ANG vessel gradually desorbed out of the adsorbent-filled vessel. However, it is not possible to lowered the pressure below atmospheric pressure by the natural means since no pressure difference is available to remove the remaining gas naturally when the storage is at the same pressure with surrounding and consequently, residual amount of methane is left in the ANG vessel even under the lowest possible rate of discharge apart from the amount that remains because of the temperature fall. From Figure 4.7, we can see that during the first 5 minutes of discharge at 1.0 l/min, pressure drops rapidly in about 78% and this profile corresponds to the removal of the first 50% of the storage gas, shown in Figure 4.8. In addition, since pressure drops so rapid, the storage temperature also drop drastically from 30 to 4 ^{o}C in correspondent during the first 5 minutes of discharge.

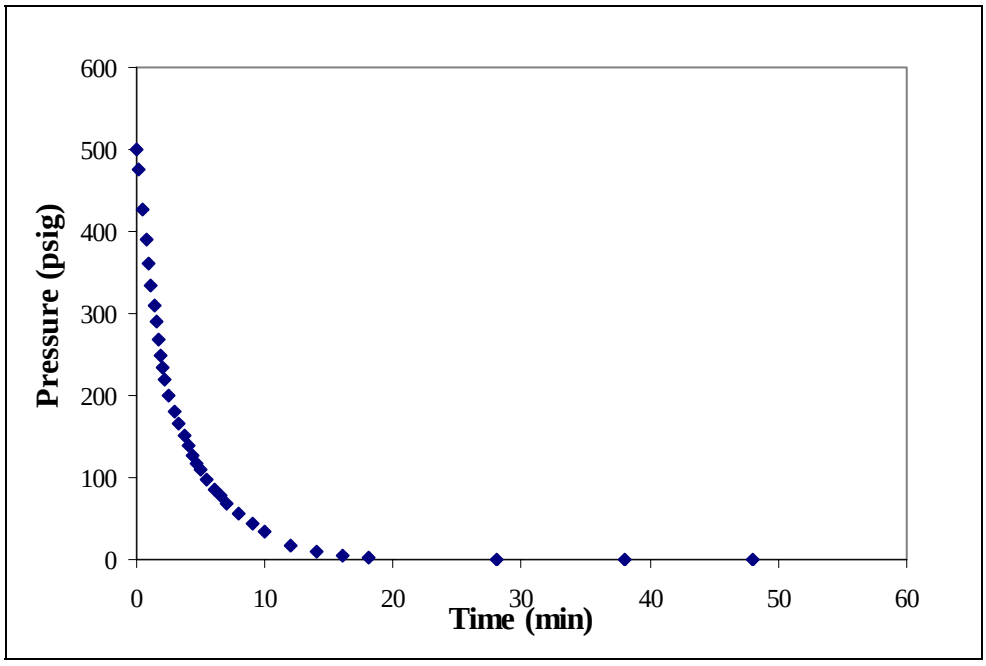

Figure 4.7: ANG storage pressure history during dynamic discharge using palm shell AC

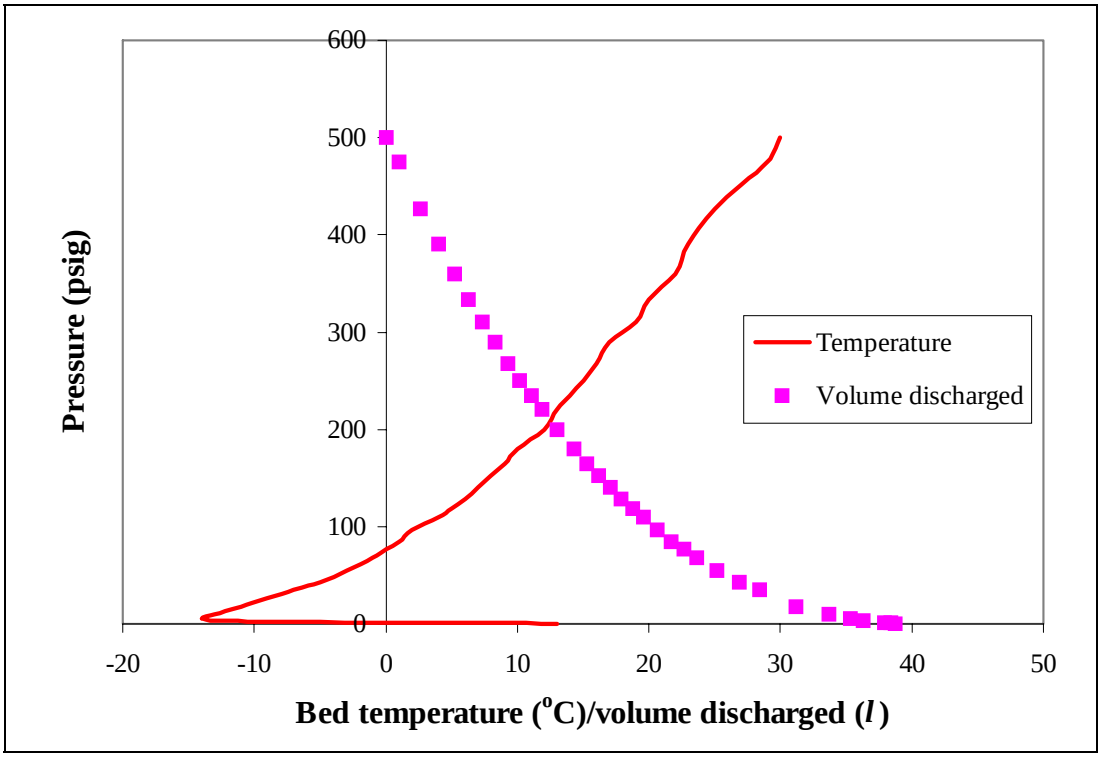

Figure 4.8: Pressure drop vs. bed temperature and volume of methane during dynamic discharged using palm shell AC

As shown in Figure 4.8, the adsorbent bed temperature begins to drop as soon as the stored gas is released. Temperature drops exponentially as storage pressure decreases and become more drastic as pressure approaching zero on gauge scale. Upon achieving 0 psig, the bed temperature begins to recover gradually to ambient value, as illustrates by the horizontal temperature line at 0 psig in the figure. As a result, a small amount of gas is gradually desorbed from the ANG vessel. However, as shown in Figure 4.8, this amount is not significant and it is delivered in an extremely small rate. Therefore, the effective delivery capacity is measured as the amount of gas discharged between 500 psig and the immediate atmospheric pressure.

4.1.2.2 Effect of Discharge Flow Rate

The rate of gas discharged from the adsorbent-filled vessel affect the delivery performance of the ANG storage. During the discharging of the palm shell AC

adsorbent-filled storage at different flow rates, it was learned that a slower discharge flow rate yields a higher gas delivery from the storage. Table 4.4 shows the delivery capacity of palm shell AC-filled storage obtained at different flow rates. Discharging the gas at 1.0 l/min yields 75.8 *l/l* of gas volume compare to 71.4 *l/l* at 6.0 l/min and 63.0 *l/l* at 10.0 l/min.

Table 4.4: Delivery capacity of palm shell AC at different flow rates

Flow rates	Delivery Capacity at 0 psig (*l/l*)
1.0 l/min	75.8
6.0 l/min	71.4
10.0 l/min	63.0

Figure 4.9 illustrates the effect of discharging rate on gas delivery. It shows the storage temperature profile in conjunction with gas delivery during discharge at different flow rates. The curves indicate that the higher the flow rate, the greater the temperature drops and the lower the delivery capacity obtained. It also shows that the total amount of gas delivered during the process to achieve thermal equilibrium, that is, during temperature recovery from the minimum level (depletion), is greater for slower discharge than for faster discharge (although both amounts is rather small compared to the amount discharged between 500 psig and the immediate depletion pressure). When discharging at 1.0 l/min, this amount of about 10% of the total amount of gas discharged while at 6.0 and 10.0 l/min, this amount is about 8% and 3% respectively. This is because at faster discharging rate, the storage system reaches a lower temperature. Since low temperature promotes adsorption, a lower temperature achieved at faster discharging rate causes more gas molecules tend to remain adsorbed than at a slower rate which yield a higher temperature (Komodromos *et al.*, 1992).

Figure 4.10 shows the adsorbent bed temperature profile at different discharge flow rate. It shows that the rate and the extent of temperature drop are greater for a faster discharge than a slower discharge. During discharge at slow rate of 1.0 l/min, bed temperature drops from 30 ^{o}C to the minimum value of –14 ^{o}C in 16 minutes while at moderate discharging rate of 6.0 l/min, temperature drops from 30

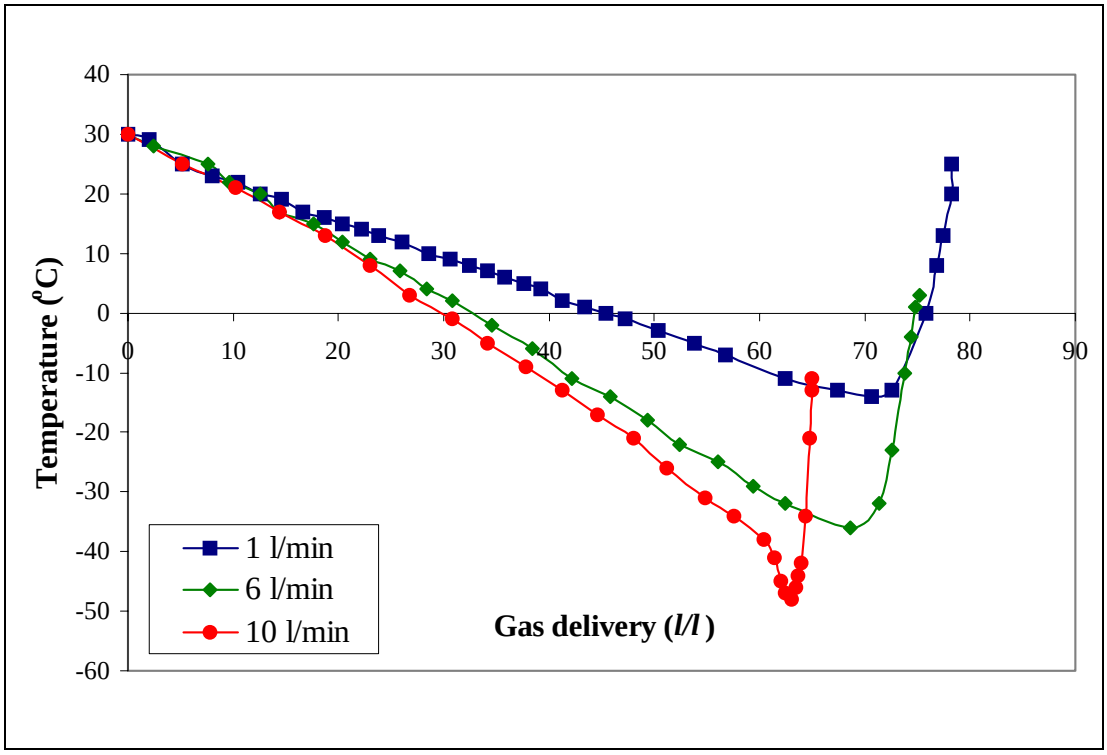

Figure 4.9: Effect of discharging rate on gas delivery using palm shell AC

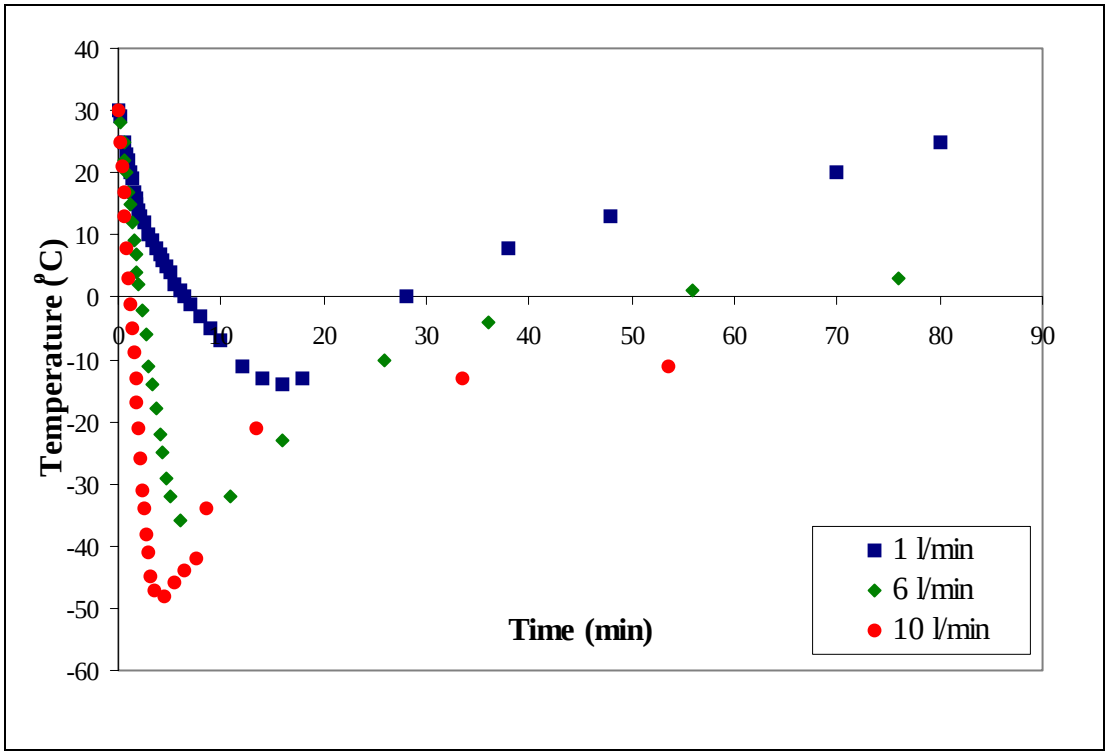

Figure 4.10: Palm shell AC adsorbent bed temperature profile at different discharge flow rate

^{o}C to the minimum –36 ^{o}C in 6 minutes. When discharging at 10.0 l/min, which depicted a fast rate, temperature falls 78 ^{o}C in 4.5 minutes from 30 ^{o}C to the minimum –48 ^{o}C. When the ANG storage reaches these very low temperatures, it is observed that fine ice film is formed, coating around the vessel wall. This happens due to condensation of water vapor from the surrounding air on the vessel wall that reaches the freezing temperature of the water vapor. After reaching the minimum points, the bed temperature for all runs begins to recover gradually in a very much longer period of time as a result of environmental heating in which the system is achieving thermal equilibrium with surrounding. As temperature gradually returns to ambient, the thin ice film slowly melts away and completely disappears upon reaching room temperature.

As mentioned before, temperature fall along with gas exhaustion happens due to the effect of the heat of desorption. The faster the discharging rate, the more methane molecules are desorbed out of the adsorbent substrate and a greater amount of heat of desorption is required by the system with time (Mota *et al.*, 1995). Therefore, a faster discharge is causing the temperature of the ANG system to drop lower because greater amount of the heat of the system is consumed. However, this is not the case under slow discharging rate. When discharging rate is slow enough, heat from the surroundings is permitted to flow into the system before the heat of the system is use up (Sejnoha *et al.*, 1995). In addition, when the stored gas is discharged faster, more gas is leaving the closed vessel with time and subsequently deteriorates the pressure, which also contributes to the temperature drop since pressure is proportional to temperature.

4.2 Storage Characteristic Study

When methane is charged into the ANG vessel, part of the gas is adsorbed on the adsorbent substrate and the other fills the free or void volume between adsorbent particles and within large pores. Therefore the total amount of gas stored inside the ANG storage is consist of the amount adsorbed and the amount of gas compressed. Since gas under compressed state is not contributing to the enhancement of methane

storage density at moderate pressure, then the significant measure of the adsorbent capability is the amount of gas adsorbed by the adsorbent substrate within the ANG vessel. This capacity measure is different from the ANG vessel storage capacity which includes the compressed gas. To differentiate the fraction of gas stored in adsorbed state and the fraction stored as compressed gas, the amount of gas adsorbed within the ANG vessel is calculated and its adsorption isotherm is plotted. To have a high ANG gas storage capacity, the amount of gas stored under adsorbed state must be maximum. Since adsorption is temperature sensitive, it is best to carry out gas charging under isothermal condition. However, it is not possible to perform isothermal discharge in realistic operation because at any finite discharge rate will result in temperature drop which is detrimental to gas desorption, unless we have a certain heat exchanger facility to control the storage temperature (Chang and Talu, 1996). Therefore, study on characteristic of gas uptake and delivery becomes important to identify the dynamic behavior of the ANG storage during charge and discharge.

4.2.1 Adsorption Isotherm

The experimental results for gas uptake under isothermal charging for the adsorbents tested are listed previously in Table 4.1. The amounts of gas uptake in the table are the working capacity of the adsorbent-filled storage and represent the amount of gas charging from 0 to 500 psig. Table 4.5, however, listed the absolute amount of gas stored by the adsorbent-filled storage that represent the amount of gas charging from vacuum to 500 psig or in particular, from 0 to 514.7 psia. Table 4.5 listed isothermal storage capacity for only three of the adsorbents tested, namely palm shell AC, MS zeolites (powder) and silica gel. Darco AC and MS zeolites (powder) are not studied since the above three already represent different types of adsorbent which are carbon-based, zeolites and silica gel.

The amounts of adsorbed gas in Table 4.5 are calculated from equation 2.12 (Malbrunot *et al.*, 1996). Details of the calculations are placed in Appendix C. For palm shell AC, the total amount of gas stored at 514.7 psia under isothermal charging

Table 4.5: Isothermal storage capacity for each type of adsorbent tested

Adsorbent	Gas stored between 0 and 514.7 psia		
	Amount uptake (g/*l*)	Amount adsorbed (g/*l*)	Volume adsorbed (*l*/g of adsorbent)
Carbon-based palm shell	66.65	58.10	0.18
Molecular sieve zeolites	37.24	27.30	0.08
Silica Gel	29.52	20.14	0.06

is 66.65 g/l. Since this is the amount charged from vacuum, it is greater than the amount listed in Table 4.1 which is 58.23 g/l. The difference between these two capacities is 8.42 g/l and it suggests that the amount of gas stored between vacuum (0 psia) and atmospheric pressure (14.7 psia) is about 13% of the total gas uptake. Meanwhile the amount of gas that is actually adsorbed within palm shell AC adsorbent is 58.10 g/l and it comprises of 87% of the total gas uptake while another 13% of the stored gas is under compressed state. Hence, the adsorptive capacity of this activated carbon is equivalent to 0.18 liter of methane per gram of adsorbent loaded. For molecular sieve zeolites, the absolute amount of gas uptake at 514.7 psia is 37.24 g/l compare to 34.58 g/l stored between atmospheric pressure and 514.7 psia. Approximately 7% of the total gas is stored between vacuum and atmospheric pressure. The amount of gas adsorbed within the zeolites substrate is 27.30 g/l which comprises of 73% of the total gas uptake while another 27% is stored as compressed gas. These values means the adsorptive capacity of MS zeolites is equivalent to 0.08 liter of methane stored per gram of zeolites loaded. For silica gel, the absolute amount of gas uptake at 514.7 psia is 29.52 g/l compared to 28.50 g/l stored between atmospheric pressure and 514.7 psia. Approximately 3.5% of the total gas is stored between vacuum and atmospheric pressure. The amount of gas adsorbed within the silica gel substrate is 20.14 g/l which comprises of 68% of the total gas uptake while another 32% is stored as compressed gas. Therefore, the adsorptive capacity of silica gel is 0.06 liter of methane stored per gram of zeolites loaded.

The adsorption isotherm of methane adsorbed on the adsorbents listed in Table 4.5 is shown in Figure 4.11. It shows the amount of gas adsorbed on those adsorbents in conjunction with pressure elevation within the ANG vessel during

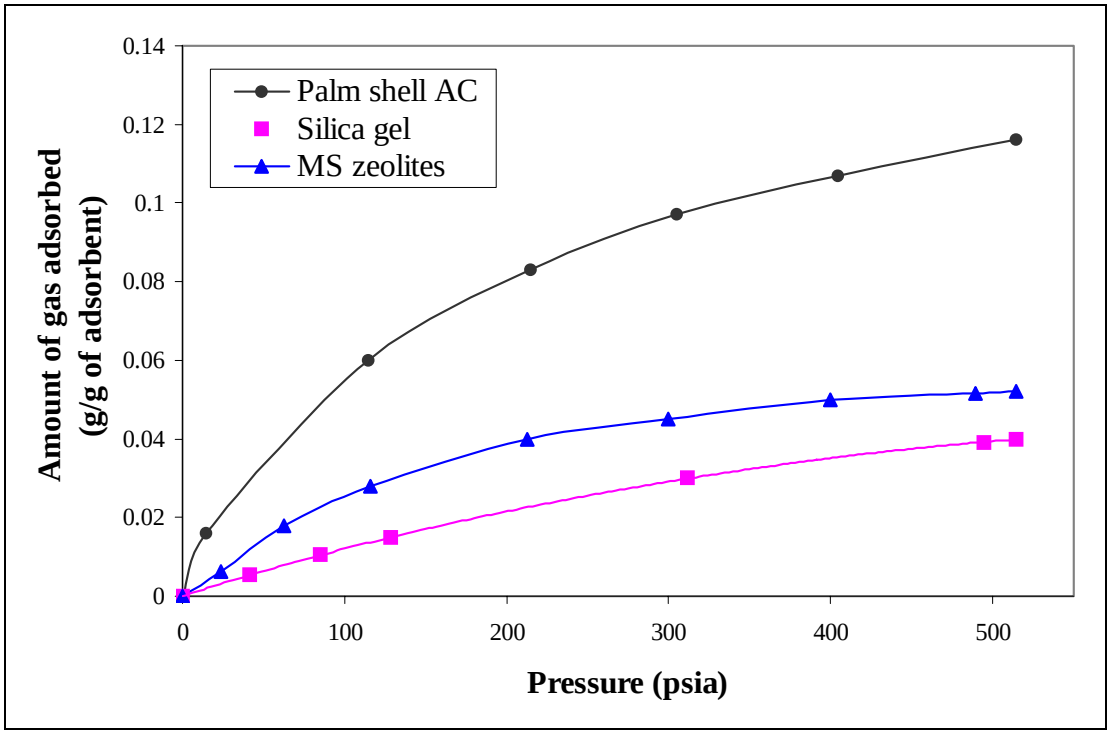

Figure 4.11: Methane adsorption isotherm on different type of adsorbents

charging at isothermal condition. During the first 10% of pressurization, we can see that palm shell AC adsorbs about 35 mg/g of gas while MS zeolites and silica gel only capable of 14 and 5 mg/g respectively. At this level, palm shell AC adsorbs 60% more gas than MS zeolites and 86% more than silica gel. At 50% of pressurization, AC adsorbs about 90 mg/g of gas while MS zeolites and silica gel adsorb about 40 and 25 mg/g of gas respectively. Up to this point, palm shell AC is capable of 56% more adsorption than MS zeolites and 72% more than silica gel. When pressurization is stopped at 514.7 psia (500 psig), palm shell AC adsorbed 120 mg/g of gas, which is about 58% more than MS zeolites and 67% more than silica gel that adsorbed 50 and 40 mg/g of gas correspondingly. Carbon-based palm shell AC obviously has a higher adsorptive capacity at all pressurization level compared to MS zeolites and silica gel. This is because activated carbon adsorbent has a larger surface area and micropore volume than zeolites and silica gel (refer to Table 3.1). In addition, according to Cracknell *et al.* (1993), activated carbon has a more suitable pore structure for methane adsorption than other type of adsorbents. Meanwhile silica gel has the poorest adsorptive capacity among the above adsorbents. It exhibits the lowest adsorptive capacity at all pressurization level. This poor performance is due to small micropore volume that silica gel had, as listed in Table 3.1 of Chapter

III since gas adsorption follows micropore-filling mechanism (Marsh, 1987). The whole accessible volume present in the micropores may be regarded as adsorption space and therefore, small micropore volume leads to less adsorption.

4.2.2 Dynamic of Gas Uptake and Delivery

The characteristic of methane uptake and delivery from the ANG storage during charge and discharge is illustrated in Figure 4.12. The figure shows the amount of gas uptake into the ANG storage in conjunction with pressurization up to 514.7 psia under isothermal condition and the reverse paths due to gas discharge from the ANG storage under both isothermal and dynamic condition. The figure shows that a considerable amount of gas is still remaining in the storage at the atmospheric pressure, which is the lowest depressurization, even under ideal (isothermal) discharge. This amount is about 15 % of the total storage capacity. This proportion of gas is quite strongly held in the adsorbent micropores and can only be delivered by unnatural means, which are by evacuating below atmospheric pressure or by heating the adsorbent (Komodromos *et al.*, 1992). This residual amount is called ‘cushion gas’. However, the residual amount left at immediate depletion of dynamic discharge is greater than the isothermal discharge because additional residual amount, about 9 % of the storage capacity, existed due to inefficient gas delivery. This additional quantity are the result of temperature fall discussed previously and it must be differentiate from the cushion gas which is the result of charging from vacuum to atmospheric pressure prior to the actual charging to the target pressure.

As shown in Figure 4.12, discharging the stored gas continuously (under dynamic condition) yield lesser amount of delivered gas than under isothermal discharge. The gap between the curves for isothermal and dynamic discharging path in the figure represent the amount of gas trapped within the adsorbent during dynamic discharge. As discussed in the previous section, the temperature behavior and the discharging rate are contributing to this condition. Note that the amount of gas left under dynamic discharge increases with depressurization. This happens

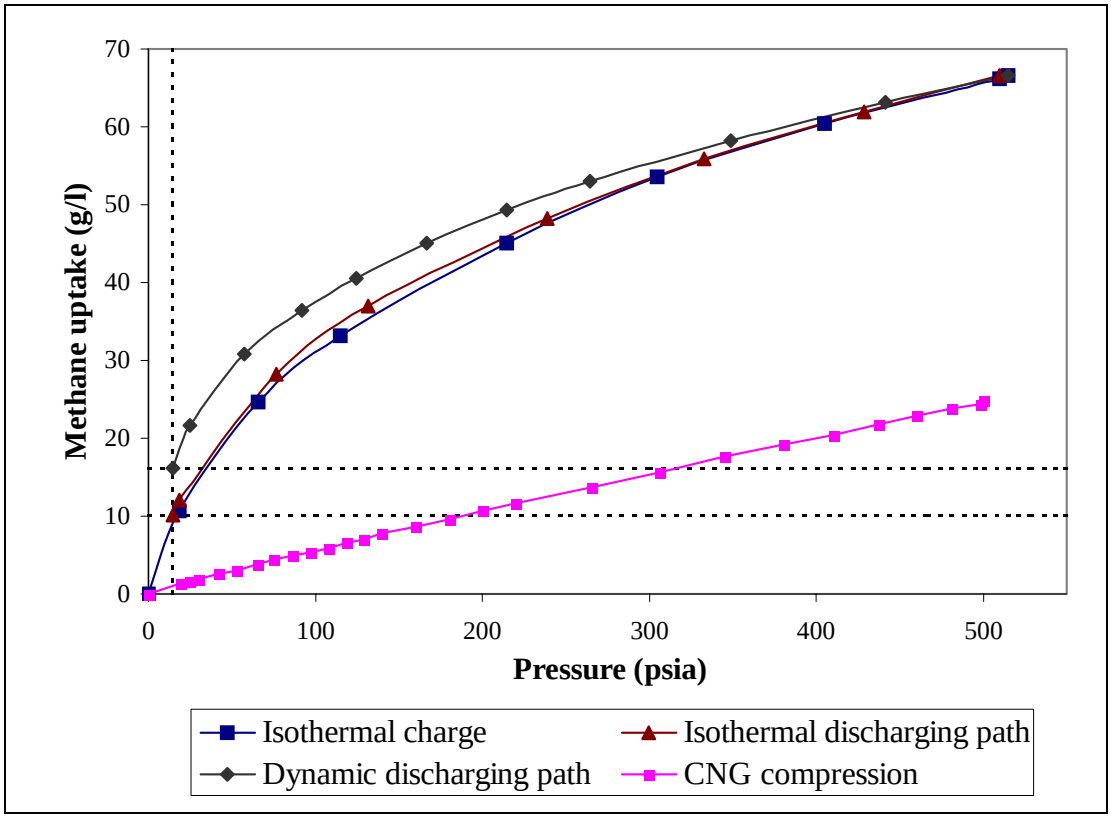

Figure 4.12: Characteristic of ANG storage during charge and discharge using palm shell AC

because as the pressure decreases, the temperature also falls down. As storage temperature getting lower, more gas is trapped within the adsorbent substrate since lower temperature promotes adsorption rather than desorption (Komodromos *et al.*, 1992). The straight line in the figure represent gas uptake for empty vessel or CNG compression. Obviously, at this range of relatively low pressure (compared to 3600 psig operating pressure of CNG storage), ANG storage stores about three times higher gas capacity than CNG storage.

For an ANG system operating under dynamic condition, storage temperature and the amount gas uptake/discharged vary significantly throughout the charge and discharge cycle. Figure 4.13 illustrates ANG parametric profile during charge and discharge at 6.0 l/min. The temperature rises exponentially as the amount of methane charged into the vessel increases with pressurization. As storage pressure approaching 35 atm (500 psig), gas uptake into the ANG vessel begins to level off while the temperature falls gradually after reaching a maximum rise. Interestingly,

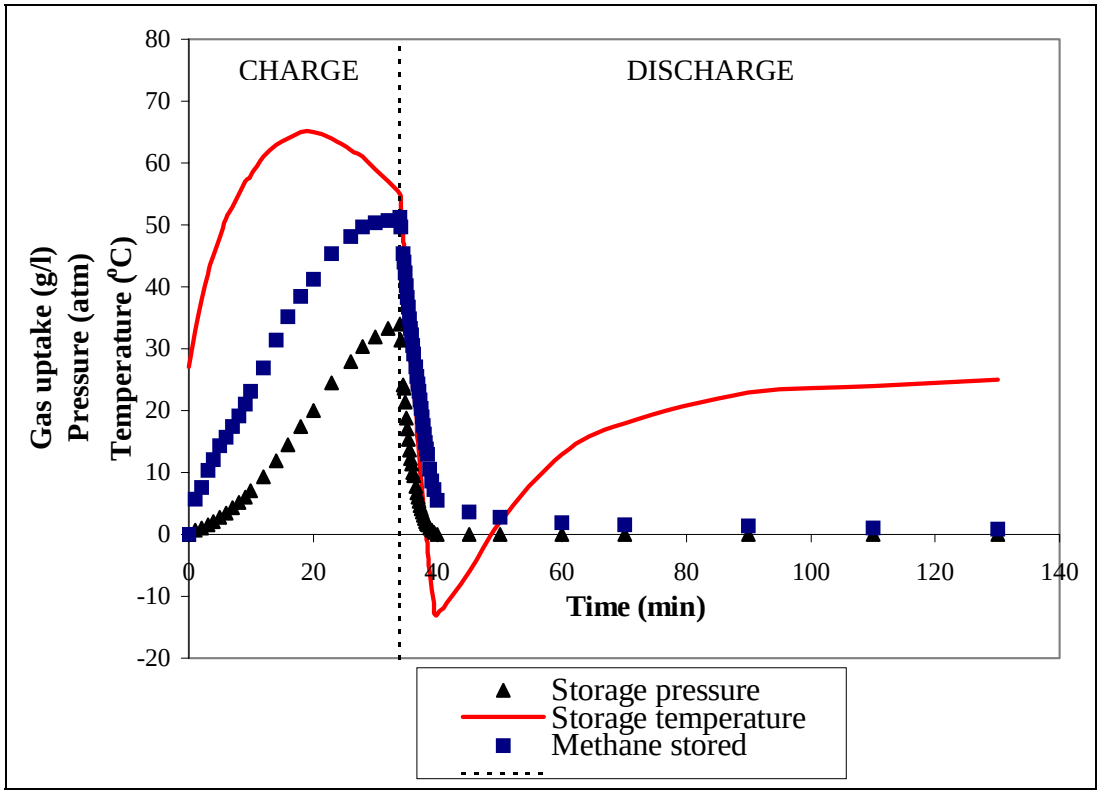

Figure 4.13: Charge and discharge profile of ANG storage using palm shell AC adsorbent

the temperature did not continue to rise when pressure approaching 35 atm but instead beginning to gradually fall. The leveling off in gas uptake suggested that the increment of gas uptake is due to mostly gas compression rather than adsorption when adsorbent micropores are getting fully occupied. Consequently, the amount of heat of adsorption generated decreases as adsorption lessens. As the rate of heat dissipation increases while heat generation decrease, the temperature begins to gradually fall. Therefore, the temperature rise is limited by the charging duration which permits the heat generated to dissipate before gas uptake finishes at 500 psig (Sejnoha *et al.*, 1995).

On the other hand, when the ANG storage is discharged upon finishing the filling process, as might be the situation of a vehicle that moves immediately after refueling (Remick and Tiller, 1985), the pressure in the vessel begins to drop as the gas leaves the storage and desorption of the stored gas leads to a sharp temperature fall. The rate of pressure and temperature drop is dictated by the discharging rate (in

vehicle application, depending on rate of engine demand) (Mota *et al.*, 1997) and the faster the discharging rate, the sharper the pressure and temperature drop (Remick and Tiller, 1985). In this study, the results show that the temperature falls very much and even well below 0 ^{o}C for carbon-based adsorbent such as palm shell AC and Darco AC. When the system reaches depletion pressure (0 or nearly 0 psig), a proportion of gas still remains on the adsorbent because of low temperature at this point. After reaching the lowest level, the temperature begins to recover gradually to ambient condition to achieve thermal equilibrium with the surrounding, and this causes the residual gas to be slowly desorbed over a much longer duration or in other words, in an extremely small rate.

4.3 Cyclic Test

In order to be reliably utilized for ANG storage, an adsorbent should perform consistent capacity in storing and delivering the amount of gas under repeated operation. In this work, each type of adsorbent is charged and discharged at slow rate (1.0 l/min) for 3 consecutive cycles to evaluate their performances under repeated operation. However, the cyclic test performed in this study is just a simple and an introductory one just to address the aspect of adsorbent performance and friability under repetitive operation. To study more comprehensive on the cyclic performance of the adsorbents, such as adsorbent life span or reliability for prolonged ANG storage application, further studies and more extensive data collections need to be carried out. Furthermore, the adsorbent used for cyclic test need to be solidified and well packed into the ANG vessel as discussed previously in page 83. In past studies, the cyclic tests performed on solidified adsorbents last between 20 and up to 100 cycles (Elliott and Topaloglu, 1986; Mota *et al.*, 1999). Apparently, such an extensive experimental works is beyond the scope this study.

Table 4.6 shows the storage and delivery capacities of each adsorbent under repeated charging/discharging and Table 4.7 shows their delivery ratio for each cycle. From Table 4.6, obviously that under cyclic operation, the adsorbents performances had deteriorated. As we can see, the dynamic storage capacity of every

Table 4.6: Storage and delivery capacity under cyclic operation

		Palm shell AC	Darco© AC	MS zeolites	Silica gel
Storage Capacity (*l*/*l*)	Cycle 1	85.74	54.96	47.94	43.53
	Cycle 2	76.10	52.41	45.57	42.75
	Cycle 3	71.10	49.77	42.78	41.20
Delivery Capacity (*l*/*l*)	Cycle 1	75.80	49.60	46.00	40.60
	Cycle 2	72.60	48.40	44.40	40.40
	Cycle 3	70.00	47.80	42.00	40.20

Table 4.7: Delivery ratio of different type of adsorbents under cyclic operation

	Palm shell AC	Darco© AC	MS zeolites	Silica gel
Cycle 1	0.88	0.90	0.96	0.93
Cycle 2	0.95	0.92	0.97	0.95
Cycle 3	0.98	0.96	0.98	0.98

adsorbent has decreased cycle upon cycle and so do the delivery capacity. Meanwhile, as the cycle continues, delivery ratio of these adsorbents on the contrary, has increased as shown is Table 4.7. Overall, although the capacities of the adsorbents had diminished, but their efficiency in delivering the stored gas on repetition had improved. However, it does not mean that the dynamic efficiency of the ANG storage has get better. Of course as the dynamic storage and delivery capacity decrease along the cycles, dynamic efficiency will also decrease. This is because dynamic efficiency measurement is based on the initial maximum storage capacity achievable and therefore reflects how far the efficiency has changed from the beginning while the delivery ratios listed in Table 4.7 represent efficiency change cycle by cycle. In other words, delivery ratio reflects the deliverability of each adsorbent as the cycle continues.

It is not surprise to know that adsorbents performances deteriorate with cyclic operation because of the nature of the ANG storage itself. As we know, ANG storage operates under a high pressure. Though the adsorbent-filled vessel could be charged slow enough so that gas from the higher-pressure supply will not causing damage to

the adsorbent surface, yet as the pressure builds up inside the vessel, the adsorbent substrate is gradually damaged.

Contrary to the capacities deterioration, the delivery ratio of the adsorbents had improved because the storage system is approaching a cyclic steady state when it operates on extended time. According to Mota (1999), when a cyclic steady state is reached, net charge capacity and net deliverable capacity are identical where the gas stored in the vessel during charge is fully delivered during discharge. That is why, as the cycle continues, the delivery ratio increases because the system is approaching a state where storage capacity equal to delivery capacity (delivery ratio =1). Therefore, since delivery capacity always decreases with cycle, then at steady state, the amount of gas storable will be minimum. However, values of delivery ratio obtained in this experiment contain experimental errors and subjected to the frailty of the adsorbent used which are in granular and powder forms compared to the solidified adsorbent briquette used by Mota. In realistic condition, several cycles are necessary before cyclic steady state could be reached. Even though these values are too good to be accurate, but they did illustrate the fact that the storage system is approaching a steady state.

The factor that could be the reason of rapid increment of the delivery ratio is the friability of the granular and powder adsorbents used. Since these forms of adsorbent are easily damaged by high pressure, as the adsorbent pores gradually ruined, the gas charged inclines to be compressed rather than adsorbed. As a result, the amount of gas charged gradually equaling amount discharged because compressed gas is fully delivered during discharge.

The amount of gas uptake during the second or following cycles does not add up to the proportion of gas retained due to heat of desorption during discharged in the first or earlier cycles. This is because the ANG system is allowed to return to ambient temperature at the end of the discharge phase, which is the pre-charging condition before subsequent cycles is carried on. Therefore, the proportion of gas retained due to temperature drop is slowly desorbed out of the storage as temperature recovers to the initial condition.

4.4 Summary

For an ANG system operating under dynamic condition, when the vessel is filled with methane, there is a significant temperature rise as adsorption takes place on the adsorbent substrate. As storage pressure approaching 500 psig, gas uptake into the ANG vessel begins to level off while the temperature is falling gradually to room temperature after reaching maximum rise. On the other hand, when the ANG storage is discharged the storage pressure begins to drop and desorption of the stored gas leads to a sharp temperature fall. The rate of pressure and temperature drop is dictated by the discharging rate. The faster the discharging rate, the sharper the pressure and temperature drop. When the ANG system reaches depletion pressure (0 or nearly 0 psig), a proportion of gas still remains on the adsorbent because of low temperature at this point. The lower the temperature, the more gas left in the vessel at the immediate depletion level. Thereafter, temperature recovers gradually to achieve thermal equilibrium with surrounding and consequently, the residual gas is slowly desorbed in an extremely slow rate. Besides the thermodynamic factor of the ANG system itself, adsorbent physical properties also play an important role for effective adsorptive storage. An adsorbent that posses a larger surface area and micropore volume, and a minimum void fraction will provide higher gas storage capacity. In addition, adsorbent with high heat capacity but low heats of methane adsorption will exhibit lesser temperature rise during adsorption and lesser temperature drop during desorption, which leads to better delivery efficiency. From the experimental results, palm shell activated carbon has the highest storage capacity while silica gel has a better delivery efficiency than the others. Meanwhile, under repetitive charge and discharge, adsorbents performances deteriorate as they are gradually damaged because of high-pressure operation.

CHAPTER V

CONCLUSION AND RECOMMENDATION

Different types of commercially available adsorbents were tested as adsorbent media for adsorbed methane storage. The storage and delivery capacity of methane of the adsorbent-filled storage are measured using a 0.5 liter pressurized vessel and are carried out under isothermal and dynamic condition in which methane is charged into the vessel until 500 psig and discharged back to atmospheric pressure at different charge/discharge flow rates. The storage and delivery performance of the adsorbents is influence by both the adsorbent physical properties such as surface area, micropore volume, interparticle void, and their thermodynamic properties such as heat capacity and heat of methane adsorption generated during adsorption and consumed during desorption. Palm shell AC adsorbent that possesses the largest surface area and micropore volume among the adsorbents tested yields the highest storage capacity of 87.35 *l/l* under isothermal condition and 85.74 *l/l* under dynamic condition at slow charging rate. On the other hand, silica gel adsorbent that has a high heat capacity but generating low heat of methane adsorption shows the highest delivery efficiency of 0.95 during slow discharge. At faster charging/discharging rate, the storage and delivery capacities achieved are lower than at slower rate as temperature changes more significantly at faster rate. Under cyclic operation, the adsorbents performance deteriorates due to high-pressure operation that damages the adsorbents structure.

According to the findings of this study, the adsorption capacity of the adsorbent is also influence by the adsorbent packing density and the structure of

adsorbent mass. Since adsorbents used in this study have low packing density and are frail under high-pressure operation, at large they yielded low storage capacities compared to the target capacity and performed poorly in cyclic operation. Therefore, it is recommended that an adsorbent employed for ANG storage should be solidified to minimize its loading voids (maximum packing density) and to strengthen its structure in order to achieve a higher ANG storage capacity and to withstand high-pressure cyclic operation. In addition, since gas adsorptive storage is very sensitive towards temperature while ANG thermal behavior is influenced by gas flow rate, hence ANG system should be equipped with heat transfer mechanism if the ANG storage is to be used in practical application in order to control the storage temperature because gas flow rate cannot be freely manipulated (it is dictated by fuel demand) to minimize the thermal problem. It is also recommended that ANG testing should be done in a large scale to meet practical specification such as for vehicle application.

REFERENCES

Abadi, Massoud Rostam (1996). “Novel Carbons From Illinois Coal For Natural Gas Storage.” Final Technical Report, ICCI Project No. 95 – ¼. 2A-4.

Alcaniz-Monge, J., de la Casa-Lillo, M. A., Cazorla-Amoros, D., and Linares-Solano, A. (1997). “Methane Storage in Activated Carbon.” *Carbon*. **35** (2). 291-297.

Asiah Hussain and Mohd.Yusni Mohd. Yunus (1992). “Kajian Sifat Permukaan dan Keliangan Serta Kesan Terma Terhadap Karbon Teraktif.” Universiti Teknologi Malaysia: Seminar Penilaian Program IRPA & UPP.

Barton, S. S., Dacey, J. R., and Quinn, D. F. (1984). “High Pressure Adsorption of Methane on Porous Carbons.” Fundamental of Adsorption. Engineering Foundation Conference, New York: AIChE

Be Vier, W. E., Mullhaupt, J. T., Notaro, F., Lewis, J. C. and Coleman, R. E. (1989). “Adsorbent-Enhances Methane Storage for Alternate Fuel Powered Vehicles.” SAE Future Transportation Technology Conf. and Exposition, Vancouver.

Brady, T. A., Rostam-Abadi, M., Sun, J., and Rood, M.J. (1995). “Development of Adsorbent Carbon from Waste Tire for Natural Gas Storage and Multicomponent Air Pollution Control.” Proc., Annual Meeting - Air Waste Management Association. 88th (Vol. 16). 95-TP51.02.

Brown, P. (Ed.) (1995). “New Promise for Adsorbent for Gaseous Fuel Storage.” CATF Review Newsletter, Issue No. 20, January, Vancouver: BC Research Inc.

Calgon Carbon Corporation (1998). Company Corporate Profile.

Chang, K. J. and Talu, O. (1996). "Behavior and Performance of Adsorptive Natural Gas Storage Cylinders During Discharge." *Applied Thermal Engineering*. **16**. 359-374.

Chemiviron Carbon Industry (1998). Company Corporate Profile.

Chen, X.S., McEnaney, B., Mays, T. J., Alcaniz-Monge, J., Cazorla-Amoros, D., and Linares-Solano, A. (1997). "Theoretical and Experimental Studies of Methane Adsorption on Microporous Carbon." *Carbon*. **35** (9). 1251-1258.

Chew, Kok Hoong (1999). "Kajian Ke Atas Silinder Tekanan Rendah untuk Kenderaan Gas Asli." Universiti Teknologi Malaysia: Projek Penyelidikan Sarjana Muda.

Cook, T. L. and Horne, D. B. (1997). "Low Pressure Adsorbed Natural Gas Vehicle Demonstration." 20th World Gas Conference, Copenhagen.

Cook, T. L., Komodromos, C., Quinn, D.F., and Ragan, S. (1999). "Adsorbent Storage for Natural Gas Vehicles." Carbon Materials for Advanced Technologies (Burchell, T. ed.). Amsterdam: Elsevier

Cracknell, R. F., Gordon, P., and Gubbins, K. E. (1993). "Influence of Pore Geometry on the Design of Microporous Materials for Methane Storage." *J. Phys. Chem.* **97**. 494-499.

Deitz, V. R. (1987). "Summary of Workshop D - Adsorbents Carbon: Structure, Preparation and Application to Gaseous System." *Carbon*. **25** (1). 155-156.

Dubinin, M. M. (1975). "Progress in Surface Membrane Science." (Cadenhead, D. A. ed.) New York: Academic Press. 1-70.

Dubinin, M. M. (1987). “Adsorption Properties and Microporous Structure of Carbonaceous Adsorbents.” *Carbon*. **25** (5). 593-598.

Elliott, D. and Topaloglu, T. (1986). “Development of New adsorbent Material for The Storage of Natural Gas On-Board Vehicles.” Gaseous Fuel For Transportation I, Conference Paper, Vancouver: Institute of Gas Technology.

Friend, D. G. (1989). “Thermophysical properties of methane.” *J. Phys. Chem. Ref. Data*. **18**. 583.

Gas Malaysia Sdn. Bhd. (1995). Company Corporate Profile.

Golovoy, A. (1983). Proc. Compressed Natural Gas. Pittsburgh: Society of Automobile Eng. 39.

Gubbins, K. E. and Jiang, S. (1997). “Adsorbing Work: Design of New Material”. University of California.

Gurdeep, H. (1974). “Adsorption and Phase Rule.” Meerut: Goel Publishing House.

Horstkamp, S. W., Starling, K. E., Harwell, J. H., and Mallinson, R. G. (1997). “High-Energy Density Storage of Natural Gas in Light Hydrocarbon Solutions.” *AIChE Journal*. **43** (4). 1108-1113.

Inform, Inc. (1992). “Natural Gas Factsheet.” New York.

Jasionowski, W. J., Tiller, A. J., Fata, J. A., Arnold, J. M., Gauthier, S. W., and Shikari, W. A. (1989). “Charge/Discharge Characteristics of High-Capacity Methane Adsorption Storage Systems.” Int. Gas Research Conf., Tokyo.

Jiang, S., Zollweg, J. A., and Gubbins, K. E. (1994). “High-Pressure Adsorption of Methane and Ethane in Activated Carbon and Carbon Fibers.” *J. Phys. Chem*. **98**. 5709-5713.

Jonas, L. A. (1987). “Summary of Workshop D - Adsorbents Carbon: Structure, Preparation and Application to Gaseous System.” *Carbon*. **25** (1). 155-156.

Komodromos, C., Pearson, S., and Grint, A. (1992). “The Potential of Adsorbed Natural Gas (ANG) for Advanced On-board Storage in Natural Gas-Fueled Vehicles.” 1992 International Gas Research Conference, Vancouver.

Komodromos, C., Fricker, N., and Horne, D. B. (1994). “Development of Carbon Adsorbent for Low Pressure Natural Gas (ANG) in Natural Gas Vehicles.” IANGV Conference, Vancouver.

Liss, W. E., Okazaki, S., Acker, Jr., G. H., and Moulton, D. S. (1992). “Fuel Issues for Liquefied Natural Gas Vehicles.” Proc. Soc. Automotive Eng., San Francisco.

Malbrunot, P., Vidal, D. and Vermesse, J. (1996). “Storage of Gases At Room Temperature by Adsorption at High Pressure.” *Applied Thermal Engineering*. **16**. 375-382.

Marsh, H. (1987). “Adsorption Methods to Study Microporosity in Coals and carbons – A Critique.” *Carbon*. **25** (1). 49-58.

Marsh, H. (1987). “Summary of Workshop C - Porosity in Carbon Adsorbents.” *Carbon*. **25** (1). 151-154.

Matranga, K. R., Stella, A., Myers, A. L., and Glandt, E. D. (1992*). Separation Sci. Tech.* **27**.1825-1831.

Matranga, K. R., Myers, A. L., and Glandt, E. D. (1996). “Storage of Natural Gas By Adsorption On Activated Carbon.” *Applied Thermal Engineering*. **47**. 1569-1578.

MacDonald, J. A. F., and Quinn, D. F. (1996). “Adsorbents for Methane Storage Made by Phosphoric Acid Activation of Peach Pits.” *Carbon*. **34** (9). 1103-1108.

Megyesy, E. F. (1989). “Pressure Vessel Handbook.” Tulsa: Publishing Inc.

Menon, V. C. (1996). “Role of Selected Sol-Gel Processing Parameters on Surface Area and Hydrophobicity of Silica Xerogels (Methane).” The Pennsylvania State University: Ph. D Thesis.

Mohd. Farid bin Kammaruddin (1999). “Kajian Kemungkinan Penggunaan Karbon Teraktif Dalam Storan Gas Asli.” Universiti Teknologi Malaysia: Projek Penyelidikan Sarjana Muda.

Mota, J. B. P., Rodrigues, A. E., Saatdjian, E., and Tondeur, D. (1995). “A Simulation Model of a High-Capacity Methane Adsorptive Storage System.” *Adsorption*. **1**. 17-27.

Mota, J. B. P., Rodrigues, A. E., Saatdjian, E., and Tondeur, D. (1997). “Charge Dynamics of a Methane Adsorption Storage System: Intraparticle Diffusional Effects.” *Adsorption*. **3** (2). 117-125.

Mota, J. P. B, Rodrigues, A. E., Saatdjian, E., and Tondeur, D. (1997). “Dynamics of Natural Gas Adsorption Storage Systems Employing Activated Carbon.” *Carbon*. **35** (9). 1259-1270.

Mota, J. B. P. (1999). “Impact of Gas Composition on Natural Gas Storage by Adsorption.” *AIChE Journal*. **45**. 986-996.

Nelson, C. R. (1993). “Carbon Adsorbents for NGV Fuel Storage.” Chicago: Gas Research Institute.

O’Brien, R. N., and Turnham, B.D. (1990). “Methane Solubility and Methane Storage in Suitable Liquid Hydrocarbon Mixtures.” Proc. Soc. Automotive Eng., Detroit.

Otto, K. (1981). “Alternative Energy Sources.” Vol. 6. 241-260.

Parent, J. D. (Ed.) (1986). “Survey and History of the Gas Industry.” IGT Home Study Course, Chicago: Institute of Gas Technology.

Parfitt, G. D., and Sing, K. S. W. (1976). “Characterization of Powder Surfaces.” London: Academic Press.

Parkyns, N. D., and Quinn, D. I. (1995). “Natural Gas Adsorbed on Carbon. Porosity in Carbons.” (Patrick, J. W. ed.). London: Arnold. Chapter 11, p. 291.

Perry, R. H. (Ed.) (1984). “Perry’s Chemical Engineer’s Handbook.” 6th Edition. New York: McGraw-Hill.

Pritchard, R., Guy, J. J., and Conner, N. E. (1977). “Handbook of Industrial Gas Utilization: Engineering Principle and Practice.” New York: Van Nostrand.

Quinn, D. F. (1990). “Carbon Adsorbent for Natural Gas.” Presentation at GURF Meeting, London.

Quinn, D. F., and MacDonald, J. A. (1992). “Natural Gas Storage.” *Carbon*. **30** (7). 1097-1103

Quinn, D. F., MacDonald, J. A., and Sosin, K. (1994). “Microporous Carbons as Adsorbents for Methane Storage.” 207th ACS National Meeting, San Diego, CA.

Remick, R. J., Elkins, R. H., Camara, E. H., and Buliez, T. (1984). “Advanced Onboard Storage Concepts for Natural Gas-Fueled Automotive Vehicles.” Rep. DOE/NASA/0327-1 prepared for U.S. Department of Energy and NASA, Washington.

Remick, R. J. and Tiller, A. J. (1985). “Advanced Methods for Low Pressure Storage of CNG.” Conference on Non-Petroleum Vehicular Fuels, Arlington VA.

Remick, R. J. and Tiller, A. J. (1985). “Heat Generation in Natural Gas Adsorption Storage System.” Gaseous Fuel for Transportation I, Conference Paper, Vancouver: Institute of Gas Technology.

Rodrigues, A. E., Levan, D. and Tondeur, D. (1989). “Adsorption: Science and Technology.” Dordrect: Kluver.

Sejnoha, M., Chahine, R., Yaici, W., and Bose, T. K. (1994). “Adsorption Storage of Natural Gas on Activated Carbon.” AIChE Meeting, San Francisco.

Sejnoha, M., Chahine, R., Yaici, W., Aube, F., and Bose, T. K. (1995). “Low Pressure Storage of Natural Gas by Adsorption on Activated Carbon.” 1995 International Gas Research Conference, Vancouver.

Senatoroff, N. K., and Forwalter, J. (1964). “Odorization and Gas Conditioning.” IGT Home Study Course, Chicago:Institute of Gas Technology.

Shakhashiri, B. Z. (2000). “Methane.” Workbook of General Chemistry, USA.

Sing, K. S. W., Everett, D. H., Paul, R. A. W., Moscou, L., Pierotti, R. A., Roquerol, J., and Siemieniewska, T. (1985). *Pure Appl. Chem.* **57**. 603-611.

Slejko, F. L. (1985). “Adsorption Technology.” New York: Marcel Dekker.

Smith, J. M., Van Ness, H. C., and Abott, M. M. (1996). “Introduction to Chemical Engineering Thermodynamics.” Fifth Edition. New York: McGraw-Hill. Smith, R. V. (1990). “Practical Natural Gas Engineering.” 2nd Edition. Tulsa: Pennwell Pub. Company.

Smirnova, L. F.,Bakaev, V. A. and Dubinin, M. M. (1987). “The Adsorption Potential of Argon in Slit-shaped Micropores of Activated Carbon.” *Carbon*. **25** (5). 599-602.

Spang, B. (1997). “Properties of Adsorbents.” About.com Network Chemical Engineering, USA.

Stodolsky, F., and Santini, D. J. (1993). “Fuel Up with Natural Gas.” *Chemical Technology*. **23**. 54-59.

Suzuki, M. (1990). “Adsorption Engineering.” Amsterdam: Elsevier.

Talu, O. (1992). “An Overview of Adsorptive Storage of Natural Gas.” Proceedings of International Conference on Fundamental of Adsorption (Suzuki, M. ed.). Kyoto. 655-662.

Tompkins, F. C. (1978). “Chemisorption of Gases on Metals.” London: Academic Press, Inc. 93-107.

Trent, R. E. (1995). “Fundamental of Adsorption.” Gas Conditioning Conference, Oklahoma.

Webster, C. E. (1999). “Modeling Adsorption: Investigating Adsorbate and Adsorbent Properties (Multiple Equilibrium Analysis)”. University of Florida: PhD Thesis.

Welder, G. (1970). “Chemisorption: An Experimental Approach.” London: Butterworth & Co Publishing Ltd.1-67.

Well, W. J. (1998). “Adsorption of Alkanes in Zeolites.” Technische Universiteit Eindhoven: PhD Thesis.

APPENDIX A1

Summary report of palm shell-derived activated carbon adsorbent surface analysis

1. Activated Carbon A

Specific surface area	: 1012.39 m^3/g
Pore volume	: 0.2142 cm^3/g
Average pore diameter	: 19.7696 Å

2. Activated Carbon B

Specific surface area	: 1107.8535 m^3/g
Pore volume	: 0.1647 cm^3/g
Average pore diameter	: 19.9606 Å

3. Activated Carbon C

Specific surface area	: 1773.9508 m^3/g
Pore volume	: 0.1583 cm^3/g
Average pore diameter	: 19.9825 Å

APPENDIX A2

Summary report of palm shell-derived activated carbon adsorbent surface analysis

1. Activated Carbon Darco (Powder)

Specific surface area	: 1488.1362 m^3/g
Pore volume	: 0/22515 cm^3/g
Average pore diameter	: 37.943 Å

2. Activated Carbon Darco (Granular)

Specific surface area	: 651.9622 m^3/g
Pore volume	: 0.01308 cm^3/g
Average pore diameter	: 49.7527 Å

APPENDIX A3

Summary report of MS zeolites (powder) adsorbent surface analysis

Molecular Sieve Zeolite Powder (MS-13X)

Specific surface area	: 435.9019 m^3/g
Pore volume	: 0.149395 cm^3/g
Average pore diameter	: 19.7790 Å

APPENDIX A4

Summary report of MS zeolites (beads) adsorbent surface analysis

Activated Carbon Darco (Powder)

Specific surface area	: 407.987 m^3/g
Pore volume	: 0.3514 cm^3/g
Average pore diameter	: 26.141 Å

Molecular Sieve Zeolite Beads (MS – 5A)

Specific surface area	: 403.188 m^3/g
Pore volume	: 0.12644 cm^3/g
Average pore diameter	: 27.3956 Å

APPENDIX A5

Summary report of silica gel adsorbent surface analysis

Silica Gel

Specific surface area	: 3792.25 m^3/g
Pore volume	: 0.90253 cm^3/g
Average pore diameter	: 62.1711 Å

APPENDIX B1

Experimental results of the isothermal adsorption

Table 1: Carbon-based Palm shell

Pressure at equilibrium (psia)	Room Temperature (^{o}C)	Gas uptake (g)	Gas uptake (g/l)
0	26	0	0
18.7	28	5.32	10.64
65.7	30	12.3	24.6
114.7	30	16.58	33.16
214.7	30	22.55	45.1
304.7	30	26.76	53.52
404.7	30	30.2	60.4
509.7	30	33.1	66.2
514.7	30	33.32	66.65

Table 2: MS zeolites (powder)

Pressure at equilibrium (psia)	Room Temperature (^{o}C)	Gas uptake (g)	Gas uptake (g/l)
0	25	0	0
23.7	28	1.9	3.8
62.7	27	5.32	10.64
115.7	28	8.47	16.94
212.7	29	12.52	25.04
299.7	29	14.86	29.72
399.7	30	16.97	33.94
489.7	29	18.17	36.34
514.7	28	18.62	37.24

Table 3: Silica gel

Pressure at equilibrium (psia)	Room Temperature (^{o}C)	Gas uptake (g)	Gas uptake (g/l)
0	26	0	0
41.7	27	1.77	3.54
84.7	28	3.42	6.84
128.7	27	4.92	9.83
311.7	27	10.41	20.82
494.7	28	14.38	28.76
514.7	28	14.76	29.52

Table 4: Carbon-based Darco

Pressure at equilibrium (psia)	Room Temperature (^{o}C)	Gas uptake (g)	Gas uptake (g/l)
0	27	0	0
34.7	29	5.23	10.46
73.7	30	8.26	16.52
120.7	30	10.75	21.5
172.7	30	12.87	25.74
312.7	30	17.04	34.08
414.7	29	19.5	39
515.7	28	21.6	43.2

APPENDIX B2

Experimental results of the dynamic charging

Table 1: Palm shell AC (charging at 1 l/min)

Cycle 1				Cycle 2				Cycle 3			
Time (min)	Pres. (psig)	Temp. (^oC)	Gas uptake (g)	Time (min)	Pres. (psig)	Temp. (^oC)	Gas uptake (g)	Time (min)	Pres. (psig)	Temp. (^oC)	Gas uptake (g)
0	0	28	0	0	0	25	0	0	0	25	0
5	10	35	3.24	5	9	32	1.82	5	9	32	1.66
10	17	38	4.26	10	17	35	3.2	10	16	35	2.97
15	25	40	5.22	15	27	38	4.17	15	25	37	3.93
20	35	41	6.23	20	38	39	5.19	20	35	38	4.95
25	46	42	7.26	25	50	40	6.03	25	47	39	5.88
30	60	43	8.31	30	62	40	6.89	30	58	40	6.83
35	71	43	9.4	35	75	40	7.79	35	72	40	7.63
40	85	43	10.41	40	90	41	8.67	40	86	40	8.48
45	100	43	11.51	45	105	41	9.62	45	100	41	9.39
50	122	43	12.56	50	121	41	10.48	50	117	41	10.26
55	135	43	13.66	55	138	40	11.66	55	135	41	11.25
60	150	43	14.73	60	157	40	12.68	60	153	41	12.03
65	170	42	15.82	65	177	40	13.74	65	173	40	12.87
70	190	42	16.75	70	197	40	14.77	70	195	40	13.8
75	210	42	17.78	75	218	39	15.79	75	215	40	14.77
80	230	41	18.81	80	240	39	16.66	80	235	39	15.56
85	250	41	19.75	85	260	39	17.5	85	255	39	16.37
90	270	40	20.66	90	280	38	18.35	90	278	39	17.29
95	290	40	21.53	95	300	38	19.16	95	298	38	18.07
100	310	39	22.34	100	322	37	19.87	100	320	37	18.78
105	329	38	23.05	105	340	37	20.52	105	340	37	19.43
110	347	38	23.83	110	360	36	21.22	110	360	37	19.96
115	365	37	24.47	115	378	36	21.79	115	377	36	20.5
120	380	37	25.02	120	395	35	22.34	120	395	35	20.98
125	396	36	25.53	125	408	35	22.84	125	410	35	21.37
130	410	36	25.95	130	423	34	23.27	130	425	34	21.79
135	430	36	26.57	135	435	34	23.69	135	438	34	22.15
140	448	35	27.1	140	445	34	23.93	140	450	34	22.5
145	465	35	27.65	145	455	33	24.21	145	460	33	22.72
150	481	35	28.04	150	463	33	24.41	150	470	33	22.95
155	495	34	28.4	155	470	32	24.6	155	478	32	23.24
157	500	34	28.58	160	483	32	25	160	485	32	23.4
				165	503	32	25.35	165	504	32	23.7

Table 2: Palm shell AC (charging at 6 and 10 l/min)

6 l/min				10 l/min			
Time (min)	Pres. (psig)	Temp. (^oC)	Gas uptake (g)	Time (min)	Pres. (psig)	Temp. (^oC)	Gas uptake (g)
0	0	27	0	0	0	27	0
1	0.61	33	2.86	0.5	8	33	1.45
2	1.02	38	3.82	1	12	36	2
3	1.57	42	5.2	1.5	17	40	2.56
4	2.11	45	6	2	23	43	3.19
5	2.79	48	7.17	2.5	30	45	3.8
6	3.47	51	7.83	3	37	48	4.42
7	4.29	53	8.7	3.5	44	50	5.03
8	5.1	55	9.58	4	52	53	5.61
9	5.99	57	10.53	4.5	61	55	6.24
10	7.14	58	11.55	5	70	57	6.9
12	9.32	61	13.41	5.5	80	59	7.52
14	11.84	63	15.68	6	90	61	8.22
16	14.43	64	17.52	6.5	100	62	8.86
18	17.35	65	19.23	7	112	63	9.5
20	20.07	65	20.64	7.5	125	65	10.24
23	24.5	64	22.7	8	136	66	10.92
26	27.9	62	24.08	9	164	68	12.5
28	30.28	61	24.87	10	191	70	14.16
30	31.98	59	25.2	11	222	71	15.9
32	33.34	57	25.33	12	253	72	16.92
34	34.02	55	25.59	13	287	73	18.6
				14	320	73	19.97
				15	354	74	21.32
				16	387	73	22.15
				17	418	73	22.88
				18	448	72	23.34
				19	474	71	23.95
				20	498	71	24.22
				20.5	507	70	24.38

Table 3: Darco AC (charging at 1 l/min)

Cycle 1				Cycle 2				Cycle 3			
Time (min)	Pres. (psig)	Temp. (^oC)	Gas uptake (g)	Time (min)	Pres. (psig)	Temp. (^oC)	Gas uptake (g)	Time (min)	Pres. (psig)	Temp. (^oC)	Gas uptake (g)
0	0	26	0	0	0	25	0	0	0	24	0
5	20	34	1.65	5	20	34	1.35	5	20	33	1.29
10	38	37	2.76	10	38	36	2.51	10	38	36	2.36
15	59	38	3.98	15	59	38	3.66	15	59	38	3.46
20	81	39	5.09	20	81	38	4.84	20	81	39	4.62
25	106	39	6.21	25	105	38	6.04	25	105	39	5.7
30	132	39	7.41	30	131	38	7.13	30	132	38	6.74
35	158	38	8.51	35	159	38	8.12	35	160	38	7.8
40	186	38	9.68	40	185	38	9.05	40	186	37	8.77
45	214	37	10.74	45	213	37	9.97	45	215	37	9.71
50	242	37	11.72	50	241	37	10.92	50	242	37	10.62
55	270	37	12.69	55	269	36	11.78	55	270	36	11.47
60	298	36	13.56	60	297	36	12.67	60	298	36	12.24
65	325	36	14.38	65	325	35	13.54	65	325	35	13.04
70	350	35	15.13	70	350	35	14.23	70	352	35	13.71
75	378	35	15.84	75	376	34	14.92	75	378	35	14.3
80	400	34	16.42	80	400	34	15.53	80	401	34	14.86
85	425	34	17	85	425	33	16.12	85	425	34	15.35
90	446	33	17.42	90	447	33	16.59	90	447	34	15.75
95	468	33	17.75	95	468	32	16.94	95	470	33	16.08
100	485	33	18.03	100	486	32	17.26	100	485	33	16.38
105	504	32	18.32	105	502	32	17.47	105	502	32	16.59

Table 4: MS zeolites (powder, charging at 1 l/min)

Cycle 1				Cycle 2				Cycle 3			
Time (min)	Pres. (psig)	Temp. (^oC)	Gas uptake (g)	Time (min)	Pres. (psig)	Temp. (^oC)	Gas uptake (g)	Time (min)	Pres. (psig)	Temp. (^oC)	Gas uptake (g)
0	0	24	0	0	0	24	0	0	0	24	0
5	24	29	2.04	5	23	29	1.59	5	23	30	1.26
10	44	32	3.13	10	42	32	2.56	10	43	33	2.32
15	68	35	4.34	15	66	35	3.93	15	66	36	3.48
20	96	37	5.57	20	94	37	4.95	20	93	38	4.76
25	127	38	6.76	25	125	38	6.08	25	123	40	5.92
30	161	39	7.81	30	160	39	7.2	30	159	41	6.88
35	197	39	9.01	35	195	40	8.4	35	194	41	7.91
40	234	39	10	40	231	40	9.55	40	230	41	8.73
45	269	39	11.12	45	267	40	10.57	45	265	41	9.7
50	305	39	11.95	50	303	40	11.39	50	300	40	10.53
55	340	38	12.87	55	338	40	12.2	55	336	39	11.26
60	372	38	13.64	60	370	39	12.96	60	368	39	11.95
65	403	37	14.19	65	400	39	13.57	65	398	39	12.52
70	430	36	14.68	70	426	39	14.13	70	423	39	12.98
75	454	36	15.13	75	450	38	14.45	75	445	38	13.33
80	475	35	15.58	80	470	38	14.7	80	467	38	13.82
85	495	35	15.91	85	490	37	14.96	85	488	37	14.1
86.217	500	34	15.98	89.167	500	36	15.19	89.7	500	36	14.26

Table 5: MS zeolites (beads, charging at 1 l/min)

Time (min)	Pres. (psig)	Temp. (^oC)	Gas uptake (g)
0	0	26	0
5	60	27	1.36
10	110	28	2.48
15	162	29	3.65
20	212	30	4.97
25	260	30	6.21
30	305	31	7.38
35	346	31	8.42
40	384	31	9.31
45	417	31	10.08
50	445	31	10.74
55	470	31	11.27
60	489	31	11.71
65	502	30	12.09

Table 6: Silica gel (charging at 1 l/min)

Cycle 1				Cycle 2				Cycle 3			
Time (min)	Pres. (psig)	Temp. (^oC)	Gas uptake (g)	Time (min)	Pres. (psig)	Temp. (^oC)	Gas uptake (g)	Time (min)	Pres. (psig)	Temp. (^oC)	Gas uptake (g)
0	0	23	0	0	0	24	0	0	0	25	0
5	44	26	1.9	5	44	27	1.85	5	50	28	1.6
10	85	28	3.17	10	84	28	3.13	10	93	30	3.08
15	125	29	4.86	15	123	29	4.57	15	133	31	4.31
20	165	30	6.06	20	163	30	5.95	20	173	31	5.92
25	204	31	7.24	25	201	31	7.18	25	211	32	7.01
30	243	31	8.77	30	240	31	8.6	30	248	33	8.42
35	280	31	9.93	35	276	31	9.51	35	285	33	9.33
40	316	31	11.19	40	312	31	10.73	40	320	33	10.45
45	350	31	12.31	45	347	31	11.88	45	352	33	11.38
50	384	31	13.08	50	380	31	12.76	50	385	33	12.32
55	417	31	13.81	55	412	31	13.38	55	415	33	12.74
60	447	31	14.22	60	440	30	13.7	60	441	32	13.15
65	475	31	14.4	65	470	30	13.99	65	467	32	13.41
70	500	30	14.51	70	495	30	14.2	70	492	32	13.66
				71.433	500	30	14.25	71.367	503	32	13.73

Table 7: CNG compression (charging at 1 l/min)

Time (min)	Pres. (psig)	Temp. (°C)	Gas uptake (g)
0	0	27	0
0.5	19	30	0.66
1	25	30	0.81
1.5	30	30	0.93
2.5	42	30	1.29
3.5	53	29	1.54
4.5	65	29	1.93
5.5	75	29	2.21
6.5	86	29	2.44
7.5	97	29	2.68
8.5	108	29	2.97
9.5	119	29	3.29
10.5	129	29	3.51
11.5	140	29	3.88
13.5	160	29	4.29
15.5	180	29	4.78
17.5	200	29	5.35
19.5	220	29	5.83
24.5	265	28	6.88
29.5	306	28	7.84
34.5	345	28	8.83
39.5	380	28	9.6
44.5	410	28	10.27
49.5	437	28	10.89
54.5	460	28	11.41
59.5	481	28	11.97
64.5	498	28	12.36
65.117	500	28	12.49

APPENDIX B3

Experimental results of the dynamic discharging

Table 1: Palm shell AC (discharging at 1 l/min)

Cycle 1				Cycle 2				Cycle 3			
Time (min)	Pres. (psig)	Temp (^oC)	Gas discharged (l)	Time (min)	Pres. (psig)	Temp (^oC)	Gas discharged (l)	Time (min)	Pres. (psig)	Temp (^oC)	Gas discharged (l)
0	497	30	0	0	500	30	0	0	501	30	0
0.167	475	29	1	0.167	482	29	0.7	0.167	470	29	1.5
0.5	427	25	2.6	0.333	440	28	2.3	0.333	425	28	3
0.833	390	23	4	0.5	400	27	3.7	0.5	392	26	4.3
1	360	22	5.2	0.667	368	25	4.9	0.667	380	25	4.8
1.167	334	20	6.3	0.833	340	23	6	0.833	350	24	5.9
1.333	310	19	7.3	1	315	22	7.2	1	325	22	7
1.5	290	17	8.3	1.333	285	20	8.6	1.333	295	21	8.2
1.667	268	16	9.3	1.667	257	18	9.9	1.667	270	19	9.4
1.833	250	15	10.2	2	235	17	11.1	2	247	18	10.6
2	235	14	11.1	2.5	210	15	12.4	2.667	220	15	12.2
2.167	220	13	11.9	3	190	13	13.7	3	202	14	13.3
2.5	200	12	13	3.333	175	12	14.7	3.333	187	13	14.1
3	180	10	14.3	3.833	155	11	16	3.667	173	12	15.1
3.333	165	9	15.3	4	145	10	16.7	4	160	11	15.9
3.667	152	8	16.2	4.333	135	9	17.6	4.333	147	10	16.8
4	140	7	17.1	4.667	123	8	18.4	4.667	135	8	17.6
4.333	128	6	17.9	5	113	7	19.3	5	125	7	18.5
4.667	118	5	18.8	5.5	102	5	20.2	5.5	113	6	19.5
5	110	4	19.6	6	90	4	21.3	6	100	5	20.6
5.5	97	2	20.6	6.5	80	3	22.3	6.5	90	4	21.6
6	85	1	21.7	7	72	2	23.3	7	80	3	22.6
6.5	77	0	22.7	8	58	0	25	8	65	0	24.3
7	68	-1	23.6	9	46	-1	26.6	9	52	-2	25.9
8	55	-3	25.2	10	36	-3	28.1	10	42	-3	27.5
9	43	-5	26.9	11	28	-5	29.7	11	28	-6	29.8
10	35	-7	28.4	13	15	-8	32.5	13	15	-9	32.5
12	18	-11	31.2	17	7	-10	33.8	17	8	-11	33.8
14	10	-13	33.7	18	5	-10	34.4	18	4	-11	34
16	5	-14	35.3	21	3	-7	35.6	21	2	-7	34.8
18	3	-13	36.3	30	0	5	36.3	30	0	4	35
28	0	0	37.9	40	0	13	36.9	40	0	15	35.8
38	0	8	38.4	50	0	18	37.2	50	0	20	36.4
48	0	13	38.7	60	0	21	37.4	60	0	22	36.8
70	0	20	39.1	70	0	23	37.5	70	0	24	37
80	0	25	39.1	80	0	25	37.5	75	0	25	37

Table 2: Palm shell AC (discharging at 6 and 10 l/min)

6 l/min				10 l/min			
Time (min)	Pres. (psig)	Temp. (^{o}C)	Gas discharged (l)	Time (min)	Pres. (psig)	Temp. (^{o}C)	Gas discharged (l)
0	500	30	0	0	500	30	0
0.167	462	28	1.2	0.167	423	25	2.6
0.5	390	25	3.8	0.333	355	21	5.1
0.667	360	22	4.8	0.5	302	17	7.2
0.833	325	20	6.3	0.667	255	13	9.4
1	310	17	7.2	0.833	215	8	11.5
1.167	269	15	8.8	1	180	3	13.4
1.333	240	12	10.2	1.167	150	-1	15.4
1.5	215	9	11.5	1.333	123	-5	17.1
1.667	190	7	12.9	1.5	100	-9	18.9
1.833	169	4	14.2	1.667	80	-13	20.6
2	150	2	15.4	1.833	65	-17	22.3
2.333	122	-2	17.3	2	50	-21	24
2.667	100	-6	19.2	2.167	38	-26	25.6
3	79	-11	21.1	2.333	26	-31	27.4
3.333	62	-14	22.9	2.5	19	-34	28.8
3.667	47	-18	24.7	2.667	14	-38	30.2
4	38	-22	26.2	2.833	9	-41	30.7
4.333	26	-25	28.0	3.167	4	-45	31
4.667	17	-29	29.7	3.5	1	-47	31.2
5	10	-32	31.2	4.5	0	-48	31.5
6	2	-36	34.3	5.5	0	-46	31.7
11	0	-32	35.7	6.5	0	-44	31.8
16	0	-23	36.3	7.5	0	-42	32
26	0	-10	36.9	8.5	0	-34	32.2
36	0	-4	37.2	13.5	0	-21	32.4
56	0	1	37.4	33.5	0	-13	32.5
76	0	3	37.6	53.5	0	-11	32.5

Table 3: Darco AC (discharging at 1 l/min)

Cycle 1				Cycle 2				Cycle 3			
Time (min)	Pres. (psig)	Temp (°C)	Gas discharged (l)	Time (min)	Pres. (psig)	Temp (°C)	Gas discharged (l)	Time (min)	Pres. (psig)	Temp (°C)	Gas discharged (l)
0	500	29	0	0	499	30	0	0	498	30	0
0.167	471	27	1.1	0.167	466	29	1.2	0.333	455	29	1.5
0.333	452	26	1.7	0.333	444	27	2	0.667	415	27	3
0.5	418	25	3	0.5	420	26	3	1	377	25	4.4
0.667	384	23	4.1	0.667	386	25	4.1	1.333	346	24	5.6
0.833	352	21	5.3	0.833	355	24	5.3	1.667	315	22	6.8
1	326	20	6.4	1	333	23	6.1	2	285	21	7.9
1.333	295	18	7.6	1.333	304	22	7.2	2.5	254	19	9.3
1.667	266	17	8.8	1.667	283	21	8.1	3	226	17	10.5
2	240	15	9.9	2	258	20	9.1	3.5	200	15	11.7
2.5	210	13	11.1	2.5	229	19	10.4	4	175	14	12.8
3	185	12	12.4	3	200	18	11.7	4.5	153	13	13.9
3.5	161	10	13.6	3.5	175	16	12.9	5	132	11	14.9
4	139	8	14.6	4	150	14	14	5.5	114	10	15.9
4.5	120	7	15.6	4.5	130	13	15.1	6	97	8	16.8
5	100	5	16.6	5	113	12	16.1	6.5	82	7	17.8
5.5	85	4	17.5	5.5	96	10	17	7	68	5	18.6
6	70	2	18.4	6	80	8	17.9	7.5	55	4	19.5
6.5	57	1	19.3	6.5	67	6	18.8	8	44	2	20.3
7	45	-1	20.2	7	55	5	19.6	9	27	0	21.7
7.5	34	-3	21.1	7.5	44	3	20.4	10	14	-3	22.5
8	24	-4	22	8	34	2	21.2	11	6	-5	23.1
9	9	-8	23.6	9	19	0	22.6	12	2	-5	23.6
10	2	-10	24.4	10	9	-3	23.5	13	0	-4	23.9
11	0	-9	24.8	11	3	-4	23.8	18	0	3	24.3
16	0	-2	25.2	12	1	-3	24	38	0	21	24.7
36	0	17	25.6	13	0	-2	24.2	56.38	0	25	24.8
56	0	22	25.7	23	0	10	25				
62.38	0	23	25.7	33	0	19	25.2				
				46	0	24	25.5				

Table 4: MS zeolites (discharging at 1 l/min)

Cycle 1				Cycle 2				Cycle 3			
Time (min)	Pres. (psig)	Temp (^oC)	Gas discharged (l)	Time (min)	Pres. (psig)	Temp (^oC)	Gas discharged (l)	Time (min)	Pres. (psig)	Temp (^oC)	Gas discharged (l)
0	497	30	0	0	496	31	0	0	496	31	0
0.167	482	29	0.5	0.167	455	30	0.5	0.167	455	30	0.4
0.333	443	28	1.7	0.333	425	29	1.5	0.333	420	29	1.5
0.5	422	27	2.3	0.5	393	28	2.5	0.5	394	28	2.3
0.667	387	26	3.4	0.667	360	27	3.6	0.667	360	27	3.3
0.833	355	25	4.4	0.833	331	26	4.5	0.833	336	26	4.1
1	335	24	5.1	1	306	25	5.4	1	306	25	5
1.167	319	23	5.7	1.167	281	24	6.2	1.167	276	23	6.1
1.333	291	22	6.6	1.333	255	23	7.1	1.333	255	22	6.9
1.5	266	21	7.5	1.5	235	22	7.9	1.5	231	21	7.8
1.667	243	20	8.3	1.667	214	21	8.7	1.667	210	20	8.6
1.833	225	19	9	1.833	195	20	9.4	1.833	190	19	9.4
2	206	18	9.7	2	180	19	10.1	2	173	18	10.1
2.333	183	17	10.7	2.333	160	18	11	2.333	152	17	11
2.667	161	16	11.5	2.667	140	17	11.9	2.667	133	15	11.8
3	143	15	12.4	3	122	16	12.8	3	115	14	12.6
3.333	125	14	13.1	3.333	107	15	13.5	3.333	100	13	13.4
3.667	110	13	14	3.667	94	14	14.3	3.667	88	12	14.2
4	97	12	14.7	4	82	13	14.9	4	75	11	14.9
4.333	85	11	15.3	4.333	70	12	15.6	4.333	65	10	15.6
4.667	75	10	16.1	4.667	59	10	16.5	4.667	55	8	16.2
5	60	9	16.7	5	46	9	17.4	5	46	7	16.9
5.5	52	7	17.5	5.5	35	8	18.2	5.5	37	6	17.7
6	41	6	18.3	6	27	6	19	6	27	5	18.5
6.5	32	4	19.1	6.5	20	5	19.8	6.5	20	3	19.2
7	25	3	19.9	7	14	3	20.5	7	14	1	19.9
7.5	17	1	20.6	7.5	5	1	21.5	7.5	9	0	20.4
8	10	0	21.4	8	0	0	22.2	8	5	-1	20.8
9	1	-3	22.8	9	0	-2	22.3	9	0	-1	21
14	0	-2	23	11	0	-2	22.4	10	0	0	21.5
24	0	4	23.2	14	0	-1	22.5	15	0	1	21.9
44	0	10	23.3	24	0	6	22.5	25	0	7	22
64	0	14	23.4	44	0	12	22.6	45	0	14	22.1
119	0	20	23.5	64	0	16	22.6	65	0	17	22.1
				104	0	20	22.6	85	0	19	22.2

Table 5: Silica gel (discharging at 1 l/min)

Cycle 1				Cycle 2				Cycle 3			
Time (min)	Pres. (psig)	Temp (^{o}C)	Gas discharged (l)	Time (min)	Pres. (psig)	Temp (^{o}C)	Gas discharged (l)	Time (min)	Pres. (psig)	Temp (^{o}C)	Gas discharged (l)
0	500	30	0	0	500	30	0	0	500	30	0
0.167	480	29	0.8	0.167	478	29	0.8	0.333	464	29	1.7
0.333	453	28	1.7	0.333	455	28	1.6	0.667	422	27	2.8
0.5	422	27	2.9	0.5	420	27	2.9	1	385	26	4.1
0.667	386	26	4.2	0.667	396	26	3.8	1.333	350	24	5.4
0.833	360	24	5.1	1	365	24	4.9	1.667	317	23	6.6
1	286	24	6.1	1.167	335	23	6.1	2	287	22	7.8
1.167	314	23	6.9	1.333	320	23	6.7	2.5	253	21	9.2
1.333	295	22	7.7	1.5	292	21	8	3	222	19	10.4
1.5	270	21	8.6	1.667	260	20	9	3.5	193	18	11.6
1.667	249	20	9.5	1.833	237	19	10	4	167	17	12.8
1.833	227	19	10.3	2	215	18	10.9	4.5	141	16	13.9
2	210	18	11	2.333	190	17	11.9	5	117	15	14.9
2.333	185	17	12	2.667	166	16	12.9	5.5	94	14	15.8
2.667	163	16	13.1	3	145	15	13.8	6	73	13	16.7
3	140	15	14.1	3.5	119	14	15	6.5	55	13	17.5
3.5	113	14	15.2	4	95	13	15.9	7	36	12	18.3
4	90	13	16.2	4.5	75	12	16.8	7.5	20	11	19.1
4.5	68	12	17.1	5	55	11	17.7	8	5	10	19.7
5	46	11	18	5.5	35	10	18.5	10	0	10	20.1
5.5	28	10	18.9	6	20	10	19.3	15	0	11	20.2
6	10	9	19.7	6.5	7	9	20	35	0	17	20.3
6.5	3	9	20.2	7	1	9	20.1	55	0	22	20.3
7	0	10	20.3	8	0	9	20.2				
8	0	10	20.3	10	0	10	20.3				
13	0	13	20.3	15	0	13	20.3				
23	0	18	20.3	35	0	21	20.4				
43	0	22	20.4	55	0	23	20.4				

Table 6: CNG decompression (discharging at 1 l/min)

Time (min)	Pres. (psig)	Temp. (^{o}C)	Gas discharged (l)
0	500	28	0
0.167	461	27	1.5
0.333	425	26	2.9
0.5	394	24	4.1
0.667	363	24	5.3
0.833	332	24	6.4
1	305	23	7.4
2	250	23	9.5
4	162	22	12.8
6	75	21	16
8	8	20	18.4
8.733	0	23	18.6
9.733	0	25	18.7
16.733	0	27	18.7

APPENDIX C

Calculations of the amount of gas adsorbed on the adsorbents substrate

The amount of gas under adsorbed state, is calculated from Equation 2.13 as shown below (Malbrunot *et al.*, 1996):

$$M_s = \rho_b m_a + \rho_g (1 - \rho_b/\rho_s) \quad (2.13)$$

where,

ρ_b = packing density of the adsorbent

m_a = amount of gas adsorbed by adsorbent (mole/gram of adsorbent)

ρ_g = molar gas density at P and T considered

ρ_s = real density of the adsorbent

The first term of the equation represents amount of the adsorbed gas and the second term represents amount of compressed gas. By calculating the value for the second term of the above equation, the amount of gas adsorbed, $\rho_b m_a$, is figured out. Value of M_s is obtained from the experiment and it is equivalent to the weight of gas uptake converted to mole amount per volume of storage. The experimental results of gas uptake at isothermal condition for each type of adsorbent tested are listed in Table C1.

Table C1: Gas uptake at 514.7 psia under isothermal condition

Adsorbent	Gas uptake at 514.7 psia	
	g/l	***mol/cm^3***
Carbon-based palm shell	66.65	4.166×10^{-3}
Molecular sieve zeolites	37.24	2.327×10^{-3}
Silica Gel	29.52	1.845×10^{-3}

Carbon-based palm shell adsorbent

The amount of adsorbed gas in the ANG storage employing palm shell adsorbent at isothermal condition is calculated as follows:

From Table C1, amount of gas uptake, M_s = 66.65 g/l = 4.166×10^{-3} mol/cm^3

From Table 3.5, packing density, ρ_b = 0.50 g/cm^3,

true density, ρ_s = 0.79 g/cm^3

Methane density, ρ_g, at 500 psig and room temperature (taken as 30 ^oC) is 23.44 g/l. This value is obtained from calculation using real gas equation where $\rho_g = MP/zRT$. Converting to mol/cm^3, ρ_g = 1.465 x 10^{-3}.

$\therefore$ Amount of adsorbed gas, $\rho_b\, m_a$ = 4.166 x 10^{-3} – 1.465 x 10^{-3} $(1 - \frac{0.5}{0.79})$

= 3.628 x 10^{-3} mol/cm^3

= 58.10 g/l

MS zeolites adsorbent

From Table C1, amount of gas uptake, M_s = 37.24 g/l = 2.161 x 10^{-3} mol/cm^3

From Table 3.5, packing density, ρ_b = 0.53 g/cm^3

true density, ρ_s = 0.92 g/cm^3

$\therefore$ Amount of adsorbed gas, $\rho_b\, m_a$ = 2.327 x 10^{-3} – 1.465 x 10^{-3} $(1 - \frac{0.53}{0.92})$

= 1.706 x 10^{-3} mol/cm^3

= 27.30 g/l

Silica gel adsorbent

From Table C1, amount of gas uptake, M_s = 29.52 g/l = 1.845 x 10^{-3} mol/cm^3

From Table 3.5, packing density, ρ_b = 0.51 g/cm^3

true density, ρ_s = 0.85 g/cm^3

$\therefore$ Amount of adsorbed gas, $\rho_b\, m_a$ = 1.845 x 10^{-3} – 1.465 x 10^{-3} $(1 - \frac{0.51}{0.85})$

= 1.259 x 10^{-3} mol/cm^3

= 20.14 g/l

Lampiran 20

UTM/RMC/F/0024(1998)

UNIVERSITI TEKNOLOGI MALAYSIA

BORANG PENGESAHAN
LAPORAN AKHIR PENYELIDIKAN

TAJUK PROJEK : **Pembagunan Storan Gas Asli Berasaskan Penjerap bagi Kegunaan Kenderaan**

Saya **PROF. MADYA DR. HANAPI BIN MAT**
(HURUF BESAR)

Mengaku membenarkan Laporan Akhir Penyelidikan ini disimpan di Perpustakaan Universiti Teknologi Malaysia dengan syarat-syarat kegunaan seperti berikut :

1. Laporan Akhir Penyelidikan ini adalah hakmilik Universiti Teknologi Malaysia.
2. Perpustakaan Universiti Teknologi Malaysia dibenarkan membuat salinan untuk tujuan rujukan sahaja.
3. Perpustakaan dibenarkan membuat penjualan salinan Laporan Akhir Penyelidikan ini bagi kategori TIDAK TERHAD.
4. * Sila tandakan (✓)

☐	SULIT	(Mengandungi maklumat yang berdarjah keselamatan atau Kepentingan Malaysia seperti yang termaktub di dalam AKTA RAHSIA RASMI 1972).
☐	TERHAD	(Mengandungi maklumat TERHAD yang telah ditentukan oleh Organisasi/badan di mana penyelidikan dijalankan).
✓	TIDAK TERHAD	

TANDATANGAN KETUA PENYELIDIK

PROF. MADYA DR. HANAPI BIN MAT

Nama & Cop Ketua Penyelidik

Tarikh: 12 hb. Jun 2006

CATATAN : ** Jika Laporan Akhir Penyelidikan ini SULIT atau TERHAD, sila lampirkan surat daripada pihak berkuasa/organisasi berkenaan dengan menyatakan sekali sebab dan tempoh laporan ini perlu dikelaskan sebagai SULIT dan TERHAD.*